Mathematical modeling in dairy cattle – nonlinear ration formulation, thermal balance, emission and excretion models

By

JINGHUI LI

DISSERTATION

Submitted in partial satisfaction of the requirements for the degree of

DOCTOR OF PHILOSOPHY

in

Animal Biology

in the

OFFICE OF GRADUATE STUDIES

of the

UNIVERSITY OF CALIFORNIA

DAVIS

Approved:

Ermias Kebreab, Chair

James G. Fadel

Vinod Narayanan

Committee in Charge

2021

Preface

This dissertation includes the work I did from 2017 to 2021 to fulfill the requirement for a Doctorate of Philosophy in Animal Biology for the Office of Graduate Studies of the University of California, Davis. Four years of PhD career in Davis are valuable experience to me, and I could not have finished my work without the help from my mentors and colleagues. I first would like to thank my dissertation committee members. I am thankful to my major advisor Dr. Ermias Kebreab for offering academic advice and opportunities to work with a wide range of researchers. I am also grateful to my co-mentor Dr. James Fadel for patiently training me and generously sharing his wisdom. In addition, I want to thank Dr. Vinod Narayanan for his engineering expertise and patience. Besides the dissertation committee members, there are many other people who have been supportive. I want to thank Dr. Kebreab for establishing the connection with Dr. Kristan Reed, an animal scientist in Cornell University, who provided the idea of ration formulation using nonlinear programming. I also would like to thank my colleague and friend, Dr. Henk van Lingen, for patiently helping me at the beginning of my PhD career and making a good researcher example. I have to thank Dr. Fadel for creating the collaboration with Dr. Hao Cheng, who kindly shared his statistical expertise and helped me as though I were under his supervision.

Finally, I must thank China Scholarship Council for the financial support. In particular, I want to thank my father, mother and grandmother for supporting and caring me throughout these years.

Table of Contents

Abstract vii

Introduction 1

Reference 5

Chapter 1: The application of nonlinear programming on designing feed formulation for dairy cattle 8

Abstract 8

Introduction 9

Methods 11

Optimization strategies 12

Simulation 15

Evaluation 15

Software 16

Results and Discussion 16

An example simulation 16

Feasibility and nutrient balance 16

Ration cost 18

Computation time 19

Conclusions 19

Acknowledgements 20

References 21

Tables and Figures 24

Appendix 1 31

Appendix 2 40
Chapter 2: A mechanistic thermal balance model of dairy cattle 43
Abstract 43
Introduction 44
Materials and Methods 45
Model Description 45
Model evaluation 56
Simulation example 57
Sensitivity analysis 58
Results and Discussion 60
Model evaluation 60
Simulation example 61
Sensitivity analysis 63
Conclusions 65
Acknowledgements 65
References 66
Tables and Figures 74
Appendix A 84
Appendix B 99
Appendix C 100
Chapter 3: A multivariate model to predict greenhouse gas emission, manure excretion and water intake in dairy cattle 105
Abstract 105

Introduction 106
Materials and Methods 107
Data Sources 107
Multivariate Model 108
Model Evaluation 110
Results and Discussion 111
GHG Production 113
Milk Production and Water Intake 114
Manure Excretion 115
Conclusions 117
Acknowledgements 118
References 118
Tables and Figures 125
Chapter 4: A simulation study at farm level using nonlinear ration formulation, thermal balance, emission and excretion models 132
Abstract 132
Introduction 133
Materials and Methods 134
Dairy herd simulation 134
Ration formulation 134
Emission and excretion 135
Thermal balance 135
Results and Discussion 136

Ration formulation..... 136
GHG emission and manure excretion..... 136
Thermal balance 138
References 139
Tables and Figures 143

Abstract

The objective of this dissertation is to integrate information from a nonlinear ration formulation model, a thermal balance model, and emission and excretion models to evaluate the environment impact of dairy cattle and the effect of climate on dairy cattle at the farm level. The first chapter investigated the application of iterative linear programming (iteLP), sequential quadratic programming (SQP) and mixed-integer nonlinear programming based deterministic global optimization (MINLP_DGO) on designing feed formulation for dairy cattle based on NRC (2001). A simulation study showed that iteLP had limited capability to design least cost diets when nonlinearity existed in the constraints. Both SQP and MINLP_DGO were able to handle nonlinear constraints well, with SQP being faster but MINLP_DGO being more reliable. In the second chapter, a thermal balance model was developed to predict the body temperature and heat fluxes for Holstein dairy cattle under heat stress conditions. The model included five nodes representing the body core, skin and coat of a dairy cow. Heat production by the animal, heat conduction through the body core, skin and coat, and heat flows between the animal and the environment, including conduction, convection, evaporation and radiation, were calculated based on existing models and physical principles. Model evaluation suggested a likely overestimation of body temperature. Sensitivity analysis showed that heat production, surface area, air pressure and the parameters relative to respiration and sweating were the most sensitive. In the third chapter, environmental impact of dairy cattle was evaluated by considering relevant outputs simultaneously. Three multivariate Bayesian regression models were developed to predict enteric methane (CH_4), carbon dioxide (CO_2), water intake ($Water_{in}$), volatile solids (VS), biodegradable VS (dVS), fecal DM (F_{DM}), fecal water (F_W), fecal carbon (F_C), fecal nitrogen (F_N), total urine (U_t), urine carbon (U_C) and urine nitrogen (U_N) for lactating cows, nonlactating cows and heifers.

Most equations predicted the response variables with reasonable accuracy, except $Water_{in}$ and U_t equations for nonlactating cows and heifers. In the last chapter, a simulation study was conducted to evaluate the environment impact of dairy cattle and the effect of climate on dairy cattle at the farm level. The ration, body temperature, heat flows, greenhouse gas emission and manure excretion were predicted for two heifer herds, three lactating cow herds and one nonlactating cow herd.

Introduction

Mathematical modeling has been widely used to evaluate and quantify different components of the dairy system, including biology (Hanigan and Baldwin, 1994; Hanigan et al., 2007), nutrition (Moraes et al., 2015; Dijkstra et al., 2018), environmental impact (Beauchemin et al., 2010; Li et al., 2012) and whole-farm systems (Beukes et al., 2008; Rotz et al., 2012). A model can be defined as one equation or a set of equations which represents the behavior of a system in a mathematical manner (Dym, 2004). There are several ways to classify models into different categories, for example, a model can be classified as an empirical or a mechanistic model based on whether the model inputs and outputs are related empirically or based on the underlying structure of the system.

Most empirical models are built based on statistical analysis, including regression analysis and analysis of variance (ANOVA). Empirical models are widely used because they are simple and can be easily implemented in well-developed packages, such as R (R Core Team, 2020), SAS (SAS Institute Inc., 2013) and SPSS (IBM Corp., 2020). One important application of empirical models is to reveal the significance of treatment effect in animal trials based on ANOVA or regression analysis. Empirical models are also widely used to build prediction equations through Bayesian or frequentist regression methods, both of which are valid approaches (Wakefield, 2013). For example, Moraes et al. (2014) developed a set of equations to predict enteric methane emissions from dairy cattle using Bayesian regression models; Appuhamy et al. (2014) developed models to predict volume and nutrient composition of fresh manure from lactating cows using frequentist regression methods. Although empirical models are commonly used, but there are some critiques of this approach. When conducting data mining, empirical models only reveal association instead of causality. In other words, the covariates in an

empirical model might be a confounder or mediator instead of the true causal factor. If only the prediction is of interest, using confounder or mediator may generate a good result, but if causal inference is also of interest, other statistical techniques are required. There are some approaches to reduce the bias from confounders, such as propensity score matching (Rosenbaum and Rubin, 1983), but these approaches were not commonly used in dairy science modeling. Another limitation of empirical models is that they are highly dependent on the dataset used for model development, which makes the model only applicable within a narrow range. For example, Niu et al. (2018) developed prediction equations for methane emissions from dairy cows using the data from several continents, and the equations for different regions had different coefficients.

Mechanistic models are developed based on the underlying mechanism of the system, and there are many of them developed for dairy cattle. Baldwin et al. (1987) developed a mechanistic model for the digestive metabolism of dairy cattle. The model contains dozens of equations describing either the mass action or Michaelis–Menten kinetics in the digestive tract. There are some other mechanistic models, such as Manure-DNDC model (Li et al., 2012) describing the biogeochemical process in the livestock manure and thermal balance model describing the heat flows for livestock (Turnpenny et al., 2000). All these models contain many equations, parameters and variables. Since mechanistic models represent the mechanism of the system, it is easy to interpret all the model components and the relationships among them, but the model complexity makes them difficult to use. Some of the mechanistic model inputs or parameters are difficult to obtain in application and need empirical equations to obtain an estimate. For example, in the thermal balance model (Turnpenny et al., 2000), the animal surface area and respiration rate are estimated through empirical equations, which make the mechanistic model not purely mechanistic. In principle, mechanistic models can be used in a much wider range than empirical

models. However, as described above, some parameters or inputs for a mechanistic model need to be estimated through empirical equations, which may require reevaluation under some situations, e.g., the empirical equation built for predicting the respiration rate of dairy cows in tropical regions might not be able to predict the cow in subtropical regions accurately without modifications.

Optimization models are another important type of mathematical models. Optimization models aim at optimizing a certain objective, which may be subject to a set of constraints. The calculation of the objective and constraints may involve empirical and mechanistic models, so it is hard to classify an optimization model as empirical or mechanistic. In animal science, one typical example of optimization model is using linear programming to formulate least-cost feed rations that meet all the nutrient requirements (Chandler et al., 1972; O'Connor, et al., 1989). There are several others, such as optimization of dairy heifer management decisions (Mourits et al., 2000), an optimization model of pasture-based model (Doole et al., 2013) and an optimization model considering multiple objectives to minimize environmental impact and maximize economic benefit (Breen et al., 2019). In the future, more complicated optimization models targeting the whole-farm system are expected, which will become an essential tool to support decision-making on farm.

The overall objective of this dissertation is to integrate information from a nonlinear ration formulation model, a thermal balance model, and emission and excretion models to evaluate the environment impact of dairy cattle and the effect of climate on dairy cattle at the farm level. The first chapter of this dissertation describes an optimization model of dairy ration formulation using nonlinear programming, which provides a framework for ration formulation based on nonlinear constraints. In the second chapter, a thermal balance model was developed to

understand the heat flows in dairy cattle under heat stress. The model can be used to guide the application of cooling strategies. The third chapter describes a multivariate Bayesian regression model for evaluating the environmental impact from dairy cattle. In the last chapter, the models developed in the previous three chapters were integrated together through a simulation study at the farm level.

Reference

Appuhamy, J. A. D. R. N., L. E. Moraes, L.E., C. Wagner-Riddle, D. P. Casper, J. France, and E. Kebreab, 2014. Development of mathematical models to predict volume and nutrient composition of fresh manure from lactating Holstein cows. Anim. Prod. Sci. 54:1927–1938.

Baldwin, R. L., J. H. Thornley, and D. E. Beever. 1987. Metabolism of the lactating cow: II. Digestive elements of a mechanistic model. J. Dairy Res. 54:107–131.

Beauchemin, K. A., H. H. Janzen, S. M. Little, T. A. McAllister, and S. M. McGinn. 2010. Life cycle assessment of greenhouse gas emissions from beef production in western Canada: A case study. Agric. Syst. 103:371–379.

Beukes, P. C., C. C. Palliser, K. A. Macdonald, J. A. Lancaster, G. Levy, B. S. Thorrold, and M. E. Wastney. 2008. Evaluation of a whole-farm model for pasture-based dairy systems. J. Dairy Sci. 91:2353–2360.

Breen, M., M. D. Murphy, and J. Upton. 2019. Development of a dairy multi-objective optimization (DAIRYMOO) method for economic and environmental optimization of dairy farms. Appl. Energy 242:1697–1711.

Chandler, P. T., and H.W. Walker. 1972. Generation of nutrient specifications for dairy cattle for computerized least cost ration formulation. J. Dairy Sci. 55:1741–1749.

Dijkstra, J., A. Bannink, P. M. Bosma, E. A. Lantinga, and J. W. Reijs. 2018. Modeling the effect of nutritional strategies for dairy cows on the composition of excreta nitrogen. Front. sustain. food syst. 2:63.

Doole, G. J., A. J. Romera, and A. A. Adler. 2013. An optimization model of a New Zealand dairy farm. J. Dairy Sci. 96:2147–2160.

Dym, C. 2004. Principles of Mathematical Modeling. Academic Press, Oxford, UK.

Hanigan, M. D., A. G. Ruis, E. S. Kolver, and C. C. Palliser. 2007. A redefinition of the representation of mammary cells and enzyme activities in a lactating dairy cow model. J. Dairy Sci. 90:3816– 3830.

Hanigan, M. D., and R. Baldwin. 1994. A mechanistic model of mammary gland metabolism in the lactating cow. Agric. Syst. 45:369– 419.

IBM Corp. 2020. IBM SPSS Statistics for Windows, Version 27.0. Armonk, NY: IBM Corp

Li, C., W. Salas, R. Zhang, C. Krauter, A. Rotz, and F. Mitloehner. 2012. Manure-DNDC: a biogeochemical process model for quantifying greenhouse gas and ammonia emissions from livestock manure systems. Nutr. Cycl. Agroecosyst. 93:163–200.

Moraes, L. E., E. Kebreab, A. B. Strathe, J. Dijkstra, J. France, D. P. Casper, and J. G. Fadel. 2015. Multivariate and univariate analysis of energy balance data from lactating dairy cows. J. Dairy Sci. 98:4012–4029.

Moraes, L. E., A. B. Strathe, J. G. Fadel, D. P. Casper, and E. Kebreab. 2014. Prediction of enteric methane emissions from cattle. Glob. Chang. Biol. 20:2140–2148.

Mourits, M. C. M., D. T. Galligan, A. A. Dijkhuizen, and R. B. M. Huirne. 2000. Optimization of dairy heifer management decisions based on production conditions of Pennsylvania. J. Dairy Sci. 83:1989–1997.

Niu, M., E. Kebreab, A. N. Hristov, J. Oh, C. Arndt, A. Bannink, A. R. Bayat, A. F. Brito, T. Boland, D. Casper, and L. A. Crompton. 2018. Prediction of enteric methane production, yield, and intensity in dairy cattle using an intercontinental database. Glob. Chang. Biol. 24:3368–3389.

O'Connor, J. D., C. J. Sniffen, D. G. Fox, and R. A. Milligan. 1989. Least cost dairy cattle ration formulation model based on the degradable protein system. J. Dairy Sci. 72:2733–2745.

Rosenbaum, P. R., and D. B. Rubin. 1983. The central role of the propensity score in observational studies for causal effects. Biometrika 70:41–55.

Rotz, C. A., M. S. Corson, D. S. Chianese, F. Montes, S. D. Hafner, and C. U. Coiner. 2012. The integrated farm system model. References manual, version, 3.

R Core Team (2020). R: A language and environment for statistical computing. R Foundation for Statistical Computing, Vienna, Austria. https://www.R-project.org/.

SAS Institute Inc. 2013. SAS® 9.4 Statements: Reference. Cary, NC: SAS Institute Inc.

Turnpenny, J. R., A. J. McArthur, J. A. Clark, and C. M. Wathes. 2000. Thermal balance of livestock: 1. A parsimonious model. Agric. For. Meteorol. 101:15–27.

Wakefield, J. 2013. Bayesian and frequentist regression methods. Springer Science & Business Media.

Chapter 1: The application of nonlinear programming on designing feed formulation for dairy cattle

J. H. Li[1], E. Kebreab[1], F. You[2], J. G. Fadel[1], T. L. Hansen[3], C. VanKerkhove[4] and K.F. Reed[3]

[1]Department of Animal Science, University of California, Davis 95616

[2] Robert Frederick Smith School of Chemical and Biomolecular Engineering, Cornell University, Ithaca, NY 14853, USA

[3] Department of Animal Science, Cornell University, Ithaca, NY 14853

[4] School of Operations Research and Information Engineering, Cornell University, Ithaca, NY 14853

Abstract

The objective of this study was to compare the application of iterative linear programming (iteLP), sequential quadratic programming (SQP) and mixed-integer nonlinear programming based deterministic global optimization (MINLP_DGO) on ration formulation for dairy cattle based on Nutrient Requirements of Dairy Cattle (NRC 2001). Least-cost diets were formulated for lactating cows, dry cows and heifers. Nutrient requirements including energy, protein and minerals, along with other limitations on dry matter intake, NDF and fat were considered as constraints. Five hundred simulations were conducted, with each simulation randomly selecting 3 roughages and 5 concentrates from the feed table in NRC (2001) as the feed resource for each of three animal groups. Among the 500 simulations for lactating cows, there were 57, 45 and 21 simulations without a feasible solution for iteLP, SQP and MINLP_DGO, respectively. All the simulations for dry cows and heifers were feasible when using SQP and MINLP_DGO, but there were 49 and 11 infeasible simulations for iteLP, respectively. Average ration costs per animal

per day obtained by iteLP, SQP and MINLP_DGO were \$4.78 (± 0.71), \$4.45 (± 0.65) and \$4.44 (± 0.65) for lactating cows, \$2.39 (± 0.52), \$1.48 (± 0.26) and \$1.48 (± 0.26) for dry cows, and \$0.98 (± 0.72), \$0.97 (± 0.15) and \$0.91 (± 0.14) for heifers, respectively. The average computation time of iteLP, SQP and MINLP_DGO were 0.59 (± 1.87) s, 1.15 (± 0.62) s and 58.69 (± 68.45) s for lactating cows; 0.041 (± 0.070) s, 0.76 (± 0.37) s and 14.84 (± 39.09) s for dry cows, and 1.60 (± 2.90) s, 0.51 (± 0.19) s and 16.45 (± 45.56) s for heifers, respectively.
Key words: feed formulation, nonlinear programming, dairy cattle, NRC (2001)

Introduction

Feed costs account for around 50 to 70% of the expenses of operating a dairy farm (Bozic et al., 2012), so it is important to control the cost when designing the feed formulation. Diet formulation relies on the nutrient requirements of the animal and nutrient compositions of feeds, which depends on systems for estimating requirements, such as Nutrient Requirements of Dairy Cattle (NRC, 2001) or Cornell Net Carbohydrates and Protein System (CNCPS, Fox, et al., 2004). Linear programming (LP) optimizes a linear objective function subject to a set of linear constraints and is a good method to formulate least-cost diets that fulfill all the nutrient requirements of dairy cattle (Chandler et al., 1972; O'Connor, et al., 1989). There are several studies considering the variation of feed compositions in the constraints (Tozer, 2000) or different objective functions (Qu, et al. 2019; Alqaisi et al. 2021) while using LP for ration formulation. However, LP only allows linear objective functions and constraints. Some equations in the dairy nutrition model are nonlinear when adapted to a LP structure. For example, the calculation of microbial protein production in NRC (2001) and digestibility of TDN in CNCPS (2004) are dependent on intake and the ration composition and therefore create nonlinear constraints for the ration optimization. In NRC (2001), nonlinearity mainly exists in the

calculation of energy and protein contents of feeds. For energy, the TDN values of feeds are corrected by the animal intake level, which consequently affects metabolizable and net energy values. For protein, the calculation of passage rates for each feed requires DMI and dietary concentrate percentage. These rates are then used to calculate rumen degradable and undegradable protein (RDP and RUP) contents. The intake level and dietary concentrate percentage are unknown before formulating the diet, so adapting these equations to an optimization programming creates the nonlinearity.

Not many studies have investigated how to handle nonlinearity in ration optimization, which is important because increasingly more nonlinear equations may appear along with the advances of dairy nutrition. Moraes et al. (2012) used an iterative linear programming (iteLP) method to deal with the nonlinearity in the NRC (2001) for ration formulation. However, iteLP has certain limitations, which will be discussed in this paper. A nonlinear programming optimizer, sequential quadratic programming (SQP, Boggs and Telle, 1995), was employed in the CPM dairy model to formulate rations based on CNCPS (Boston et al., 2000), but the performance of using SQP based on NRC (2001) is unknown. Mixed-integer nonlinear programming based deterministic global optimization (MINLP_DGO) algorithms are able to solve a broader range of nonlinear programming problems compared to SQP.

Mathematical modeling has been an important technique to evaluate production and environmental impacts of dairy systems (France and Kebreab, 2008). Whole farm models like the Integrated Farm Systems Model (IFSM) can provide holistic estimates of production and environmental outcomes in response to changes in weather and management (Rotz et al., 2016; Veltman et al., 2018) and require a method to determine feed use and delivery. The IFSM currently uses an iteLP approach for ration formulation with requirements modified from the

NRC (2001) (Rotz et al., 2016). The limitations of the ration formulation method in IFSM are among the factors that have led our group to develop a new, flexible whole-farm model to evaluate connections between dairy system components, including animal husbandry and feeding, manure management, field and crop management, and feed storage (Kebreab et al., 2019). The nonlinear programming framework for ration formulation developed in this study will automate simulation of feed use and production within the Ruminant Farm Systems Model and represent an advancement over extant whole-farm models (Kebreab et al., 2019). The objectives of this study are to (1) introduce a methodology to use MINLP_DGO to find least-cost ration solutions that depend on with nonlinear nutrition equations of the NRC (2001) and (2) compare the performance of iteLP, SQP and MINLP_DGO on designing feed formulation based on NRC (2001).

Methods

Least-cost diets were formulated to meet the nutrient requirements of dairy cattle in different life-stages with the nutrient compositions of feeds as described by the NRC (2001). Model constraints created to meet the animal's requirements for nutrients were drawn directly from the recommendations of the NRC (2001) and included net energy requirements for maintenance (NE_M), lactation (NE_L) and growth (NE_G), metabolizable protein (MP) requirement, and calcium and phosphorus requirements. Additional constraints were introduced to guide formulation of diets that meet requirements for rumen function. These included a fat constraint of less than 7% of diet DM (NRC, 2001), an NDF constraint of greater than 25 % and less than 40 % of diet DM (NRC, 2001; Moraes et al., 2012), and a constraint of forage NDF greater than 19% of diet DM (NRC, 2001). Finally, DMI was limited to be less than the predicted DMI in NRC (2001), so that low quality feeds would not be overfed in the case of low feed prices.

Detailed information of all the constraints is shown in the Appendix 1. Three optimization strategies, iteLP, SQP and MINLP_DGO, use different approaches to deal with the nonlinearity existing in the energy and protein constraints as described below.

Optimization strategies

iteLP. Moraes et al. (2012) reported solving LP iteratively to deal with the nonlinearity in the NRC (2001). Formulating least-cost diets using LP can be written as:

$$\text{Min } Z = \sum_{j=1}^{m} c_j x_j$$

$$\text{Subject to } \sum_{j=1}^{m} a_{ij} x_j \geq b_i \text{ for } i = 1, 2, \ldots, n$$

where Z (\$) is the diet cost; c_j (\$/kg DM) is the feed price of feed j; x_j (kg DM) is the amount of feed j; a_{ij} is the coefficient for x_j in constraint i; b_i is the lower bound of constraint i. For example, if constraint i represents NE_M requirement, then b_i is the minimum NE_M requirement and a_{ij} are the NRC (2001) predicted amount of NE_M in feed j (Mcal/kg DM). To ensure that energy and protein requirements are met, the feed ingredients (a_{ij}) start at certain initial values, and then are updated according to the DMI at the solution. The iteration process is repeated until DMI and dietary concentrate percent at the solution are relatively constant (Moraes et al., 2012). However, we found that iterating based on DMI and dietary concentrate percent does not always result in a satisfactory solution depending on the feed ingredients. During the iteration process, two solutions may have very similar DMI and concentrate percentage but very different values of dietary TDN and RDP intake, leading to a large discrepancy between nutrient requirement and nutrient supply at the final solution. Therefore, the iteration was based on intake level and MCP production in this study. The algorithm stopped when the differences of intake level and MCP production between two iterations were both lower than 0.1%. In order to prevent infinite

iterations when intake level or MCP does not converge, the maximum number of iterations was set to be 1000.

SQP. Sequential quadratic programming allows nonlinear constraints, so the nutrient requirement constraints can be built according to NRC (2001) directly. The basic structure of an SQP problem is:

$$\text{Min } Z = \sum_{j=1}^{m} c_j x_j$$

$$\text{Subject to } g_i(\boldsymbol{x}) \leq 0, \text{ for } i = 1, 2, \ldots, n$$

where $\boldsymbol{x}$ is a vector of x_j and $g_i(x)$ is constraint i, which must be twice continuously differentiable with respect to all x_j in $\boldsymbol{x}$. However, there are several equations in NRC (2001) that result in either nondifferentiable or discrete constraints. For example, the calculation of feed energy values requires intake level, which is calculated as:

$$\text{IntakeLevel} = \begin{cases} 1, \text{ if TotalTDN} < 0.35\ \text{BW}^{0.75} \\ \frac{\text{TotalTDN}}{0.35\ \text{BW}^{0.75}}, \text{ if TotalTDN} \geq 0.35\ \text{BW}^{0.75} \end{cases} \quad [1]$$

where IntakeLevel (dimensionless) is the incremental intake above maintenance; TotalTDN (%) is dietary TDN percentage. Intake level is used to adjust the TDN value of feeds since feed intake above maintenance would decrease the nutrient digestibility (NRC, 2001). This equation is not differentiable at the point TotalTDN equal to $0.35\ \text{BW}^{0.75}$ and IntakeLevel equal to 1. Besides, the calculation of microbial crude protein (MCP, kg) production is discrete:

$$\text{MCP} = \min(0.13\ \text{TDN}_{\text{intake}}, 0.85\ \text{RDP}_{\text{intake}}) \quad [2]$$

where $\text{TDN}_{\text{intake}}$ (kg) is discounted TDN intake; $\text{RDP}_{\text{intake}}$ (kg) is RDP intake. These constraints present challenges to formulating diets with SQP, which will be discussed in the results and discussion section. Additionally, SQP algorithm converges to a local optimal, which could be far away from the global optimal solution of a non-convex nonlinear optimization problem.

MINLP_DGO. Another optimization strategy MINLP_DGO allows a mixture of continuous and binary deision variables. Note that MINLP includes a wide range of nonlinear optimization problems containing continuous and integer variables. Solving an MINLP problem usually involves multiple algorithms and techniques (Kronqvist et al., 2019). Several solvers, including Couenne (Burer, 2009), BARON (Tawarmalani and Sahinidis, 2013) and Gurobi (Gurobi Optimization, LLC, 2021), are able to find deterministic global solutions in MINLP problems. The basic structure of an MINLP problem is:

$$\text{Min } Z = \sum_{j=1}^{\text{m}} c_j x_j$$

$$\text{Subject to } g_i(\boldsymbol{x}, \boldsymbol{y}) \leq 0, \text{ for } i = 1, 2, \ldots, \text{n}$$

where $\boldsymbol{y}$ is a binary variable vector. Using binary variables enables the conversion of Eq. [1] and [2] into several constraints. For Eq. [1], the intake level calculation can be written into 3 equations:

$$1 - M \times (1 - y_1) \leq \text{IntakeLevel} \leq 1 + M \times (1 - y_1) \quad [3]$$

$$0.035\ \text{BW}^{0.75} - M \times y_1 \leq \text{TotalTDN} \leq 0.035\ \text{BW}^{0.75} + M \times (1 - y_1) \quad [4]$$

$$\frac{\text{TotalTDN}}{0.035\ \text{BW}^{0.75}} - M \times y_1 \leq \text{IntakeLevel} \leq \frac{\text{TotalTDN}}{0.035\ \text{BW}^{0.75}} + M \times y_1 \quad [5]$$

where M is a large positive number (suppose $M = 100000$) and y_1 is a binary variable. If y_1 is equal to 0, then Eq. [3] models an intake level greater than a very small number and smaller than a very large number, which makes Eq. [3] ineffective. Eq. [4] models a TotalTDN greater than $0.035\ \text{BW}^{0.75}$ and smaller than a large number, which is equivalent to TotalTDN greater than $0.035\ \text{BW}^{0.75}$. Eq. [3] models an intake level greater or equal to TotalTDN/$0.035\ \text{BW}^{0.75}$ and smaller than or equal to TotalTDN/$0.035\ \text{BW}^{0.75}$, which is equivalent to intake level equal to TotalTDN/$0.035\ \text{BW}^{0.75}$. Similarly, if y_1 is equal to 1, Eq. [5] is ineffective. Eq. [4] is equivalent

to TotalTDN smaller than 0.035 $BW^{0.75}$, and Eq. [3] is equivalent to intake level equal to 1. In summary, Eq. [3] to [5] together are equivalent to Eq. [1]. The same technique can be used for the conversion of Eq. [2]:

$$0.13\ TDN_{intake} - M \times y_2 \leq MCP \leq 0.13\ TDN_{intake} + M \times y_2 \quad [6]$$

$$0.85\ RDP_{intake} - M \times (1 - y_2) \leq MCP \leq 0.85\ RDP_{intake} + M \times (1 - y_2) \quad [7]$$

$$0.13\ TDN_{intake} - M \times y_2 \leq 0.85\ RDP_{intake} \leq 0.13\ TDN_{intake} + M \times (1 - y_2) \quad [8]$$

where y_2 is a binary variable. Similar as Eq. [3] to [5], if $0.13\ TDN_{intake} \geqslant 0.85\ RDP_{intake}$, $y_2 = 1$, $MCP = 0.85\ RDP_{intake}$; if $0.13\ TDN_{intake} < 0.85\ RDP_{intake}$, $y_2 = 0$, $MCP = 0.13\ TDN_{intake}$.

Simulation

A simulation study was conducted to compare the three optimization strategies, iteLP, SQP and MINLP_DGO. We simulated three animal groups: lactating cows, dry cows and heifers. The animal inputs needed to define the nutrient requirement constraints are summarized in Table 1. A total of 500 simulations were conducted by randomly selecting a set of feeds containing five concentrates and three forages from 100 feeds (details in Appendix 2) in the feed table provided by NRC (2001). Calcium phosphate (monobasic) was kept for all 500 sets of feeds to minimize excess mineral feeding. The 2020 annual average feed prices were taken from the Pennsylvania State University feed price list (https://extension.psu.edu/files/feed-price-lists). For each animal group, three least-cost diets were designed based on each set of the randomly selected feeds using iteLP, SQP and MINLP_DGO, respectively, which gave 4500 (3 × 3 × 500) diets in total.

Evaluation

To demonstrate the validity of each optimizer, all the formulated diets were evaluated with the NRC (2001) equations to examine whether all the nutrient requirements were truly met by the feed supply. The difference between requirement and supply was calculated for all the

nutrient constraints. In addition, diet cost and computation time for three optimizers were compared with an i7-5500U computer processor (2.40 GHz).

Software

All the simulation and computation were conducted in Python 3.7.4 (Van Rossum and Drake, 2009). The SciPy package (Virtanen et al., 2020) was used as solvers for iteLP and SQP. Gurobi (Gurobi Optimization, LLC, 2021) is free to academic users and can be easily implemented in Python, so it was used as the solver for MINLP_DGO in this study.

Results and Discussion

An example simulation

A set of feeds in one simulation is shown in Table 2. The diets formulated based on the feeds by iteLP, SQP and MINLP are shown in Table 3. For lactating and dry cows, the rations obtained by SQP and MINLP_DGO were the same, but the ones obtained by iteLP were more expensive. For heifers, the rations obtained by three optimizers were close.

Feasibility and nutrient balance

While formulating diets for lactating cows, there were 57 (11.4%) infeasible simulations for iteLP, 6 of which were infeasible because the SciPy package could not find a feasible solution in the first several iterations. The other 51 simulations were infeasible because the maximum number of iterations was reached before the convergence of intake level and MCP. In these cases, the value of intake level or MCP oscillated between two or several values and failed to converge during the iteration process (Figure 1), which highlights a flaw of iteLP. For MINLP_DGO, there were 21 simulations without feasible solutions. In order to investigate the reason of infeasibility, the 21 simulations were rerun after adding two dummy feed variables, including a “supper protein” feed with 100% of protein and a “supper energy” feed with 30 Mcal

of digestible energy. Both feeds were set to be very expensive (i.e., $100 per kg of DM), so that they would not be used when feeds can fulfill the protein and energy requirements. The appearance of them in the solution indicates a lack of protein or energy from feeds. The results showed that all 21 simulations were infeasible due to protein deficiency. The same 21 simulations were also infeasible for SQP and there were 24 additional infeasible simulations due to a failure to fulfill the protein requirement. These 24 simulations were feasible when using MINLP_DGO, which means SQP did not fully explore the feed potential in these cases. Optimization with SQP relies on the gradient of the objective function and constraints, but the MP constraint is not continuous due to the discrete choice between prediction of MCP based on energy or protein availability represented in Eq. [2]. The SciPy package calculates the gradient numerically instead of analytically, which makes fitting a discrete constraint into SQP possible. In the MP constraint, the MCP production is either limited by TDN intake or RDP intake, which creates two discrete value domains. In most cases, the optimum exists in one of the domains and is far away from the other, so SQP solver is able to search for the optimum within one domain without the influence from discreteness. However, sometimes when the optimum is close to the boundaries of two domains, SQP may not be able to find a proper solution based on the gradient due to the discreteness on the optimum direction. On the other hand, by including binary variables, MINLP_DGO is able to find the optimum through the branch and bound approach (Land and Doig, 1960), which is able to evaluate the suboptimal solutions in each domain and to find the best one (Taylor, 2009). Heuristically, MINLP_DGO will consider both TDN limited and RDP limited cases for MCP production and select the better solution. The requirement of NE_L did not result in any infeasible solutions for SQP, even though the NE_L constraint contained a nondifferentiable function (Eq. [1]). Since Intake Level represents the incremental intake above

maintenance, the Intake Level value of diets fulfilling the requirements of NE_M, NE_L and NE_G at the same time was always greater than 1, and the nondifferentiable point (Intake Level = 1) does not disrupt the solution. All the infeasible simulations for SQP and MINLP were also infeasible for iteLP. While formulating diets for dry cows and heifers, a feasible solution was obtained for all the simulations using SQP and MINLP_DGO, but there were 49 and 11 infeasible simulations for iteLP, respectively. For dry cows and heifers, the protein requirement did not cause infeasibility in SQP, probably due to much smaller nutrient requirement of dry cows and heifers. All the infeasible simulations were removed for the following analysis.

Boxplots of the difference between requirements and estimated nutrient delivery of the ration solutions for lactating cows from all feasible simulations are shown in Figure 2. Only NE_L and MP balance values are shown because the other constraints were linear and did not differ greatly between the three optimizers. The NE_L and MP balance values were positive for the solutions obtained by iteLP, SQP and MINLP_DGO in all feasible simulations, but the NE_L balance values were higher for iteLP, which suggests a tendency for rations formulated with iteLP to overfeed energy. Differences between the rations simulated for dry cows and heifers (Figure 3 and 4) by iteLP, SQP and MINLP_DGO were similar to those for lactating cows.

Ration cost

Average ration costs per animal obtained by iteLP, SQP and MINLP were \$4.78 (± 0.71), \$4.45 (± 0.65), \$4.44 (± 0.65) for lactating cows, \$2.39 (± 0.52), \$1.48 (± 0.26), \$1.48 (± 0.26) for dry cows, and \$0.98 (± 0.72), \$0.97 (± 0.15), \$0.91 (± 0.14) for heifers, respectively (Figure 2, 3 and 4). Ration costs were similar for SQP and MINLP_DGO, which indicated that the solution obtained through SQP was very close to the global optimum in ration optimization. However, the costs obtained by iteLP were greater, especially for dry cows. The iterations in

iteLP do not push the solution along the optimum direction, but blindly replaces the initial value with the solution from last iteration, therefore, the ration cost is only minimized within each iteration instead of the whole process and is likely to be greater than the one obtained by SQP or MINLP_DGO.

Computation time

The average computation time of iteLP, SQP and MINLP_DGO were 0.59 (± 1.87) s, 1.15 (± 0.62) s and 58.69 (± 68.45) s for lactating cows, 0.041 (± 0.070) s, 0.76 (± 0.37) s and 14.84 (± 39.09) s for dry cows, and 1.60 (± 2.90) s, 0.51 (± 0.19) s and 16.45(± 45.56) s for heifers, respectively (Figure 2, 3 and 4). The computation time of iteLP and SQP was much shorter than that of MINLP_DGO, especially when formulating diets for lactation cows. Since MINLP_DGO solves the problem involving integers, the resulting problem becomes computationally expensive. When the solver Gurobi solves MIMLP problems, the best bound and the suboptimal solution are updated throughout the computation. The best bound is the upper bound of the objective function value for a maximization problem (or the lower bound of a minimization problem), and the suboptimal solution is the best feasible solution found so far. By default, the computation stops when the gap between the two values decreases below 0.01%, but it may take hours to obtain such a solution. The computation time was limited within 3 min in this study. In total, 98, 21 and 33 simulations for lactating cows, dry cows and heifers exceeded the time limit (computation time equal to 3 min), respectively, but the gaps for them were all less than 0.1%, meaning the solution found was close enough to the true optimum.

Conclusions

Our study investigated various optimization approaches to design least-cost diets given nonlinear constraints, which provides a framework for future ration formulation when the

constraint equations are nonlinear. We considered the most important nutrient constraints based on NRC (2001), but other constraints, such as mineral requirements apart from calcium and phosphorus, vitamin requirements and feedstuff limitations, can be easily fitted in the nonlinear programming framework. In conclusion, iteLP had limited capability to formulate least-cost diets when nonlinearity existed in the constraints. Both SQP and MINLP_DGO were able to handle nonlinear constraints well, with SQP being faster but MINLP_DGO being more reliable. Thus, both nonlinear programming frameworks for least-cost ration formulation represent an advancement over previous linear programming techniques. Either can be used to find the least-cost ration for a given set of feed and nutrient constraints within ration formulation software or whole-farm simulation models. The current presentation based on the NRC (2001) will be integrated within a new whole-farm model, the Ruminant Farm Systems model (Kebreab, et al., 2019), to enable simulation of feed delivery, consumption, and production for multiple groups of animals over time.

Acknowledgements

Research was partially supported by the University of California, Davis Sesnon Endowed Chair program, and the USDA National Institute of Food and Agriculture Multistate Research Project NC-2040 (University of California–Davis).

References

Alqaisi, O., and E. Schlecht. 2021. Feeding models to optimize dairy feed rations in view of feed availability, feed prices and milk production scenarios. Sustainability 13:215.

Boggs, P. T., and J. W. Tolle. 1995. Sequential quadratic programming. Acta Numer. 4:1–51.

Boston, R., D. Fox, C. Sniffen, E. Janczewski, R. Munson, and W. Chalupa. 2000. The conversion of a scientific model describing dairy cow nutrition and production to an industry tool: The CPM-Dairy project. Pages 361–377 in Modeling Nutrition of Farm Animals. J. P. McNamara, J. France, and D. E. Beever, ed. CAB Int., Oxford, UK.

Bozic, M., J. Newton, C.S. Thraen, and B.W. Gould. 2012. Mean-reversion in income over feed cost margins: Evidence and implications for managing margin risk by US dairy producers. J. Dairy Sci. 95:7417–7428.

Burer, S. 2009. On the copositive representation of binary and continuous nonconvex quadratic programs. Math. Program. 120:479–495.

Chandler, P.T., and H.W. Walker. 1972. Generation of nutrient specifications for dairy cattle for computerized least cost ration formulation. J. Dairy Sci. 55:1741–1749.

Fox, D.G., L.O. Tedeschi, T.P. Tylutki, J.B. Russell, M.E. Van Amburgh, L.E. Chase, A.N. Pell, and T.R. Overton. 2004. The Cornell Net Carbohydrate and Protein System model for evaluating herd nutrition and nutrient excretion. Anim. Feed Sci. Technol. 112:29–78.

France, J., and E. Kebreab. 2008. Mathematical modelling in animal nutrition. Page 574. CAB Int., Wallingford, UK.

Gurobi Optimization, LLC, 2021, Gurobi Optimizer Reference Manual, http://www.gurobi.com.

Kebreab, E., K.F. Reed, V.E. Cabrera, P.A. Vadas, G. Thoma, and J.M. Tricarico. 2019. A new modeling environment for integrated dairy system management. Anim. Front. 9:25–32.

Kronqvist, J., D.E. Bernal, A. Lundell, and I.E. Grossmann. 2019. A review and comparison of solvers for convex MINLP. Eng. Optim. 20:397–455.

Land, A.H., and A.G. Doig. 1960. An automatic method of solving discrete programming problems. Econometrica 28: 497–520.

Moraes, L.E., J.E. Wilen, P.H. Robinson, and J.G. Fadel,.2012. A linear programming model to optimize diets in environmental policy scenarios. J. Dairy Sci. 95:1267–1282.

NRC. 2001. Nutrient Requirements of Dairy Cattle. 7th ed. National Academy Press, Washington, DC.

O'Connor, J.D., C.J. Sniffen, D.G. Fox, and R.A. Milligan. 1989. Least cost dairy cattle ration formulation model based on the degradable protein system. J. Dairy Sci. 72:2733–2745.

Penn State Feed Price List. 2020. Pennsylvania State University Cooperative Extension. Accessed Jan. 15, 2021. https://extension.psu.edu/files/feed-price-lists.

Qu, J., T.C. Hsiao, E.J. DePeters, D. Zaccaria, R.L. Snyder, and J. G. Fadel. 2019. A goal programming approach for balancing diet costs and feed water use under different environmental conditions. J. Dairy Sci. 102:11504–11522.

Rotz, C.A., M.S. Corson, D.S. Chianese, F. Montes, S.D. Hafner, and C.U. Coiner. 2016. The integrated farm systems model: Reference manual. USDA Agricultural Research Service: University Park, PA.

Tawarmalani, M., and N.V. Sahinidis. 2013. Convexification and global optimization in continuous and mixed-integer nonlinear programming: theory, algorithms, software, and applications (Vol. 65). Springer Science & Business Media.

Taylor, B. 2009. Introduction to management science. Module C. Integer programming: The branch and bound method. Pearson.

Tozer, P.R. 2000. Least-cost ration formulations for Holstein dairy heifers by using linear and stochastic programming. J. Dairy Sci. 83:443–451.

Van Rossum, G., and F. L. Drake. 2009. Python 3 reference manual. CreateSpace, Scotts Valley, CA.

Veltman, K., C.A. Rotz, L.E. Chase, J. Cooper, P. Ingraham, R.C. Izaurralde, C.D. Jones, R. Gaillard, R.A. Larson, M. Ruark, W. Salas, G. Thoma, and O. Jolliet. 2018. A quantitative assessment of Beneficial Management Practices to reduce carbon and reactive nitrogen footprints and phosphorus losses on dairy farms in the US Great Lakes regin. Ag. Systems. 166:10-25.

Virtanen, P., R. Gommers, T. E. Oliphant, M. Haberland, T. Reddy, D. Cournapeau, E. Burovski, P. Peterson, W. Weckesser, J. Bright, and S. J. van der Walt. 2020. SciPy 1.0: Fundamental algorithms for scientific computing in Python. Nat. Methods 17:261–272.

Tables and Figures

Table 1. Animal attributes of the lactating cows, dry cows and heifers for the simulation study

	Latating cows	Dry cows	Heifers
Body weight, kg	650	720	300
Parity	2	3	0
Milk production, kg	35	-	-
Milk protein, %	3.0	-	-
Milk fat, %	3.5	-	-
Days in milk, d	100	-	-
Days of pregnancy, d	0	260	0
Age, month	-	-	9.5
Calving interval, d	370	370	370

Table 2. Chemical compositions (% of DM) and price ($/kg of DM) of an example feed set

Feed	CP	EE	NDF	ADF	Ca	P	TDN*	Price
Almond hulls	6.5	2.9	36.8	28.7	0.28	0.13	58.36	0.16
Canola meal	37.8	5.4	29.8	20.5	0.75	1.10	69.88	0.31
Steam flaked corn	9.4	4.2	9.5	3.4	0.04	0.30	91.67	0.18
Corn silage	8.8	3.2	45.0	28.1	0.28	0.26	68.82	0.18
Cotton seed	23.5	19.3	50.3	40.1	0.17	0.60	77.22	0.26
Grass hay	13.3	2.5	57.7	36.9	0.66	0.29	59.72	0.24
Legume hay	20.2	2.1	39.6	31.2	1.52	0.26	58.95	0.31
Soybean meal	46.3	8.1	21.7	10.4	0.36	0.66	88.53	0.37
Calcium phosphate monobasic	0	0	0	0	16.40	21.60	0	0.96

*TDN are the standard values from the NRC (2001) table.

Table 3. Feed ration designed by iterative linear programming (iteLP), sequential quadratic programming (SQP) and mixed-integer nonlinear programming based deterministic global optimization (MINLP_DGO) given an example feed set.

	Lactating cow			Dry cow			Heifer		
	iteLP	SQP	MINLP_ DGO	iteLP	SQP	MINLP_ DGO	iteLP	SQP	MINLP_ DGO
Ingredient (% of DM)									
Almond hulls	0	0	0	7.72	0	0	0	0	0
Canola meal	0	0	0	0	0	0	0	0	0
Steam flaked corn	10.42	7.73	7.73	5.60	3.23	3.23	2.09	2.30	2.03
Corn silage	10.02	8.42	8.42	0	3.01	3.01	1.81	2.06	1.90
Cotton seed	0	0	0	0	0	0	0	0	0
Grass hay	0	0	0	0	0	0	0	0	0
Legume hay	0	0	0	0	0	0	0	0	0
Soybean meal	2.99	3.49	3.49	0.54	0.73	0.73	0.48	0.43	0.48
Calcium phosphate monobasic	0.30	0.31	0.31	0.10	0.17	0.17	0.09	0.09	0.09
Chemical composition (% of DM)									
CP	13.67	15.45	13.67	9.15	12.69	12.69	12.89	12.19	12.86
NDF	25.90	26.47	25.90	25.00	25.51	25.51	25.00	25.37	25.58
ADF	14.67	15.00	14.67	17.64	14.46	14.46	14.09	14.38	14.50
Fat	4.21	4.39	4.21	3.60	4.08	4.08	4.12	4.04	4.10
Ca	0.39	0.45	0.39	0.30	0.56	0.56	0.52	0.48	0.52
P	0.60	0.68	0.60	0.37	0.83	0.83	0.77	0.72	0.77
Diet cost ($/animal)									
	5.08	4.96	5.08	2.54	1.56	1.56	0.97	1.03	0.97

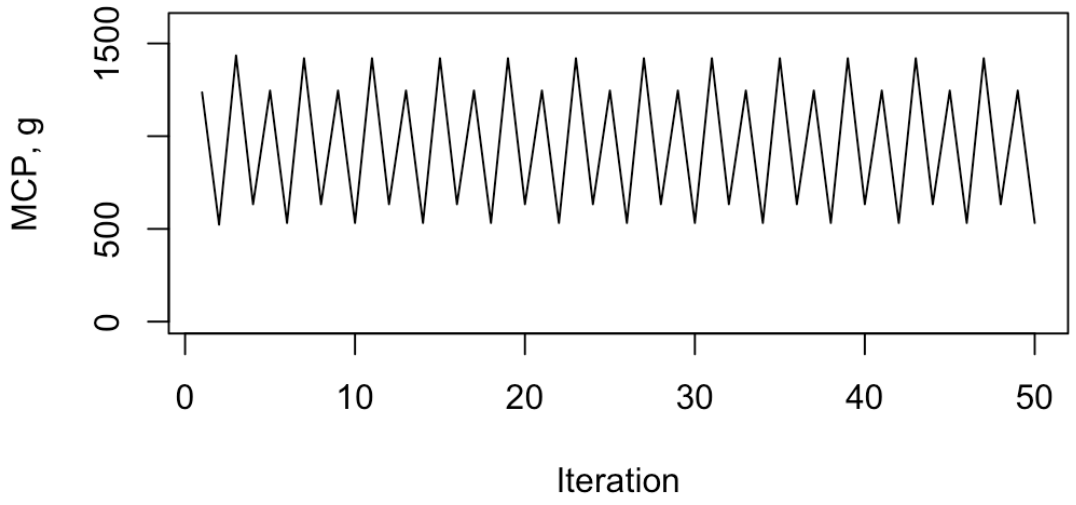

Figure 1. An example of microbial crude protein (MCP) production oscillating between several values and failing to converge when using iterative linear programming (iteLP) to design feed formulation for lactating cows (using corn grain, cotton seed meal, corn distillers, corn cob, canola meal, mixed grass-legume hay, alfalfa meal, mixed grass-legume silage and calcium phosphate monobasic). formulation for lactating cows (using corn grain, cotton seed meal, corn distillers, corn cob, canola meal, mixed grass-legume hay, alfalfa meal, mixed grass-legume silage and calcium phosphate monobasic).

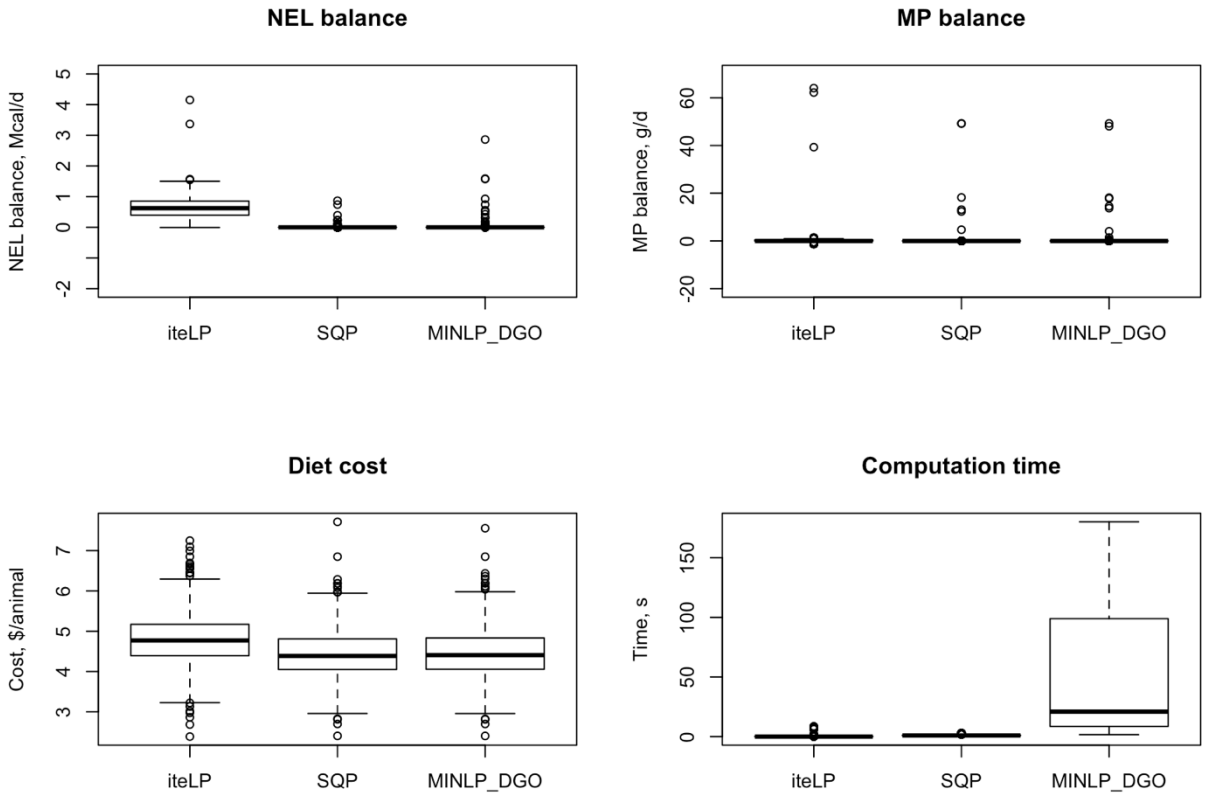

Figure 2. NE_L balance (diet NE_L supply – animal NE_L requirement), MP balance (diet MP supply – animal MP requirement), diet cost and computation time of 500 simulations for lactating cows based on three optimizers. iteLP = Iterative linear programming, SQP = Sequential quadratic programming, MINLP_DGO = mixed-integer nonlinear programming based deterministic global optimization.

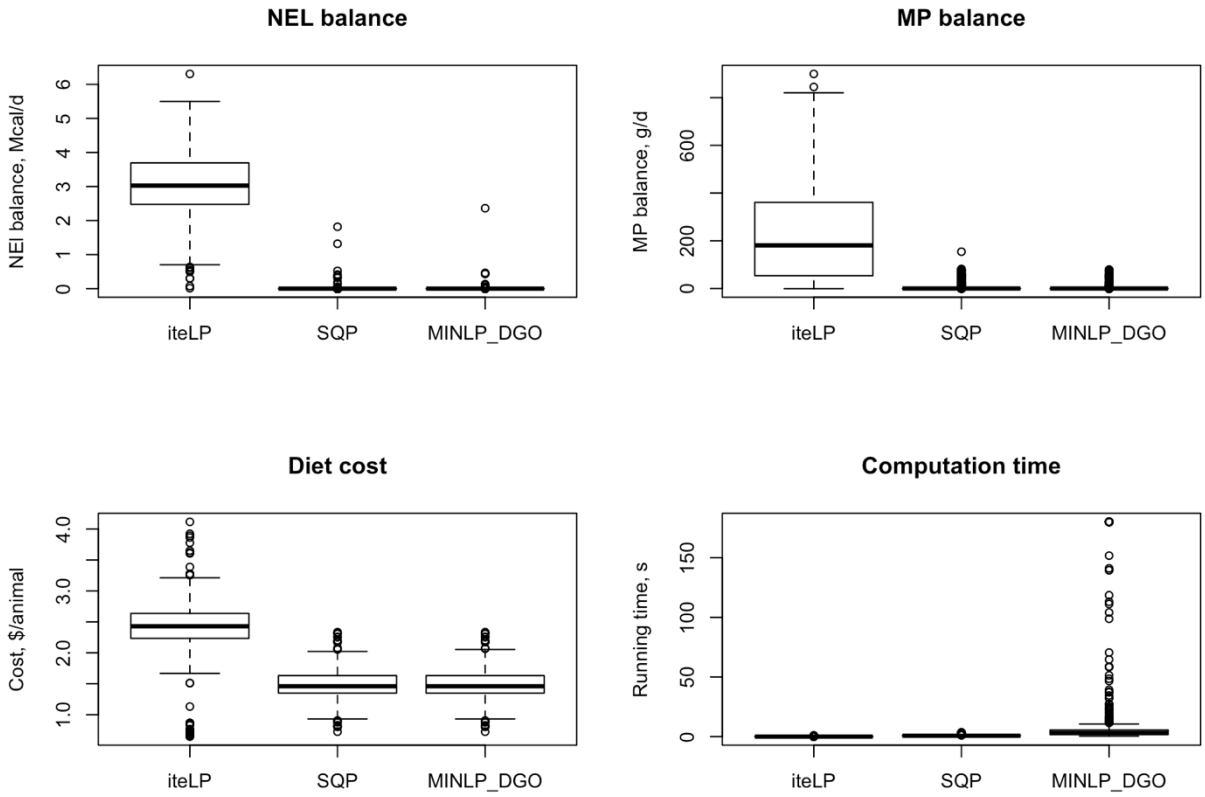

Figure 3. NE_L balance (diet NE_L supply – animal NE_L requirement), MP balance (diet MP supply – animal MP requirement), diet cost and computation time of 500 simulations for dry cows. iteLP = Iterative linear programming, SQP = Sequential quadratic programming, MINLP_DGO = mixed-integer nonlinear programming based deterministic global optimization.

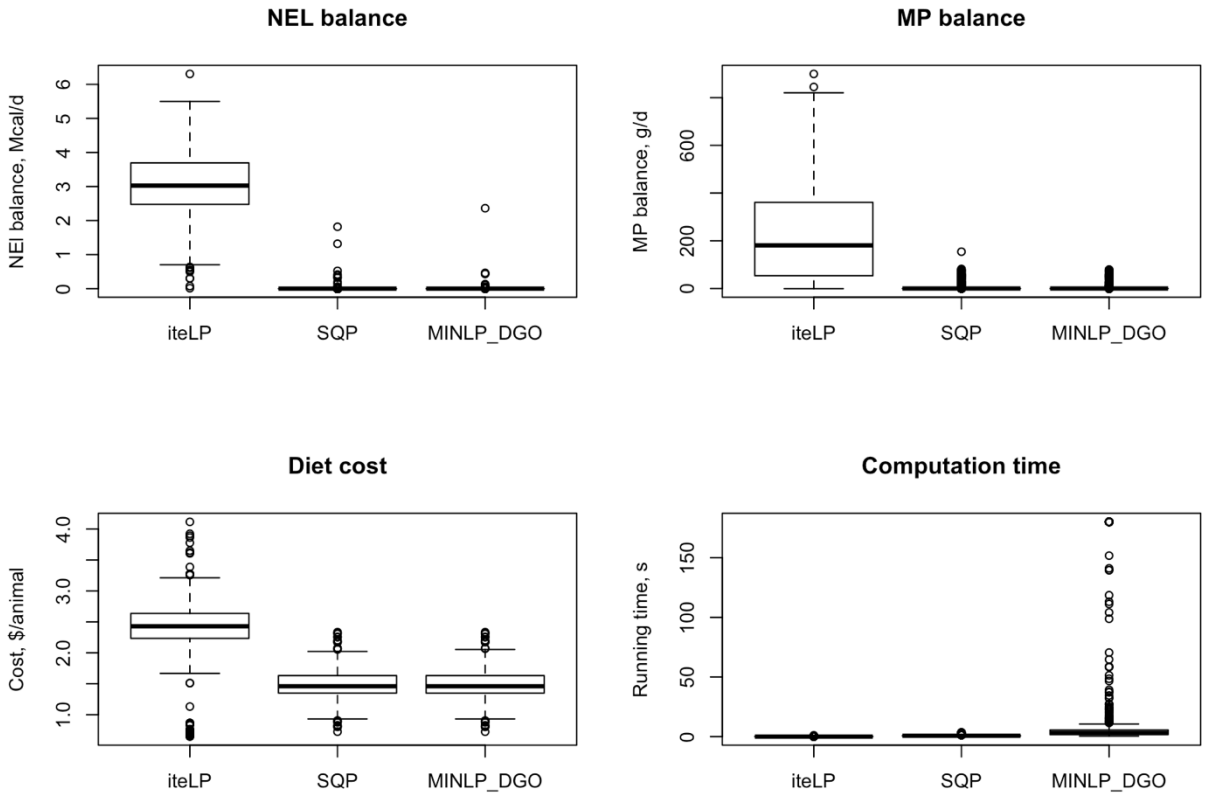

Figure 4. NE_L balance (diet NE_L supply – animal NE_L requirement), MP balance (diet MP supply – animal MP requirement), diet cost and computation time of 500 simulations for heifers. iteLP = Iterative linear programming, SQP = Sequential quadratic programming, MINLP_DGO = mixed-integer nonlinear programming based deterministic global optimization.

Appendix 1

The equations in the NRC (2001) used to calculate nutrient requirements of animals and nutrient supply from feeds on a daily basis is shown below. Nutrient requirements include net energy requirements for maintenance (NE_M), lactation (NE_L) and growth (NE_G), metabolizable protein (MP) requirement, calcium and phosphorus requirements. Additional constraints included a fat constraint of less than 7% of diet DM, an NDF constraint of greater than 25 % and less than 40 % of diet DM, a constraint of forage NDF greater than 19% of diet DM, and DMI less than the predicted DMI in NRC (2001). Equations are shared by lactating cows, dry cows and heifer or indicated otherwise.

NE_M requirement

Net energy requirements for maintenance requirement includes two parts: maintenance requirement and activity requirement.

$$\text{CBW} = \text{MW} \times 0.06275 \quad [A.1]$$

where CBW = Calf birth weight (kg); MW = Mature body weight (kg), 682 kg for Holstein cow by default.

$$\text{CW} = \begin{cases} (18 + (\text{DOP} - 190) \times 0.665) \times \left(\frac{\text{CBW}}{45}\right), \text{ if DOP} > 190 \\ 0, \text{ otherwise} \end{cases} \quad [A.2]$$

where CW = Conceptus weight (kg); DOP = Days of pregnancy.

$$\text{NEmaint} = \begin{cases} 0.08 \times (\text{BW} - \text{CW})^{0.75}, \text{ for cows} \\ ((\text{SBW} - \text{CW})^{0.75}) \times \left(0.086 \times \text{COMP} + 0.0007 \times (20 - \text{PrevTemp})\right), \text{ for heifers} \end{cases} \quad [A.3]$$

where NEmaint = Maintenance requirement, Mcal; SBW = shrunk body weight, kg; COMP = 0.8 + (CS9 – 1) × 0.05; CS9 = Body condition score based on a 1 to 9 system; PrevTemp = Average ambient temperature for last month, °C.

$$NEa1 = \begin{cases} c_G \times BW, \text{ if Housing} = \text{Grazing} \\ 0, \text{ otherwise} \end{cases} \quad [A.4]$$

where NEa1 = Net energy for activity requirement caused by grazing system, Mcal; c_G = Grazing coefficient (0.0012 for cows and 0.0025 for heifers).

$$NEa2 = \begin{cases} 0.006 \times BW, \text{ if Topography} = \text{Hilly} \\ 0, \text{ otherwise} \end{cases} \quad [A.5]$$

where NEa2 = Net energy for activity requirement caused by hilly topography, Mcal.

$$NEa = \text{Distance} \times 0.00045 \times BW + NEa1 + NEa2 \quad [A.6]$$

where NEa = Total net energy for activity requirement, Mcal; Distance = Daily walking distance, km.

$$NEMNE_M = NEmaint + NEa \quad [A.7]$$

where NE_M = Net energy requirements for maintenance, Mcal.

NE_G requirement

$$MSBW = 0.96 \times MW \quad [A.8]$$

where MSBW = Mature shrunk body weight, kg.

$$SBW = 0.96 \times BW \quad [A.9]$$

where SBW = Shrunk body weight, kg.

$$EBW = 0.891 \times SBW \quad [A.10]$$

where EBW = Empty body weight, kg.

$$EQSBW = (SBW - CW) \times \frac{478}{MSBW} \quad [A.11]$$

where EQSBW = Equivalent shrunk body weight, kg.

$$ADG = \begin{cases} \frac{(0.92 - 0.82) \times MSBW}{CI}, \text{ if Parity} = 1 \\ \frac{(1 - 0.92) \times MSBW}{CI}, \text{ if Parity} = 2 \\ 0, \text{ if Parity} > 2 \\ \frac{(0.55 \times MSBW - SBW)}{(Age1stBred - Age) \times 30.4}, \text{ for heifers before breeding} \\ \frac{(0.82 \times MSBW - SBW)}{(Age1st - Age) \times 30.4}, \text{ for heifers after breeding} \end{cases} \quad [A.12]$$

where ADG = Average daily gain, kg; CI = Calving interval, d; Age1stBred = First breeding age, month; Age = Current age, month; Age1st = First calving age, month.

$$EQEBG = 0.956 \times ADG \quad [A.13]$$

where EQEBG = Equivalent empty weight gain, kg.

$$EQEBW = 0.891 \times EQSBW \quad [A.14]$$

where EBW = Equivalent shrunk body weight, kg.

$$NE_G = 0.0635 \times EQEBW^{0.75} \times EQEBG^{1.097} \quad [A.15]$$

where NE_G = Net energy for growth requirement, Mcal.

NE_L requirement

Net energy requirements for lactation requirement includes two parts: lactation requirement and pregnancy requirement.

$$Milken = 0.0929 \times Fat\_Milk + \frac{0.0547}{0.93} \times TP\_Milk + 0.0395 \times Lactose\_Milk \quad [A.16]$$

where Milken = Milk energy, Mcal/kg of milk production; Fat_Milk = Milk fat proportion; TP_Milk = Milk true protein proportion; Lactose_Milk = Milk lactose proportion.

$$NElact = Milken \times Milk \quad [A.17]$$

where NElact = Net energy requirement for lactation, Mcal.

$$MEpreg = \begin{cases} (2 \times 0.00159 \times DOP - 0.0352) \times \frac{CBW}{45 \times 0.14}, \text{ if DOP} > 190 \\ 0, \text{ otherwise} \end{cases} \quad [A.18]$$

where MEpreg = Metabolizable energy requirement for pregnancy, Mcal.

$$NEpreg = MEpreg \times 0.64 \quad [A.19]$$

where NEpreg = Net energy requirement for pregnancy, Mcal.

$$NE_L = NElact + NEpreg \quad [A.20]$$

where NE_L = Net energy for lactation requirement, Mcal.

Protein requirements

Protein requirement is divided into 4 components: maintenance, growth, pregnancy and lactation (all in metabolizable protein, g).

$$MPm = 0.3 \times (BW - CW)^{0.6} + 4.1 \times (BW - CW)^{0.5} + (30 \times DMI - 0.125 \times MPbact) + 7.045 \times DMI \quad [A.21]$$

where MPm = Metabolizable protein requirement for maintenance, g; MPbact = Bacteria metabolizable protein production, g.

$$NPg = \begin{cases} 0, \text{ if } ADG = 0 \\ ADG \times (268 - 29.4 \times \frac{NEg}{ADG}) \end{cases} \quad [A.22]$$

where NPg = Net protein requirement for growth, g.

$$EffMP\_NPg = \begin{cases} \frac{(83.4 - 0.114 \times EQSBW)}{100}, \text{ if } EQSBW \leq 478 \\ 0.28908, \text{ otherwise} \end{cases} \quad [A.23]$$

where EffMP_NPg = Efficiency of converting metabolizable protein to net protein.

$$MPg = \frac{NPg}{EffMP\_NPg} \quad [A.24]$$

where MPg = Metabolizable protein requirement for growth, g.

$$MPpreg = \begin{cases} (0.69 \times DOP - 69.2) \times \frac{CBW}{45 \times 0.33}, \text{ if } DOP > 190 \\ 0, \text{ otherwise} \end{cases} \quad [A.25]$$

where MPpreg = Metabolizable protein requirement for pregnancy, g.

$$MPlact = Milk \times \frac{TP_{Milk}}{100} \times \frac{1000}{0.67} \quad [A.26]$$

where MPlact = Metabolizable protein requirement for lactation, g.

$$MPreq = MPm + MPg + MPpreg + MPlact \quad [A.27]$$

Calcium requirement

Calcium requirement is divided into 4 components: maintenance, growth, pregnancy and lactation (all in g).

$$Ca_{main} = \begin{cases} 0.031 \times BW + 0.08 \times \frac{BW}{100}, \text{ if } DOP > 0 \\ 0.0154 \times BW + 0.08 \times \frac{BW}{100}, \text{ if } DOP = 0 \end{cases} \quad [A.28]$$

where Ca_{main} = Maintenance calcium requirement, g.

$$Ca_{growth} = 9.83 \times MW^{0.22} \times BW^{-0.22} \times \frac{ADG}{0.96} \quad [A.29]$$

where Ca_{growth} = Calcium growth requirement, g.

$$Ca_{preg} = \begin{cases} 0.02456 \times \exp\left((0.05581 - 0.00007 \times DOP) \times DOP\right) - 0.02456 \times \\ \exp\left(\left(0.05581 - 0.00007 \times (DOP - 1)\right) \times (DOP - 1)\right), \text{ if } DOP > 190 \\ 0, \text{ if } DOP \leq 190 \end{cases} \quad [A.30]$$

where Ca_{preg} = Calcium pregnancy requirement, g; DOP = Days of pregnancy.

$$Ca_{lact} = 1.22 \times Milk \quad [A.31]$$

where Ca_{lact} = Calcium lactation requirement, g; Milk = Milk production, kg.

$$Ca_{req} = Ca_{main} + Ca_{growth} + Ca_{preg} + Ca_{lact} \quad [A.32]$$

where Ca_{req} = Total calcium requirement, g.

Phosphorus requirement

Phosphorus requirement is divided into 4 components: maintenance, growth, pregnancy and lactation (all in g).

$$P_{main} = \begin{cases} DMI + 0.002 \times BW, \text{ for lactating cows and dry cows} \\ 0.8 \times DMI + 0.002 \times BW, \text{ for heifers} \end{cases} \quad [A.33]$$

where P_{main} = Phosphorus maintenance requirement, g.

$$P_{growth} = \left(1.2 + 4.635 \times MW^{0.22} \times BW^{-0.22}\right) \times \frac{ADG}{0.96} \quad [A.34]$$

where P_{growth} = Phosphorus growth requirement, g.

$$Ppreg = \begin{cases} 0.02743 \times \exp\left((0.05527 - 0.000075 \times DOP) \times DOP\right) - \\ 0.02743 \times \exp\left(\left(0.05527 - 0.000075 \times (DOP - 1)\right) \times (DOP - 1)\right), \text{ if } DOP > 190 \\ 0, \text{ if } DOP \leq 190 \end{cases} \quad [A.35]$$

where P_{preg} = Phosphorus pregnancy requirement, g.

$$P_{lact} = 0.9 \times Milk \quad [A.36]$$

where P_{lact} = Phosphorus lactation requirement, g.

$$P_{req} = P_{main} + P_{growth} + P_{preg} + P_{lact} \quad [A.37]$$

where P_{req} = Total phosphorus requirement, g.

Dry matter intake estimation

Dry matter intake was estimated for lactating cow and dry cow, but not for heifers.

$$FCM = (0.4 \times Milk) + (15 \times Fat\_Milk \times \frac{Milk}{100}) \quad [A.38]$$

where FCM = Fat corrected milk, kg.

$$DMIest = \begin{cases} (0.372 \times FCM + 0.0968 \times BW^{0.75}) \times (1 - \exp\left(-0.192 \times (WOL + 3.67)\right), \text{ for lactating cows} \\ \frac{\left(1.97 - 0.75 \times \exp\left(0.16 \times (DOP - 280)\right)\right)}{100} \times BW, \text{ for dry cows} \end{cases} \quad [A.39]$$

where DMIest = Dry matter intake estimation, kg; WOL = Week of lactation, which is the integer part of days in milk (DIM) divided by 7; DOP = Days of pregnancy.

Energy supply

Energy supply from the feed include NEm, NEl and NEg. NEm provides energy for maintenance and activity requirement; NEl provides energy for lactation and pregnancy; NEg

provides energy for growth. Values of NEl are corrected based on the intake level, but NEm and NEg are not affected by the intake according to NRC (2001).

$$\text{TotalTDN} = \sum_i \text{Feed}_i \times \frac{\text{TDN}_i}{100} \quad [A.40]$$

TotalTDN = Dietary TDN content, kg; Feed_i = The amount of feed i in the diet, kg; TDN_i = standard TDN value of feed i in NRC (2001).

$$\text{TDNconc} = \frac{\text{TotalTDN}}{\text{DMI}} \times 100 \quad [A.41]$$

where TDNconc = TDN concentration, %.

$$\text{IntakeLevel} = \begin{cases} 1, \text{ if TotalTDN} < 0.035 \times \text{BW}^{0.75} \\ \frac{\text{TotalTDN}}{0.035 \times \text{BW}^{0.75}}, \text{ otherwise} \end{cases} \quad [A.42]$$

where IntakeLevel = is the incremental intake above maintenance, dimensionless.

$$\text{Discount} = \begin{cases} 1, \text{ if TDNconc} < 60 \\ \frac{(\text{TDNconc} - (0.18 \times \text{TDNconc} - 10.3) \times (\text{IntakeLevel} - 1))}{\text{TDNconc}}, \text{ otherwise} \end{cases} \quad [A.43]$$

where Discount = TDN discount, TDN digestibility decrease caused by DMI and TDNconc.

$$\text{TDNact}_i = \text{TDN}_i \times \text{Discount} \quad [A.44]$$

where TDNact_i = Actual TDN content of feed i, %; TDN_i = Standard TDN content of feed i, %.

$$\text{DEact}_i = \text{DE}_i \times \text{Discount} \quad [A.45]$$

where DEact_i = Actual digestible energy of feed i, Mcal/kg; DE_i = Standard DE feed i in NRC (2001), Mcal/kg.

$$\text{MEact}_i = \begin{cases} 1.01 \times \text{DEact}_i - 0.45 + 0.0046 \times (\text{EE}_i - 3), \text{ if feed type is not fat and} \\ \text{fat content} \geq 3\%; \\ 1.01 \times \text{DEact}_i - 0.45, \text{ if feed type is not fat and fat content} \leq 3\%; \\ \text{DE}_i, \text{ if feed type is fat} \end{cases} \quad [A.46]$$

where MEact_i = Corrected metabolizable energy of feed i, Mcal/kg; EE_i = Fat content of feed i, %.

$$NElact_i = \begin{cases} 0.703 \times MEact_i - 0.19 + \frac{0.097 \times MEact_i + 0.19}{97} \times (EE_i - 3), \text{ if feed} \\ \text{type is not fat and fat content} \geq 3\%; \\ 0.703 \times MEact_i - 0.19, \text{ if feed type is not fat and fat content} \leq 3\%; \\ DEact_i \times 0.8, \text{ if feed type is fat} \end{cases} \quad [A.47]$$

where $NElact_i$ = Corrected net energy for lactation of feed i, Mcal/kg.

$$NEm_i = \begin{cases} 1.37 \times ME_i - 0.138 \times ME_i^2 + 0.0105 \times ME_i^3 - 1.12, \text{ if feed type is not fat} \\ MEact_i \times 0.8, \text{ if feed type is fat} \end{cases} \quad [A.48]$$

where NEm_i = Net energy for maintenance of feed i, Mcal/kg; ME_i = Standard metabolizable energy of feed i in NRC (2001), Mcal/kg.

$$NEg_i = \begin{cases} 1.42 \times ME_i - 0.174 \times ME_i^2 + 0.0122 \times ME^3 - 1.65, \text{ if feed type is not fat} \\ ME_i \times 0.55, \text{ if feed type is fat} \end{cases} \quad [A.49]$$

where NEg_i = Net energy for growth of feed i, Mcal/kg.

Protein supply

Protein supply from the feed include 2 parts: digestible rumen undegradable protein (RUP) and digestible microbial crude protein (MCP), which is produced through rumen degradable protein (RDP). Production of MCP requires nitrogen source and energy source, so MCP is either nitrogen limited or energy limited.

$$Kp_i = \begin{cases} 2.904 + 1.375 \times \frac{DMI}{BW} \times 100 - 0.02 \times \text{PercentConc}, \text{ if feed}_i \text{ is concentrate} \\ 3.362 + 0.479 \times \frac{DMI}{BW} \times 100 - 0.017 \times NDF_i - 0.007 \times \text{PercentConc}, \text{ if feed}_i \text{ is forage} \\ 3.054 + 0.614 \times \frac{DMI}{BW} \times 100, \text{ if feed}_i \text{ is wet forage} \end{cases}$$

[A.50]

where Kp_i = Protein passage rate of feed i, %/h; PercentConc = Dietary concentrate percentage, % of DM; NDF_i = Neutral detergent fiber (ether extract) content of feed i, %.

$$RDP_i = \begin{cases} \frac{Kd_i}{Kd_i + Kp_i} \times \frac{N_{B_i}}{100} \times CP_i + \frac{N_{A_i}}{100} \times CP_i, \text{ if } Kp_i + Kd_i > 0 \\ 0, \text{ if } Kp_i + Kd_i \leq 0 \end{cases} \quad [A.51]$$

where RDP_i = Rumen degradable protein of feed i, % of DM; Kd_i = Protein degradation rate of feed i, %/h; N_{Ai} = Fraction A of protein of feed i, % of CP; N_{Bi} = Fraction B of protein of feed i, % of CP.

$$RUP_i = CP_i - RDP_i \quad [A.52]$$

where RUP_i = Rumen undegradable protein of feed i, % of DM.

$$MPbact = 0.64 \times \min (1000 \times 0.13 \times TDNact_{diet}, 1000 \times 0.85 \times RDP_{diet}) \quad [A.53]$$

where MPbact = Metabolizable bacterial protein production, g; $TDNact_{diet}$ = Dietary actual TDN, kg; RDP_{diet} = Dietary RDP, kg.

$$RUP_{diet} = \sum_i feed_i \times RUP_i \times dRUP_i \quad [A.54]$$

where RUP_{diet} = Dietary digestible RUP, kg; $feed_i$ = Dry matter intake of feed i, kg; $dRUP_i$ = RUP digestibility of feed i, % of RUP.

$$MP_{supply} = MPbact + RUP_{diet} + 0.4 \times 11.8 \times DMI \quad [A.55]$$

where MP_{supply} = Total metabolizable protein supply; $0.4 \times 11.8 \times DMI$ = Endogenous protein.

Mineral supply

$$Ca_{supply} = \sum_i feed_i \times Ca_i \times \frac{dCa_i}{100} \quad [A.56]$$

where Ca_{supply} = Dietary calcium supply, kg; Ca_i = Calcium content of feed i, % of DM; dCa_i = Calcium digestibility of feed i, % of Ca.

$$P_{supply} = \sum_i feed_i \times P_i \times \frac{dP_i}{100} \quad [A.57]$$

where P_{supply} = Dietary phosphorus supply, kg; P_i = Phosphorus content of feed i, % of DM; dP_i = Phosphorus digestibility of feed i, % of P.

Appendix 2

Table A2.1. Feeds from NRC (2001) used in 500 simulations

Entry[1]	Feed	Description	Type[2]	Price[3]
1	Alfalfa	Meal, 17% CP	Forage	0.32
2	Almond	Hulls	Conc	0.16
3	Apple	Pomace, wet	Conc	0.24
4	Bakery byproduct	Byproduct meal	Conc	0.15
5	Bakery byproduct	Bread, waste	Conc	0.15
6	Bakery byproduct	Cereal byproduct	Conc	0.15
7	Bakery byproduct	Cookie byproduct	Conc	0.15
8	Barley	Grain, rolled	Conc	0.18
9	Barley	Malt sprouts	Conc	0.18
10	Barley	Silage, headed	Forage	0.18
11	Beet, sugar	Pulp dried	Conc	0.27
12	Bermudagrass	Coastal, hay, early head	Forage	0.16
13	Bermudagrass	Tifton-85, hay, 3-4wk growth	Forage	0.16
14	Blood	Meal, ring dried	Conc	0.86
15	Blood	Meal, batch dried	Conc	0.86
16	Brewers grains	Dried	Conc	0.23
17	Brewers grains	Wet	Conc	0.23
18	Canola	Seed	Conc	0.31
19	Canola	Meal, mech. Extracted	Conc	0.31
20	Chocolate	Byproduct	Conc	0.18
21	Citrus	Pulp dried	Conc	0.03
22	Corn, yellow	Cobs	Conc	0.18
23	Corn, yellow	Distillers grains with solubles, dried	Conc	0.23
24	Corn, yellow	Gluten feed, dried	Conc	0.19
25	Corn, yellow	Gluten meal, dried	Conc	0.57
26	Corn, yellow	Grain, cracked, dry	Conc	0.18
27	Corn, yellow	Grain, ground, dry	Conc	0.18
28	Corn, yellow	Grain, steam-flaked	Conc	0.18
29	Corn, yellow	Grain, rolled, high moisture	Conc	0.18
30	Corn, yellow	Grain, ground, high moisture	Conc	0.18
31	Corn, yellow	Grain and cob, dry, ground	Conc	0.18
32	Corn, yellow	Grain and cob, high moisture, ground	Conc	0.18
33	Corn, yellow	Hominy	Conc	0.18
34	Corn, yellow	Silage, immature <25% DM	Forage	0.18
35	Corn, yellow	Silage, normal 32-38% DM	Forage	0.18
36	Corn, yellow	Silage, mature >40% DM	Forage	0.18
37	Cotton seed	Whole seeds with lint	Conc	0.26
39	Cotton seed	Meal, solvent, 41% CP	Conc	0.36
43	Fats and oils	Tallow	Fat	0.94
45	Feathers	Hydrolyzed meal	Conc	0.38

49	Grasses, cool season	Pasture, intensively managed	Forage	0.21
50	Grasses, cool season	Hay, all samples	Forage	0.24
51	Grasses, cool season	Hay, immature <55% NDF	Forage	0.24
52	Grasses, cool season	Hay, mid maturity 55-60% NDF	Forage	0.24
53	Grasses, cool season	Hay, mature >60% NDF	Forage	0.24
54	Grasses, cool season	Silage, all samples	Forage	0.24
55	Grasses, cool season	Silage, immature <55% NDF	Forage	0.24
56	Grasses, cool season	Silage, mid maturity 55-60% NDF	Forage	0.24
57	Grasses, cool season	Silage, mature >60% NDF	Forage	0.24
58	Grass-legume mixtures pr. gr. (17-22% hcel.)	Hay, immature <51% NDF	Forage	0.24
59	Grass-legume mixtures pr. gr. (17-22% hcel.)	Hay, mid maturity 51-57% NDF	Forage	0.24
60	Grass-legume mixtures pr. gr. (17-22% hcel.)	Hay, mature >57% NDF	Forage	0.24
61	Grass-legume mixtures pr. gr. (17-22% hcel.)	Silage, immature <51% NDF	Forage	0.24
62	grass-legume mixtures pr. gr. (17-22% hcel.)	Silage, mid maturity 51-57% NDF	Forage	0.24
63	Grass-legume mixtures pr. gr. (17-22% hcel.)	Silage, mature >57% NDF	Forage	0.24
64	Mixed grass-legume (12-15% hcel.)	Hay, immature <47% NDF	Forage	0.26
65	Mixed grass-legume (12-15% hcel.)	Hay, mid maturity 47-53% NDF	Forage	0.26
66	Mixed grass-legume (12-15% hcel.)	Hay, mature >53% NDF	Forage	0.26
67	Mixed grass-legume (12-15% hcel.)	Silage, immature <47% NDF	Forage	0.26
68	Mixed grass-legume (12-15% hcel.)	Silage, mid maturity 47-53% NDF	Forage	0.26
69	Mixed grass-legume (12-15% hcel.)	Silage, mature >53% NDF	Forage	0.26
70	Grass-legume mixtures pr. lg. (10-13% hcel.)	Hay, immature <44% NDF	Forage	0.24
71	Grass-legume mixtures pr. lg. (10-13% hcel.)	Hay, mid maturity 44-50% NDF	Forage	0.24
72	Grass-legume mixtures pr. lg. (10-13% hcel.)	Hay, mature >50% NDF	Forage	0.24
73	Grass-legume mixtures pr. lg. (10-13% hcel.)	Silage, immature <44% NDF	Forage	0.24
74	Grass-legume mixtures pr. lg. (10-13% hcel.)	Silage, mid maturity 44-50% NDF	Forage	0.24
75	Grass-legume mixtures pr. lg. (10-13% hcel.)	Silage, mid maturity >50% NDF	Forage	0.24

76	Legumes, forage	Pasture, intensively managed	Forage	0.23
77	Legumes, forage	Hay, all samples	Forage	0.31
78	Legumes, forage	Hay, immature <40% NDF	Forage	0.31
79	Legumes, forage	Hay, mid maturity 40-46% NDF	Forage	0.31
80	Legumes, forage	Hay, mature >46% NDF	Forage	0.31
81	Legumes, forage	Silage, all samples	Forage	0.31
82	Legumes, forage	Silage, immature <40% NDF	Forage	0.31
83	Legumes, forage	Silage, mid maturity 40-46% NDF	Forage	0.31
84	Legumes, forage	Silage, mature >46% NDF	Forage	0.31
85	Linseed (flax)	Meal, solvent	Conc	0.35
88	Molasses	Beet sugar	Conc	0.25
89	Molasses	Sugarcane	Conc	0.25
90	Oats	Grain, rolled	Conc	0.22
91	Oats	Hay, headed	Forage	0.12
92	Oats	Silage, headed	Forage	0.12
98	Sorghum, grain type	Grain, dry rolled	Conc	0.14
99	Sorghum, grain type	Grain, steam-flaked	Conc	0.14
100	Sorghum, grain type	Silage	Forage	0.26
101	Sorghum, sudan type	Hay	Forage	0.21
102	Sorghum, sudan type	Silage	Forage	0.26
104	Soybean	Meal, expellers, 45% CP	Conc	0.37
105	Soybean	Meal, nonenzymatically browned	Conc	0.37
106	Soybean	Meal, solvent, 44% CP	Conc	0.38
107	Soybean	Meal, solvent, 48% CP	Conc	0.38
108	Soybean	Seeds, whole	Conc	0.41
109	Soybean	Seeds, whole roasted	Conc	0.41
110	Soybean	Silage, early maturity	Forage	0.26
111	Sunflower	Meal, solvent	Conc	0.26
114	Triticale	Silage, headed	Forage	0.21
115	Wheat	Bran	Conc	0.19
116	Wheat	Grain, rolled	Conc	0.21
118	Wheat	Middlings	Conc	0.16
122	Calcium Phosphate monobasic	Ca(H2PO4)2	Mineral	0.96

[1]Entry numbers refer to Tables 15–1 and 15–2a in NRC (2001).

[2]Feed type, Conc = concentrate.

[3]Feed price in $/kg of DM based on Penn State University feed price list.

Chapter 2: A mechanistic thermal balance model of dairy cattle

Jinghui Li[1], Vinod Narayanan[2], Ermias Kebreab[1], Serdal Dikmen[3], James G. Fadel[1]

[1] Department of Animal Science, University of California, Davis CA 95616, USA

[2] Department of Mechanical and Aerospace Engineering, University of California, Davis CA 95616, USA

[3] Faculty of Veterinary Medicine, Department of Animal Science, Bursa Uludag University, Bursa, 16059, Turkey

Abstract

A dynamic model describing the thermal balance of Holstein dairy cattle was developed. The model quantified the heat flow of five main nodes at the body core, top and bottom skin, and top and bottom coat of a dairy cow. Heat production by the animal, heat conduction through the body core, skin and coat, and heat flows between the animal and the environment, including convection, evaporation, radiation and conduction to the ground while lying down, were calculated based on existing models and physical principles. The model requires climate information (Julian day number, air temperature, relative humidity, wind speed and annual average air temperature), animal information (body weight, milk production, feed intake and feed ingredients) and location (latitude and altitude) as inputs, and returns body core, skin and coat temperatures as outputs. The thermal balance model was evaluated through two datasets. The root mean squared error of prediction for body temperature was 1.16 °C (2.9% of the observation mean) and 0.40 °C (1.0% of the observation mean) for the two datasets, respectively. A simulation study was conducted based on a Holstein dairy cow with 600 kg of body weight and 25 kg of daily milk yield under a typical California summer environment for three days. The average simulated temperatures of body, top and bottom skin, and top and bottom coat were

40.9, 35.6, 35.9, 34.1 and 33.7 ℃, respectively. A local and a global sensitivity analyses showed that heat production, surface area and the parameters relative to respiration and sweating were the most sensitive. The model is able to predict the dynamic change of body temperature under hot weather, and to guide the use of physical cooling strategies, such as shade, fans, sprinklers and cooling mats in dairy facilities.

Key words: dairy cow, thermal balance model, heat stress

Introduction

Thermal stress is a major factor that can cause losses in production of dairy cows, who prefer an ambient temperature between 5 and 25 ℃ (Roenfeldt, 1998). Heat stress can be defined as the sum of external forces (dry bulb temperature, humidity, wind speed and radiation) that act to displace the animal's body temperature from ground state (Hansen et al., 2020). Heat stress negatively affects the health of animals through their physiology (Lacetera et al., 1996), metabolism (Nardone et al., 2010) and immune system (Das et al., 2016), resulting in decreased production. Temperature humidity index (THI), calculated using air temperature and relative humidity, has been used as a way to express heat stress experienced by animals (Mader et al., 2006). However, THI evaluates the thermal environment instead of the thermal condition of the animal, therefore it is not accurate enough to evaluate thermal stress. Body temperature of dairy cattle shows great susceptibility to hot weather (Akari et al., 1984), which makes it a more sensitive indicator of thermal stress. When the body temperature is over 39 ℃ under hot weather conditions, cows are likely to be in heat stress (Zimbelman et al., 2009). It has been suggested that milk production significantly decreases when rectal temperature is over 39 ℃ for more than 16 h (Igono et al., 1990), with 1.8 kg of production decline for every 0.55 ℃ increase in rectal temperature (West, 2003). Increase of body temperature also depresses the conception rate

(Nabenishi et al., 2011) and cause severe damage on follicles when body temperature is over 40 ℃ (Roth et al., 2000).

Many attempts have been made to investigate the heat flow and temperature change of dairy cows under different climate conditions. Some studies focused on certain types of heat transfer mechanisms, including evaporative cooling (Gebremedhin et al., 2001; Maia et al., 2005a; Berman, 2006), respiratory heat loss (da Silva et al., 2002; Maia et al., 2005) and solar radiation (Yamamoto et al., 1994). However, this approach does not connect heat transfer with body temperature. McArthur (1987) developed a comprehensive model describing the thermal interaction between animal and microclimate, which was modified by Turnpenny et al. (2000a), but their model was not evaluated thoroughly and can only predict body temperature under a static environment (i.e., environmental conditions do not change). Thompson et al. (2014a) developed a thermal balance model for beef cattle by connecting the heat flows with body temperature. Their model structure allows for the prediction of dynamic body temperature under a constantly changing environment, thus was used in this study. We aim to develop a thermal balance model for dairy cows in order to understand the thermal conditions of the animal and to improve the heat mitigation strategies under hot climate.

Materials and Methods

Model Description

The most important difference between our model and previous ones (McGovern and Bruce, 2000; Turnpenny et al., 2000a; Thompson et al., 2014a) is that our model includes heat conduction between the animal and the ground surface when the animal lies down, while previous ones do not. Although cows in heat stress tend to stand rather than lie down (Shultz,

1984; Chen et al., 2016), lying down still accounts for about one third of the total time budgets of dairy cows in summer (Cook et al., 2007), therefore it is necessary to consider it.

The heat balance model developed in this study requires climate information (Julian day number, air temperature, relative humidity, wind speed and annual average air temperature), animal information (body weight, milk production, feed intake and feed ingredients), location (latitude and altitude) and timing of behaviors (lying down and standing up) as inputs for animals outdoor, and returns body core, skin and coat temperatures as outputs. Black globe temperature is required as an additional input for animals located indoor. The temperatures of body core, skin and coat were calculated in absolute units (Kelvin) in the model but converted to Celsius degree in results for ease of understanding. The model and all the analyses were coded in R statistical software (Version 3.5.3, R core team, 2019). The FME package (Soetaert and Petzoldt, 2010) was used to solve the differential equations.

Differential equations. A heat balance model with five main nodes (the surface layer of body core, top and bottom skin and, top and bottom coat) was developed. A similar model structure was adopted in previous studies (McGovern and Bruce, 2000; Thompson et al., 2014a) to represent different temperatures and thermal properties (conductivity, specific heat, etc.) of each node. The skin and coat were divided into top and bottom parts to account for different heat transfer mechanisms occurring in these regions when the animal lies down, with the bottom skin and coat representing the part in contact with the ground surface (0.2; Ortiz et al., 2015) and the top part representing the rest (0.8). The geometry of the nodes is represented by three concentric cylinders (top and bottom skin and coat consist of two cylinders), and the control volume surrounding each node has uniform internal temperature and thermal properties. The temperature of each node is regulated by different heat flows as shown in Fig. 1. The dynamic change of heat

at each node results in temperature changes. For the body core node, the heat flows include heat production by the animal, heat dissipation through respiration, and heat conduction between body core and skin. For the top skin node, the heat flows include heat conduction between body core and skin, heat conduction between skin and coat, and heat dissipation through evaporation. The bottom skin node shares the same heat flows as the top one when the animal stands up. When the animal lies down, we assumed that evaporation does not happen at the bottom skin, therefore the heat flows include the conduction between body core and skin and the conduction between skin and ground surface. For the top coat node, the heat flows include solar radiation, heat conduction between skin and coat, heat convection at the coat surface, and long wave radiation between the coat and the surrounding. The bottom coat node has the same heat flows as the top one when the animal stands up. When the animal lies down, no heat transfer was considered for the bottom coat, and we assumed that it has the same temperature as bottom skin. Besides, we also assumed that no heat transfer occurs between top and bottom skin, or between top and bottom coat. Heat flows are in the unit of W to represent heat transfer rate in Fig. 1 and can be converted to heat flux ($W \cdot m^{-2}$) by dividing by the surface area to represent the heat transfer rate per unit of area. Five differential equations representing the dynamic heat and temperature change of body core, top and bottom skin, and top and bottom coat can be developed based on the nodal energy balances as follows:

Body core node: $$d(M_b\, c_{pb}\, T_b)/dt = HE - A\,[p_c\, q''_{cond,\, b\text{-}s1} + (1 - p_c)\, q''_{cond,\, b\text{-}s2} + q''_{resp}] \quad (1.1)$$

Top skin node: $$d[(1 - p_c)M_s\, c_{ps}\, T_{s1}]/dt = (1 - p_c)\, A\, (q''_{cond,\, b\text{-}s1} - q''_{cond,\, s1\text{-}c1} - q''_{evap1}) \quad (1.2)$$

Bottom skin node:

$$d(p_c\, M_s\, c_{ps}\, T_{s2})/dt = \begin{cases} p_c\, A\, (q''_{cond,\, b\text{-}s2} - q''_{cond,\, s2\text{-}c2} - q''_{evap2}), \text{ when standing up} \\ p_c\, A\, (q''_{cond,\, b\text{-}s2} - q''_{cond,\, s2\text{-}g}), \text{ when lying down} \end{cases} \quad (1.3)$$

Top coat node: $$d[(1 - p_c)M_c\, c_{pc}\, T_{c1}]/dt = (1 - p_c)\, A\, (q''_{cond,\, s1\text{-}c1} + q''_{sol1} - q''_{conv1} - q''_{lw1}) \quad (1.4)$$

Bottom coat node:

$$d(p_c M_c c_{pc} T_{c2})/dt = \begin{cases} p_c A (q''_{cond,\ s2\text{-}c2} + q''_{sol2} - q''_{conv2} - q''_{lw2}), & \text{when standing up} \\ 0, & \text{when lying down} \end{cases} \quad (1.5)$$

where A (m^2) is animal surface area; M_b, M_s and M_c (kg) are the mass of body core, skin and coat, respectively; c_{pb}, c_{ps} and c_{pc} (J kg^{-1} K^{-1}) are the specific heat capacity of body core, skin and coat, respectively; T_b, T_{s1}, T_{s2}, T_{c1} and T_{c2} (K) are the temperature of body core, top skin, bottom skin, top coat and bottom coat, respectively; p_c (dimension less) is the proportion of contacting surface to the animal surface area when the animal lies down, taken equal to 0.2 (Ortiz et al., 2015); HE (W) is the heat production by animal; $q''_{cond,\ b\text{-}s1}$ and $q''_{cond,\ b\text{-}s2}$ (W m^{-2}) are heat conduction between body core and top and bottom skin, respectively; q''_{resp} (W m^{-2}) is heat loss through respiration; $q''_{cond,\ s1\text{-}c1}$ and $q''_{cond,\ s2\text{-}c2}$ (W m^{-2}) are heat conduction between top skin and coat and between bottom skin and coat, respectively; q''_{evap1} and q''_{evap2} (W m^{-2}) are heat evaporation through sweating at top and bottom skin, respectively; $q''_{cond,\ s2\text{-}g}$ (W m^{-2}) are heat conduction between bottom skin and ground surface; q''_{sol1} and q''_{sol2} (W m^{-2}) is solar radiation at top and bottom coat, respectively; q''_{conv1} and q''_{conv2} (W m^{-2}) are heat convection at top and bottom coat, respectively; q''_{lw1} and q''_{lw2} (W m^{-2}) are the net heat flux from the animal to the environment through long wave radiation at top and bottom coat, respectively. One should note that all the heat transfer could happen in both directions depending on the temperature difference between two surfaces, except evaporation and solar radiation. For example, $q''_{cond,\ b\text{-}s1}$ is subtracted in equation 1.1 to indicate a heat outflow from the body core, which is true when the body temperature is higher than the top skin temperature. When the top skin temperature is higher, $q''_{cond,\ b\text{-}s1}$ is negative and becomes a heat inflow from top skin to body core.

The condensed model equations are shown below, and detailed description of the model equations is presented in Appendix A. The differential equations allow for solving the five unknowns, T_b, T_{s1}, T_{s2}, T_{c1} and T_{c2} after quantifying all the other variables.

Heat production by the Animal. The average daily heat production (HE, W) can be calculated as:

$$HE = (ME - RE)/86400 \quad (2.1)$$

where ME is daily metabolizable energy intake (J); RE is daily retained energy (J); 86400 is the amount of time per day in second. Given the feed ingredients of a diet, feed intake, milk production and body weight change, ME and RE can be estimated based on NRC (2001). Heat production can also be roughly estimated through an empirical equation (Purwanto et al., 1990) when detailed dietary information is not available:

$$HE = c_h BW^{0.75}/3.6 \quad (2.2)$$

where c_h (dimensionless) is the heat production coefficient equal to 44.1 for high production cows (daily milk yield $\geqslant$ 30 kg), 37.8 for intermediate production cows (daily milk yield < 30 kg) and 29.7 for dry cows. Some researchers have claimed that drinking cold water helps with heat mitigation in summer (Bewley et al., 2008) while others only found transient effect of cold water (Baker et al., 1988). We roughly estimated the heat mitigation through drinking water by assuming a cow drinking 100 L of 25 °C water per day and heating all of it up to the body temperature (38.5 °C). All water consumed would be lost through manure, milk or sweat. The amount of heat absorbed by the consumed water (5.6×10^6 J approximately) is less than 1% of the total heat production by the animal based on our calculation, therefore the cooling effect of drinking water is not considered in the model.

Heat conduction between body core and skin. Heat conduction between body core and top skin surface ($q''_{cond, b\text{-}s}$, W m^{-2}) can be calculated based on McArthur (1987):

$$q''_{cond,\ b\text{-}s1} = \rho c_p\ (T_b - T_{s1})/r_{s1} \quad (3.1)$$

where ρc_p (J m^{-3} K^{-1}) is volumetric heat capacity of air and r_{s1} (s m^{-1}) is skin resistance. Skin resistance is a function of T_{s1}, reflecting the change of skin conductivity in response to heat stress (McArthur, 1987):

$$r_{s1} = \max\ (-5.44\ (T_{s1} - 273.15) + 225, 29) \quad (3.2)$$

where 29 s m^{-1} is the minimum of skin resistance. The conduction between body core and bottom skin surface can be calculated by replacing T_{s1} with T_{s2} in equations 3.1 and 3.2.

Heat loss through respiration Heat loss through respiration (q''_{resp}, W m^{-2}) consists of sensible heat transfer (q''_{sen}, W m^{-2}) and latent heat transfer (q''_{lat}, W m^{-2}):

$$q''_{resp} = q''_{sen} + q''_{lat} \quad (4.1)$$

Sensible heat transfer happens between inhaled air and exhaled air due to temperature difference, while latent heat transfer happens due to the transformation of water from liquid to vapor at lung without temperature change. The equations are described as follows (McGovern, 2000; Monteith and Unsworth, 2013):

$$q''_{sen} = V_t\ RR\ \rho c_p\ (Tv_e - Tv_a)/A \quad (4.2)$$

$$q''_{lat} = \lambda\ V_t\ RR\ (\chi_e - \chi_a)/A \quad (4.3)$$

where V_t (m^3 $breath^{-1}$) is tidal volume; RR (breath s^{-1}) is respiration rate; Tv_e (K) and Tv_a (K) are virtual temperatures of exhaled air and inhaled air, respectively; λ (2430 J g^{-1}) is latent heat of vaporization of water (Monteith and Unsworth, 2013); A (m^2) is area of animal body surface; χ_e (g m^{-3}) and χ_a (g m^{-3}) are absolute humidity of exhaled air and inhaled air, respectively.

Heat conduction between skin and coat. Heat conduction between top skin and top coat ($q''_{cond,\ s\text{-}c}$, W m^{-2}) is calculated as:

$$q''_{cond,\ s1\text{-}c1} = k_{eff}\ (T_{s1} - T_{c1})/d_c \quad (5.1)$$

where k_{eff} (W m^{-1} K^{-1}) is effective thermal conductivity of coat, and d_c (0.0025 m) is the coat thickness (Bertipaglia et al., 2005). Coat layer is a mixture of fur and air, the thermal conductivity for which is derived by Gebremedhin et al. (2001) as:

$$k_{eff} = 0.5\ (k_x + k_y) \tag{5.2}$$

$$k_x = (\rho_h\ \pi\ d_h^2/4)\ k_f + (1 - \rho_h\ \pi\ d_h^2/4)\ k_a \tag{5.3}$$

$$k_y = k_a\ (1/\rho_h^{0.5} - d_h)\ \rho_h^{0.5} + d_h\ k_a\ k_f/(d_h\ k_a + (1/\rho_h^{0.5} - d_h)\ k_f) \tag{5.4}$$

where k_x (W m^{-1} K^{-1}) is horizontal thermal conductivity; k_y (W m^{-1} K^{-1}) is vertical thermal conductivity; ρ_h (9.87 hairs mm^{-2}) is fur density (Bertipaglia et al., 2005); d_h (0.0625 mm) is hair diameter (Bertipaglia et al., 2005); k_f (0.26 W m^{-1} K^{-1}) is fur conductivity (Gebremedhin et al., 2016); k_a (0.024 W m^{-1} K^{-1}) is air conductivity. Based on the above parameter values, k_{eff} = 0.028 W m^{-1} K^{-1}. The conduction between bottom skin and bottom coat can be calculated by replacing T_{s1} and T_{c1} with T_{s2} and T_{c2} in equation 5.1.

Heat evaporation through sweating. Heat loss through sweating is limited by either sweating rate or potential evaporation rate, which is dependent on the environmental conditions (Thompson et al., 2014a). Therefore, the minimum value of two functions (Gebremedhin and Wu, 2001; Silva and Maia, 2011) based on sweating rate and potential evaporation rate is used to represent the heat evaporation at the top skin (q''_{evap1}, W m^{-2}):

$$q''_{evap1} = \min (31.5 + 3.67 \exp[(T_{s1} - 301.05)/2.19],\ \lambda\ (\chi_{s1} - \chi_a)/[1/h_m + (d_c + d_a)/D]) \tag{6.1}$$

where χ_{s1} (g m^{-3}) is absolute humidity at the top skin; χ_a (g m^{-3}) is absolute humidity of air, which is the same as the absolute humidity of inhaled air in equation 4.3; h_m (m s^{-1}) is mass transfer coefficient; d_a (m) is laminar thickness; D (dimensionless) is diffusion coefficient of water vapor in air. The first part is an empirical equation representing q''_{evap1} through sweating rate based on T_{s1}, while the second part describes the potential evaporation rate based on the environmental air

conditions. Heat evaporation at the bottom skin can be calculated by replacing T_{s1} with T_{s2} in equation 6.1.

Heat convection at coat surface. Conduction occurs between two still surface while convection occurs between a still surface and fluid in motion, therefore the heat transfer between coat surface and air is considered as convection. Heat convection at the top coat surface (q''_{conv1}, W m^{-2}) can be expressed using Newton's law of cooling as:

$$q''_{conv1} = h_c (T_{c1} - T_a) \quad (7.1)$$

where h_c (W m^{-2} K^{-1}) is the convection heat transfer coefficient, which is a function of Nusselt number and surface properties (Monteith and Unsworth, 2013). The calculation of Nusselt number is based on Reynolds number, which is dependent on the nature of the fluid motion, surface geometry and the assortment of fluid thermodynamic (Gebremedhin and Wu, 2001). The convection at the bottom coat can be calculated by replacing T_{c1} with T_{c2} in equation 7.1.

Heat flux through long wave radiation. Thermal radiation is the energy emitted by matter that is at a nonzero absolute temperature. The radiation between the top coat surface and surroundings (q''_{lw1}, W m^{-2}) has longer wavelength than solar radiation, and can be prescribed by the Stefan-Boltzmann law:

$$q''_{lw1} = \sigma \varepsilon_c (T_{c1}^4 - T_r^4) \quad (8.1)$$

where σ (5.67×10^{-8} W m^{-2} K^{-4}) is Stefan-Boltzmann constant; ε_c (0.98, dimensionless) is the emissivity of coat (Maia and Loureiro, 2005); T_r (K) is the average radiant temperature of the surrounding. When the animal is outdoor, T_r is calculated as the average of sky temperature (T_{sky}, K) and ground temperature (T_g, K):

$$T_r = (T_{sky} + T_g)/2 \quad (8.2)$$

Similarly, when the animal is indoor, T_r can be calculated as the average of roof temperature and floor temperature. However, estimating roof temperature is difficult, therefore indoor T_r is estimated through black globe temperature (Kuehn et al., 1970; Thorsson et al., 2007):

$$T_r = (T_{black}^4 + 1.1 \times 10^{-8} u^{0.6} (T_{black} - T_a)/2.029)^{0.25} \quad (8.3)$$

where T_{black} (K) is black globe temperature and u (m s^{-1}) is wind speed. The long radiation between the bottom coat and surroundings can be calculated by replacing T_{c1} with T_{c2} in equation 8.1.

Heat flux through solar radiation. Solar radiation is an important heat input to animals when exposed to the sun. Turnpenny et al. (2000a) divided heat flux through solar radiation (q''_{sol}, W m^{-2}) into three parts, including direct and diffusive radiation from the sun, and the radiation reflected by the ground:

$$q''_{sol} = (1 - \rho_c) [(A_h/A) S_b + 0.5 S_d + 0.5 \rho_g (S_b + S_d)] \quad (9.1)$$

where ρ_c (0.3, dimensionless) is the reflection coefficient of coat (Turnpenny et al., 2000b); A_h/A (dimensionless) is the proportion of body surface the receives the direct solar radiation, taking the orientation of the animal and the solar altitude angle into account; S_b (W m^{-2}) is the direct radiation from the sun; S_d (W m^{-2}) is the diffusive radiation from the sun; ρ_g (dimensionless) is the reflection coefficient of ground. The coefficient 0.5 represents the assumption that half of the body surface faces towards the sky and receives diffusive solar radiation, while the other half faces towards the ground and receives the reflected radiation from the ground. Then the heat flow through solar radiation (q_{sol}, W) received by the animal is:

$$q_{sol} = A\, q''_{sol} \quad (9.2)$$

Since the coat was divided into top and bottom parts in this study, the equation was modified to quantify the solar radiation at the top (q_{sol1}, W) and bottom coat (q_{sol2}, W) separately:

$$q_{sol1} = A\ (1 - \rho_c)\ (A_h/A)\ S_b + 0.5\ A\ S_d + (0.5 - p_c)\ A\ \rho_g\ (S_b + S_d) \quad (9.3)$$

$$q_{sol2} = p_c\ A\ \rho_g\ (S_b + S_d) \quad (9.4)$$

We assumed that the direct radiation and diffusive radiation are received the top coat, and that the bottom coat only receives the reflected radiation from the ground. Since the proportion of bottom coat to the total coat ($p_c = 0.2$) is smaller than 0.5, the rest of the reflected radiation from the ground is received by the top coat. Then the heat flux of solar radiation in the equation 1.4 and 1.5 can be calculated by dividing the heat flow by the area:

$$q''_{sol1} = q_{sol1}/[(1 - p_c)\ A] \quad (9.5)$$

$$q''_{sol2} = q_{sol2}/(p_c\ A) \quad (9.6)$$

Solar radiation is affected by cloud (Hottel, 1976), which was not considered in this study. Cloudiness is difficult to quantify and highly varied, therefore it is better to obtain solar radiation through direct measurement instead of estimation on cloudy days.

Heat conduction between animal and ground when lying down. A finite difference method (Bastian et al., 2003) was used to quantify the heat conduction between the animal and the ground through dividing the vertical distance between contacting surface and an adiabatic layer underground into many small nodes. The adiabatic layer was estimated using thermal penetration depth $2.3\ (\alpha_{soil}\ t)^{0.5}$ (Bergman et al., 2011), where α_{soil} ($m^2\ s^{-1}$) is the thermal diffusivity and t (s) is the time after lying down. In this study, we assumed a soil type of heavy clay with thermal diffusivity equal to $5.9 \times 10^{-7}\ m^2\ s^{-1}$ (Najib et al., 2020). To estimate the thermal penetration conservatively, the undisturbed depth was set to be 0.5 m when the animal lies down for the whole day (t = 86400 s). The vertical distance from the contact surface to the adiabatic layer was divided into 50 nodes, with the distance of d_i equal to 0.01 m between each of two nodes (Fig. 1).

The heat conduction ($q''_{cond,\,1}$, W m^{-2}) into the first node, i.e., the conduction between the animal and the ground surface ($q''_{cond,\,s2\text{-}g}$), was calculated as (Radoń et al., 2014):

$$q''_{cond,\,s2\text{-}g} = (T_{s'} - T_{g,\,1})/r_{sg} \quad (10.1)$$

where $T_{g,\,1}$ (K) is the ground temperature at the first node; r_{sg} (0.1 m^2 K W^{-1}) is the thermal contact resistance between the skin and the ground surface (Radoń et al., 2014). We assume that $T_{g,\,1}$ is equal to the ground surface temperature (T_g) at the beginning of animal lying down. The net heat flux into interior control volume ($q''_{cond,\,1}$, W m^{-2}) of node 1 was calculated as the conduction from the bottom skin minus the conduction to node 2:

$$q''_{cond,\,1} = q''_{cond,\,s2\text{-}g} - (T_{g,\,1} - T_{g,\,2})/(d_i/2) \quad (10.2)$$

where $T_{g,\,2}$ (K) is the underground temperature at node 2. Node spacing was set to be $d_i/2$ for the first and last nodes, and to be d_i for all the other nodes (Bastian et al., 2003). The net heat flux into each interior control volume ($q''_{cond,\,i}$, W m^{-2}) from nodes i = 2 to 49 was calculated as the conduction input from node i – 1 minus the conduction output to node i + 1:

$$q''_{cond,\,i} = k_{soil}\,[(T_{g,\,i-1} - T_{g,\,i}) - (T_{g,\,i} - T_{g,\,i+1})]/d_i \quad (10.3)$$

where k_{soil} (W m^{-1} K^{-1}) is the thermal conductivity of soil; $T_{g,\,i-1}$, $T_{g,\,i}$ and $T_{g,\,i+1}$ (K) are the underground temperature at node i – 1, i and i + 1, respectively. The heat flux at the last node (0.5 m deep underground, $q''_{cond,\,50}$, W m^{-2}) was calculated as the conduction input from node 49 minus the conduction output to the adiabatic layer:

$$q''_{cond,\,50} = k_{soil}\,[(T_{g,\,49} - T_{g,\,50}) - (T_{g,\,50} - T_{adl})]/(d_i/2) \quad (10.4)$$

where $T_{g,\,49}$ (K) the temperature at node 49; $T_{g,\,50}$ (K) is the temperature at node 50; T_{adl} (K) is the temperature at the adiabatic layer, which was assumed to be a constant equal to the annual average air temperature of the location (Zarrella & De Carli, 2013). We assumed that the heat conduction among the nodes is one-dimensional and shares the same contact area as that between

the animal and the ground surface. The net heat flux into each control volume in the soil is equal to the thermal storage in that control volume with time:

$$d(M_{soil}\, c_{psoil}\, T_{g,\,i})/dt = p_c\, A\, q''_{cond,\,i} \quad (10.5)$$

where M_{soil} (kg) is the soil mass for each node; c_{psoil} (J kg^{-1} K^{-1}) is the specific heat capacity of soil. Soil mass can be written as the product of volume and density ($M_{soil} = p_c\, A\, d_i\, \rho_{soil}$), which converts the above equation to:

$$d(\rho_{soil}\, c_{psoil}\, T_{g,\,i}\, d_i)/dt = q''_{cond,\,i} \quad (10.6)$$

where ρ_{soil} (kg m^{-3}) is the soil density. Different soil has different thermal properties; we assume a heavy clay soil with c_{psoil} = 1784 J kg^{-1} K^{-1}, ρ_{soil} = 1784 kg m^{-3} and k_{soil} = 1.64 W m^{-1} K^{-1} in this study, which is typical in the Central Valley in California (Najib et al., 2020).

Model evaluation

Two datasets (Dikmen & Hansen, 2009; Chen et al., 2015) were used to evaluate the predictability of the model for body temperature. Both datasets were collected in the afternoon based on the experimental design. The body temperature data from Dikmen & Hansen (2009) were collected indoor in the afternoon from June to September 2007 in Florida, thus solar radiation was considered to be 0. Measurements were taken over 2 h when the animals were standing up. After removing the data collected from animals exposed to sprinklers, 347 observations from 304 animals were used for evaluation. The dataset from (Chen et al., 2015) is publicly available on the Dryad Digital Repository (https://doi.org/10.25338/B88P7H). They collected body temperature data over 1 h when the cows were standing up under the sun in the afternoon from June to August 2011 in California. Only the data collected from animals without any cooling treatment were used (486 observations from 18 animals). Climate data near the animal including air temperature, relative humidity, wind speed and black globe temperature

were recorded when the rectal temperature was measured every 1 to 3 min for 2 h in the dataset of Dikmen & Hansen (2009) and every 5 to 10 min for 1 h in the dataset of Chen et al. (2015). The weather data were assumed to change linearly between each time point. The heat production was estimated based on the herd average body weight and milk production. The dataset of Chen et al. (2015) also contained RR measurements for all the 486 observations, which were used to compare two RR estimation equations (Thompson et al., 2011; Atkins et al., 2017). Both are linear equations regressed on T_b: $RR = 37T_b - 1385$ (Thompson et al., 2011) and $RR = 19.8T_b - 707$ (Atkins et al., 2017), where T_b is in °C and RR is in breath min^{-1}.

Correlation between observations and predictions (r^2), root mean squared error of prediction (RMSEP) and concordance correlation coefficient (CCC; Lawrence and Lin, 1989) were used to evaluate the accuracy and precision of the model on body temperature and respiration rate estimation.

Simulation example

A simulation example was conducted based on a Holstein dairy cow weighing 600 kg, with 176 MJ of metabolizable energy intake per day, producing 25 kg of milk (3.2% of milk protein, 3.5% of milk fat and 4.85% of lactose) per day and having no body weight change. The heat production rate was estimated to be 1240 W based on NRC (2001). Milk production was set to be low because the simulation was conducted under an outdoor environment in hot summer when the animal was likely under heat stress. Three days of simulation were run based on the weather condition in Davis, California from July 26 to 28, 2019. Hourly air temperature, relative humidity and wind speed were obtained from Weather Underground (https://www.wunderground.com/weather/us/ca/davis). Weather data were interpolated linearly to provide information of inputs varying on a per second basis (Fig. 2), with the average

air temperature, relative humidity and wind speed being 25.8 °C (min = 13.3 °C, max = 37.7 °C), 51.0% (min = 16.0 %, max = 95 %) and 2.0 m/s (min = 0.67 m s^{-1}, max = 3.8 m s^{-1}), respectively. Annual average temperature in Davis (16.2 °C) was obtained from U.S. Climate Data (https://www.usclimatedata.com/climate/davis/california/united-states/usca0284). The timing of animal lying down and standing up is also required to quantify the conduction between animal and ground. In the simulation, we assumed that the animal did not lie down when the ground surface temperature was higher than the lower skin temperature. The proportion of lying down during other time was set based on Drwencke et al. (2020), resulting 7.5 h of lying down per day (details in Appendix B).

Sensitivity analysis

Sensitivity measures how influential a parameter is on the model output. A local and a global sensitivity analyses were conducted to estimate the sensitivities of the model parameters. The local sensitivity analysis evaluates the effect of each parameter at a steady state, while the global sensitivity analysis evaluates them dynamically.

Local sensitivity analysis. In the local sensitivity analysis, 50 model parameters (detailed information in Appendix B), three of which were climate variables (air temperature, relative humidity and wind speed), were analyzed. The climate variables were set to nominal values, with air temperature being 34 °C, relative humidity being 18 % and wind speed being 2.8 m s^{-1}, which mimicked a typical summer afternoon in Davis, California. The model was run with the baseline values of all the parameters ($\overline{p}_i$, i = 1, ..., 50) until the outcome T_b reached a steady state (the outcome does not change more than 0.01 % within 1 h). Then the model was rerun twice for each parameter after changing the baseline value by ± 3% (Thompson et al., 2014b) and fixing all the others. The sensitivity S_i (dimensionless) for parameter i was calculated as:

$$S_i = (\Delta T_{bi}/\Delta p_i)\ (\overline{p}_i/\overline{T}_b) \quad \text{(S.1)}$$

where ΔT_{bi} is the change of T_b caused by the change of parameter i (Δp_i), and $\overline{T}_b$ is the outcome of T_b under the baseline value of parameter $\overline{p}_i$. In order to investigate the difference of sensitivity between cows standing up and lying down, two local sensitivity analyses were conducted using the same procedures as described above, except that the animal was assumed to stand up in one analysis while to lie down in the other.

Global sensitivity analysis. Global sensitivity analysis measured the sensitivity of each parameter throughout 24 h based on the method described by Saltelli et al. (2008) and Thompson et al. (2014b). The three climate parameters changed across time and could not be included in the global sensitivity analysis, thus only the rest 47 parameters were included. A parameter matrix X (x_{ij}, i = 1, ...,10000 and j = 1, ..., 47) was constructed with each column representing a parameter and each row representing a simulation. The values for each parameter were drawn from a uniform distribution, with upper and lower bounds given as ± 3% of the baseline value. In total, 10000 simulations were performed, with the parameter inputs for each simulation given by a row from the parameter matrix. The T_b outputs were saved from each run every 15 min throughout 24 h (96 outcomes in total) and stored in a model output matrix Y (y_{ik}, i = 1, ...,10000 and k = 1, ..., 96).

All columns of the parameter matrix and the output matrix were standardized to X' and Y' as:

$$x'_{ij} = (x_{ij} - \overline{x}_{.j})/s_{xj} \text{ and } y'_{ik} = (y_{ik} - \overline{y}_{.k})/s_{yk} \quad \text{(S.2)}$$

where $\overline{x}_{.j}$ and s_{xj} are the mean and standard deviation of column j in the parameter matrix X, $\overline{y}_{.k}$ and s_{yk} are the mean standard deviation of column k in the output matrix Y. Then each column of the standardized output matrix was regressed on the standardized parameter matrix as:

$$Y'_k = X' \beta_k + e_k \quad (S.3)$$

where Y'_k is a vector (10000 × 1) of column k in the standardized output matrix, X' (10000 × 47) is the standardized parameter matrix, β_k is a regression coefficient vector (47 × 1), and e_k (10000 × 1) is a residual vector.

In a standardized regression setting, the total variation of the output equals one and the sensitivity of a parameter can be represented by its regression coefficient squared, which describes the fraction of the model variance that is accounted for by variation of the parameter. As a result, each parameter had 96 sensitivities corresponding to each time point. The R^2, the coefficient of determination, from the standardized regression will be close to 1 if the model is linear in its parameters. The global sensitivity analysis was conducted using the same lying time as that in the simulation, and climate condition in Davis, California on July 26, 2019.

Results and Discussion

Model evaluation

The RMSEP of the thermal balance model prediction of body temperature on the data from Dikmen & Hansen (2009) was 1.16 °C (2.9% of the observation mean), while the data from Chen et al. (2015) was 0.40 °C (1.0% of the observation mean). The prediction on the data from Dikmen & Hansen (2009) had lower r^2 (0.43 vs 0.91, respectively) and CCC (0.36 vs 0.79, respectively) than the data from Chen et al. (2015). Fig. 3 suggests that the model was likely to overestimate the body temperature for both datasets, given many predictions were higher than the observations. Cows stood indoor for 2 h in Dikmen & Hansen (2009) while cows were forced to stand under the sun for 1 h in Chen et al. (2015) when sampling, which resulted in a higher average body temperature from Chen et al. (2015) than that from Dikmen & Hansen (2009). The variance of the body temperature in the dataset of Dikmen & Hansen (2009) was 0.62, while that

in the dataset of Chen et al. (2015) was 0.39. The thermal balance model fitted the dataset from Chen et al. (2015) better, probably because Dikmen & Hansen (2009) collected 347 observations from 304 animals, which resulted in a larger animal variation. In contrast, Chen et al. (2015) collected 486 observations of body temperature from 18 animals consecutively, which can be better described by our model. However, we did not have data from cows lying down, so the evaluation of the conduction between the animal and ground requires future experimentation to take the appropriate measurements.

For respiration rate prediction (Fig. 4), the equation from Thompson et al. (2011) had a similar RMSEP (25.0 vs 23.5 breath s^{-1}, respectively; 26.4% vs 24.8% of the observation mean, respectively) as the one from Atkins et al. (2017), but a greater CCC value (0.45 vs 0.33, respectively). Both equations predict respiration rate by a linear regression on body temperature, thus had the same r^2 of 0.66. Thompson's equation had a slightly larger RMSEP but a better CCC value, thus was used in our model. Thompson's equation was derived through a meta-analysis using data from *Bos taurus* cattle, which included animals other than dairy cows (Thompson et al., 2011), while Atkins's equation was developed based on an animal trial using only 8 cows (Atkins, et al., 2017). Both equations may not be accurate enough, therefore a meta-analysis on dairy cattle respiration rate should be conducted in the future to refine the respiration rate equation.

Simulation example

The simulated temperature of body core, skin and coat is shown in Fig. 5. The average temperatures of body, top and bottom skin, and top and bottom coat were 40.9 °C (min = 39.0 °C, max = 42.1 °C), 35.6 °C (min = 32.5 °C, max = 38.6 °C), 35.9 °C (min = 32.5 °C, max = 40.8 °C), 34.1 °C (min = 21.6 °C, max = 48.1 °C) and 33.7 °C (min = 21.7 °C, max = 40.8 °C),

respectively. The body temperature was higher than normal (38.5 ℃), probably due to the assumption that the animal was unshaded and had no access to any cooling equipment (roofs, fans or sprinklers). The variation of body core temperature is the smallest, followed by skin temperature, and coat temperature. The body temperature oscillated every 24 h, with the peak occurring around 1600 to 1700 h and the minimum occurring around 0400 to 0500 h. The top skin and coat temperatures followed the same pattern, with the peak occurring around 3 h earlier and the minimum occurring 1 h earlier than the body temperature. Environmentally, the peak temperature of top coat and skin temperatures occurred around 1 h after the solar radiation peak, while body temperature reached a peak around 1 h after peak air temperature. A similar pattern was also reported by Scott et al. (1983), indicating the process of heat accumulation. The bottom skin and coat temperature changed periodically because of lying down and standing up. When the animal lied down, the bottom skin temperature was higher than the top skin temperature due to lack of evaporation. After standing up, the bottom skin and coat temperature gradually changed to the same as the top skin and coat temperature due to the same heat transfer mechanism happening to top and bottom parts. However, when the animal keeps standing when the ground surface temperature was higher the bottom skin temperature, bottom skin and coat temperatures were lower than the top ones because of the stronger solar radiation received by the top coat.

The proportions of five ways of heat dissipation are shown in Table 1. Evaporation accounted for 48.0% of the total amount of dissipated heat on average throughout the simulation, followed by long wave radiation (18.2%), respiration (16.2%), convection (14.9%), and conduction (2.7%). Fig. 6 shows the heat flux over the three days. Evaporation, convection, solar radiation, long wave radiation are shown as the weighted average heat flux at the top and bottom

nodes (e.g., evaporation = 0.8 evaporation at the top skin + 0.2 evaporation at the bottom skin). Solar radiation was an important heat source thus shading is essential in summer to prevent heat stress. Evaporation was the major way to dissipate heat in the afternoon when the air temperature was high and relative humidity was low, which is also suggested by previous studies (McGovern and Bruce, 2000; Thompson et al., 2014a). Heat dissipation through respiration followed a similar pattern as air temperature while long wave radiation showed an opposite pattern to air temperature, because respiration is mainly dependent on the air temperature and body temperature while long wave radiation depends on the difference between coat temperature and surrounding radiant temperature, which was smaller at noon and larger at midnight. Heat convection increased when solar radiation increased, because coat temperature increased due to solar radiation and caused a larger driving temperature difference for convection from the coat surface. Heat conduction between the animal and surface ground accounted for a very low percentage of the total heat dissipation, because only 20% of the animal surface is in contact with the ground when lying down (Ortiz et al., 2015). Based on our assumption, the animal did not lie down during most of the daytime when the temperature of ground surface was higher than skin temperature. Although the total heat dissipation through conduction was small, the heat flux of it showed a peak every time when the animal lied down between midnight and sunrise, which agrees with Bastian et al. (2003) reporting a great amount of heat dissipation through conduction when the ground temperature is low.

Sensitivity analysis

Local sensitivities of the top 10 parameters are shown in Fig. 7. Two analyses shared the same top 10 parameters with small differences in the rank. Air temperature was the most sensitive among the 10 parameters for both animal standing up and lying down. Besides, two

parameters (qevap_c and qevap_d) related to heat evaporation and four parameters (RR_a, RR_b, Vt_b and Te_b) related to respiration were also sensitive for both animal standing up and lying down. The other three top 10 sensitive parameters were heat production, surface area and air pressure, probably because heat production and surface area were in the differential equations and directly determine the gain and loss of heat, and air pressure was used to calculate multiple heat transfer mechanisms, including conduction, evaporation and respiration. The average R^2 of the regressions in the global sensitivity analysis was 0.96, indicating that the heat balance model was linear in the parameters and regression was a valid technique to investigate the global sensitivities. Six parameters with minimum global sensitivity greater than 0.05 are shown in Fig. 8. Two respiration parameters were the most sensitive before around 8 am, while the evaporation rate parameter became the most sensitive afterwards. All the six parameters were also within the top 10 local sensitivities.

The sensitivity analysis suggests that the parameters related to respiration and heat evaporation through sweating must be well quantified since small changes in those parameters can change the outcome considerably. Most of these parameters were derived from either old or small datasets, thus reevaluation of them with a large and recent dataset may improve the model accuracy and resolve the model overestimation. Heat production is assumed to be constant in our model, which does not account for the heat increment effect of feeding (Sprinkle, et al., 2000). In addition, heat stress induces behavioral and metabolic changes in cattle including reduced dry matter intake, selective consumption and reduced heat production (Fox and Tylutki, 1998), while the estimation of heat production in our model is based on a non-stressed condition. Since heat production is also a sensitive parameter, the bias of the overall heat production estimation may impact the model outcome. Besides, the long-term effect of heat stress and resulting

physiological changes were not considered in our model, and if incorporated, may change the sensitivity values.

Conclusions

In conclusion, a dynamic model describing the thermal balance of Holstein dairy cattle was developed in this study. Heat production by the animal, heat conduction among the body core, skin and coat, and heat flows between the animal and the environment, including conduction, convection, evaporation and radiation were considered. The model had an overestimation for the body temperature based on two real datasets, which may be resolved by reevaluating several sensitive parameters including respiration and evaporation coefficients using recent data. Despite some limitations, the thermal balance model can provide a guideline on the thermal condition of the animal under hot climate and a mechanistic modeling framework for future studies. Our future work will focus on evaluating and guiding the use of cooling strategies based on the thermal balance model.

Acknowledgements

This research was supported in part by the W. K. Kellogg Endowment and USDA National Institute of Food and Agriculture (Washington, DC) Multistate Research Project NC-2040. We gratefully acknowledge the infrastructure support of the Department of Animal Science, College of Agricultural and Environmental Sciences, and the California Agricultural Experiment Station of the University of California, Davis. We are grateful to Drs. Peter J. Hansen (University of Florida), Jennifer MC Van Os (University of Wisconsin, Madison), and Cassandra B Tucker (University of California, Davis) for generously sharing their experimental data.

References

Araki, C. T., R. M. Nakamura, L. W. G. Kam, and N. Clarke. 1984. Effect of lactation on diurnal temperature patterns of dairy cattle in hot environments. J. Dairy Sci. 67:1752–1760.

Atkins, I. K., N. B. Cook, M.R. Mondaca, and C.Y. Choi. 2018. Continuous respiration rate measurement of heat-stressed dairy cows and relation to environment, body temperature, and lying time. Trans. ASABE. 61: 1475–1485.

Baker, C. C., C. E. Coppock, J. K. Lanham, D. H. Nave, J. M. Labore, C. F. Brasington, and R. A. Stermer. 1988. Chilled drinking water effects on lactating Holstein cows in summer. J. Dairy Sci. 71:2699–2708.

Bastian, K. R., K. G. Gebremedhin, and N. R. Scott. 2003. A finite difference model to determine conduction heat loss to a water-filled mattress for dairy cows. Trans. ASAE. 46:773–780.

Bergman, T. L., F. P. Incropera, A. S. Lavine, and D.P. Dewitt. 2011. Introduction to heat transfer. John Wiley & Sons, (Chapter 5).

Berman, A. 2006. Extending the potential of evaporative cooling for heat-stress relief. J. Dairy Sci. 89:3817–3825.

Berman, A. 2008. Increasing heat stress relief produced by coupled coat wetting and forced ventilation. J. Dairy Sci. 91:4571–4578.

Bertipaglia, E. C. A., R. G. Silva, and A. S. C. Maia. 2005. Fertility and hair coat characteristics of Holstein cows in a tropical environment. Anim. Reprod. 2:187–194.

Bewley, J. M., M. W. Grott, M. E. Einstein, and M. M. Schutz. 2008. Impact of intake water temperatures on reticular temperatures of lactating dairy cows. J. Dairy Sci. 91:3880–3887.

Brody, S. 1945. Bioenergetics and growth. Reinhold Publishing Corporation, New York.

Campbell G. S., and J. M. Norman. 1998. An introduction to environmental biophysics, 2nd ed. Springer, New York.

Chen, J. M., K. E. Schütz, and C. B. Tucker. 2015. Cooling cows efficiently with sprinklers: Physiological responses to water spray. J. Dairy Sci. 98:6925–6938.

Chen, J. M., K. E. Schütz, and C. B. Tucker. 2016. Cooling cows efficiently with water spray: Behavioral, physiological, and production responses to sprinklers at the feed bunk. J. Dairy Sci. 99:4607–4618.

Cook, N. B., R. L. Mentink, T. B. Bennett, and K. Burgi. 2007. The effect of heat stress and lameness on time budgets of lactating dairy cows. J. Dairy Sci. 90:1674–1682.

da Silva, R. G., N. LaScala, A. Lima Filho, and M. Catharin. 2002. Respiratory heat loss in the sheep: a comprehensive model. Int. J. Biometeorol. 46:136–140.

Das, R., L. Sailo, N. Verma, P. Bharti, and J. Saikia. 2016. Impact of heat stress on health and performance of dairy animals: A review. Vet. World. 9:260.

Dikmen, S., and P. J. Hansen. 2009. Is the temperature-humidity index the best indicator of heat stress in lactating dairy cows in a subtropical environment?. J. Dairy Sci. 92:109–116.

Drwencke, A. M., G. Tresoldi, M. M. Stevens, V. Narayanan, A. V. Carrazco, F. M. Mitloehner, T. E. Pistochini, and C. B. Tucker. 2020. Innovative cooling strategies: Dairy cow responses and water and energy use. J. Dairy Sci. 103:5440–5454.

Duffie, J. A., and A. B. William. 2013. Solar engineering of thermal processes, 4th ed. John Wiley & Sons, Inc., Hoboken, New Jersey.

Ehrlemark, A. 1988. Calculation of sensible heat and moisture loss from housed cattle using a heat balance model. Department of Farm Buildings, Swedish University of Agricultural Sciences, Uppsala, Sweden.

Fox, D. G., and T. P. Tylutki. 1998. Accounting for the effects of environment on the nutrient requirements of dairy cattle. J. Dairy Sci. 81:3085–3095.

Gebremedhin, K. G., and B. Wu. 2001. A model of evaporative cooling of wet skin surface and fur layer. J. Therm. Biol. 26:537–545.

Gebremedhin, K. G., B. Wu, and K. Perano. 2016. Modeling conductive cooling for thermally stressed dairy cows. J. Therm. Biol. 56:91–99.

Hansen, P. J. 2020. Prospects for gene introgression or gene editing as a strategy for reduction of the impact of heat stress on production and reproduction in cattle. Theriogenology. 154:190–202.

Hottel, H. C. 1976. A simple model for estimating the transmittance of direct solar radiation through clear atmospheres. Sol. Energy. 18:129–134.

Kuehn, L. A., R. A. Stubbs, and R. S. Weaver. 1970. Theory of the globe thermometer. J. Appl. Physiol. 29:750–757.

Lacetera, N., U. Bernabucci, B. Ronchi, and A. Nardone. 1996. Body condition score, metabolic status and milk production of early lactating dairy cows exposed to warm environment. Riv. Agric. Subtrop. Trop. 90:43–55.

Lawrence, I., and K. Lin. 1989. A concordance correlation coefficient to evaluate reproducibility. Biometrics. 45: 255–268.

Liu, B. Y., and R. C. Jordan. 1960. The interrelationship and characteristic distribution of direct, diffuse and total solar radiation. Sol. energy. 4:1–19.

Mader, T. L., M. S. Davis, and T. Brown-Brandl. 2006. Environmental factors influencing heat stress in feedlot cattle. J. Anim. Sci. 84:712–719.

Maia, A. S. C., and C. B. Loureiro. 2005. Sensible and latent heat loss from the body surface of Holstein cows in a tropical environment. Int. J. Biometeorol. 50:17–22.

Maia, A. S. C., R. G. DaSilva, and C. M. B. Loureiro. 2005. Respiratory heat loss of Holstein cows in a tropical environment. Int. J. Biometeorol. 49:332–336.

McArthur, A. J. 1981. Thermal resistance and sensible heat loss from animals. J. Therm. Biol. 6:43–47.

McArthur, A. J. 1987. Thermal interaction between animal and microclimate: a comprehensive model. J. Theor. Biol. 126:203–238.

McGovern, R. E., and J. M. Bruce. 2000. AP—Animal Production Technology: A model of the thermal balance for cattle in hot conditions. J. Agric. Eng. Res. 77:81–92.

Monteith, J., and M. Unsworth. 2013. Principles of environmental physics: plants, animals, and the atmosphere. Academic Press, Oxford, UK.

Murray, F.W. 1967. On the computation of saturation vapor pressure. J. Appl. Meteor. 6:203–204.

Nabenishi, H., H. Ohta, T. Nishimoto, T. Morita, K. Ashizawa, and Y. Tsuzuki. 2011. Effect of the temperature-humidity index on body temperature and conception rate of lactating dairy cows in southwestern Japan. J. Repro. Develop. 1104050364–1104050364.

Najib, A., A. Zarrella, V. Narayanan, R. Bourne, and C. Harrington. 2020. Techno-economic parametric analysis of large diameter shallow ground heat exchanger in California climates. Energ. Buildings, 228:110444.

Nardone, A., B. Ronchi, N. Lacetera, M. S. Ranieri, and U. Bernabucci. 2010. Effects of climate changes on animal production and sustainability of livestock systems. Livest. Sci. 130:57–69.

Nay, T., and R. H. Hayman. 1963. Some skin characters in five breeds of European (Bos taurus) dairy cattle. Aust. J. Agric. Res. 14:294–302.

NRC. 2001. Nutrient Requirements of Dairy Cattle. 7th rev. ed. National Academy Press, Washington, DC.

Ortiz, X.A., J. F. Smith, F. Rojano, C. Y. Choi, J. Bruer, T. Steele, N. Schuring, J. Allen, and R. J. Collier. 2015. Evaluation of conductive cooling of lactating dairy cows under controlled environmental conditions. J. Dairy Sci. 98:1759–1771.

Purwanto, B. P., Y. Abo, R. Sakamoto, F. Furumoto, and S. Yamamoto. 1990. Diurnal patterns of heat production and heart rate under thermoneutral conditions in Holstein Friesian cows differing in milk production. J. Agric. Sci. 114:139–142.

Radoń, J., W. Bieda, J. Lendelová, and Š. Pogran. 2014. Computational model of heat exchange between dairy cow and bedding. Comp. Electron. Agric. 107:29–37.

Roenfeldt, S. 1998. You can't afford to ignore heat stress. Dairy Herd Manag. 35:6–12.

Roth, Z., R. Meidan, R. Braw-Tal, and D. Wolfenson. 2000. Immediate and delayed effects of heat stress on follicular development and its association with plasma FSH and inhibin concentration in cows. J. Rep. Fer. 120:83–90.

Saltelli, A., M. Ratto, T. Andres, F. Campolongo, J. Cariboni, D. Gatelli, M. Saisana, and S. Tarantola. 2008. Global sensitivity analysis: the primer. John Wiley & Sons Ltd, West Sussex, England.

Scott, I. M., H. D. Johnson, and G. L. Hahn. 1983. Effect of programmed diurnal temperature cycles on plasma thyroxine level, body temperature, and feed intake of Holstein dairy cows. Int. J. Biometeorol. 27:47–62.

Shultz, T. A. 1984. Weather and shade effects on cow corral activities. J. Dairy Sci. 67:868–873.

Silva, R. G. D., and A. S. C. Maia. 2011. Evaporative cooling and cutaneous surface temperature of Holstein cows in tropical conditions. Revista Brasileira de Zootecnia. 40:1143–1147.

Smith, N. E., and R. L. Baldwin. 1974. Effects of breed, pregnancy, and lactation on weight of organs and tissues in dairy cattle. J Dairy Sci. 57:1055–1060.

Soetaert, K., and T. Petzoldt. 2010. Inverse modelling, sensitivity and Monte Carlo analysis in R using package FME. J. Stat. Softw. 33:1–28.

Sonntag, D. 1990. Important new values of the physical constants of 1986, vapour pressure formulations based on the ITS-90, and psychrometer formulae. Zeitschrift für Meteorologie. 40:340–344.

Sprinkle, J. E., J. W. Holloway, B. G. Warrington, W. C. Ellist, J. W. Stuth, T. D. A. Forbes, and L.W. Greene. 2000. Digesta kinetics, energy intake, grazing behavior, and body temperature of grazing beef cattle differing in adaptation to heat. J. Anim. Sci. 78:1608–1624.

Stevens, D. G. 1981. A model of respiratory vapor loss in Holstein dairy cattle. Trans. ASAE. 24:151–0153.

Thompson, V. A. 2011. Development and Evaluation of a Dynamic, Mechanistic, Thermal Balance Model for Bos indicus and Bos taurus. University of California, Davis.

Thompson, V. A., J. G. Fadel, and R. D. Sainz. 2011. Meta-analysis to predict sweating and respiration rates for Bos indicus, Bos taurus, and their crossbreds. J. Anim. Sci. 89:3973–3982.

Thompson, V. A., L. G. Barioni, T. R. Rumsey, J. G. Fadel, and R. D. Sainz. 2014a. The development of a dynamic, mechanistic, thermal balance model for Bos indicus and Bos taurus. J. Agric. Sci. 152:464.

Thompson, V. A., R. D. Sainz, A. B. Strathe, T. R. Rumsey, and J. G. Fadel. 2014b. The evaluation of a dynamic, mechanistic, thermal balance model for Bos indicus and Bos taurus. J. Agric. Sci. 152:483.

Thorsson, S., F. Lindberg, I. Eliasson, and B. Holmer. 2007. Different methods for estimating the mean radiant temperature in an outdoor urban setting. Int. J. Climatol. 27:1983–1993.

Tucker, C. B., K. E. Schütz, and M. Jennifer. 2020. Data from: Cooling cows efficiently with sprinklers: physiological responses to water spray. Accessed May 28, 2020. https://doi.org/10.25338/B88P7H.

Turnpenny, J. R., A. J. McArthur, J. A. Clark, and C. M. Wathes. 2000a. Thermal balance of livestock: 1. A parsimonious model. Agric. For. Meteorol. 101:15–27.

Turnpenny, J. R., C. M. Wathes, J. A. Clark, and A. J. McArthur. 2000b. Thermal balance of livestock: 2. Applications of a parsimonious model. Agric. For. Meteorol. 101:29–52.

U. S. Climate Data. (2021). Climate Davis – California. Accessed April 3, 2021. https://www.usclimatedata.com/climate/davis/california/united-states/usca0284.

Weather Underground. 2019. Davis, CA weather condition. Accessed July 29, 2019. https://www.wunderground.com/weather/us/ca/davis.

West, J. W. 2003. Effects of heat-stress on production in dairy cattle. J. Dairy Sci. 86:2131–2144.

Yamamoto, S., B. A. Young, B. P. Purwanto, F. Nakamasu, and T. Matsumoto. 1994. Effect of solar radiation on the heat load of dairy heifers. Aust. J. Agric. Res. 45:1741–1749.

Zarrella, A., and M. De Carli. 2013. Heat transfer analysis of short helical borehole heat exchangers. Appl. Energy 102:1477–1491.

Zimbelman, R. B., R. P. Rhoads, M. L. Rhoads, G. C. Duff, L. H. Baumgard, and R. J. Collier. 2009. A re-evaluation of the impact of temperature humidity index (THI) and black globe humidity index (BGHI) on milk production in high producing dairy cows. Proceedings of the 24th Southwest Nutrition and Management Conference, pp 158–169.

Tables and Figures

Table 1. The average percentage (%) of heat dissipation through convection, evaporation, long wave radiation, respiration and conduction between animal and ground surface to the sum of them during different time periods for the simulation based on the weather condition in Davis (CA) from July 26 to 28, 2019.

	0000 to 0600 h	0600 to 1200 h	1200 to 1800 h	1800 to 2400 h	Entire day
Convection	14.1	19.8	14.9	8.0	14.9
Evaporation	32.6	49.3	57.0	45.7	48.0
Long wave radiation	28.7	16.6	11.5	21.8	18.2
Respiration	15.9	13.8	16.6	19.7	16.2
Conduction	8.7	0.5	-	4.8	2.7

A: Standing up

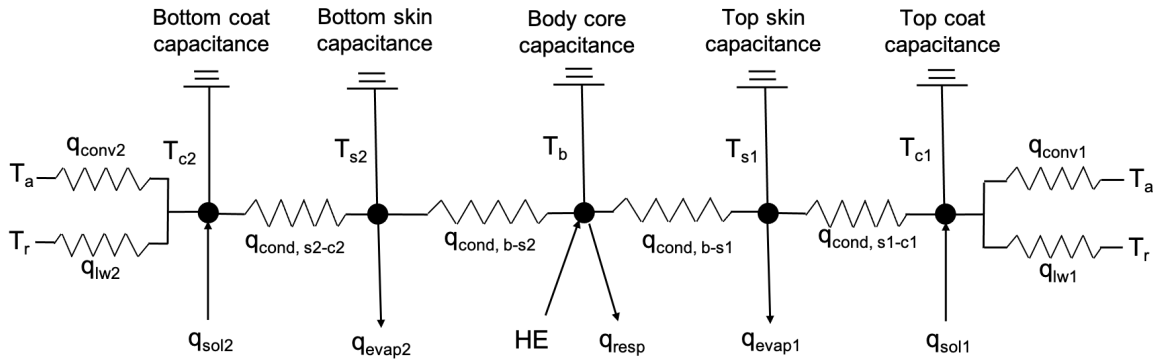

B: Lying down

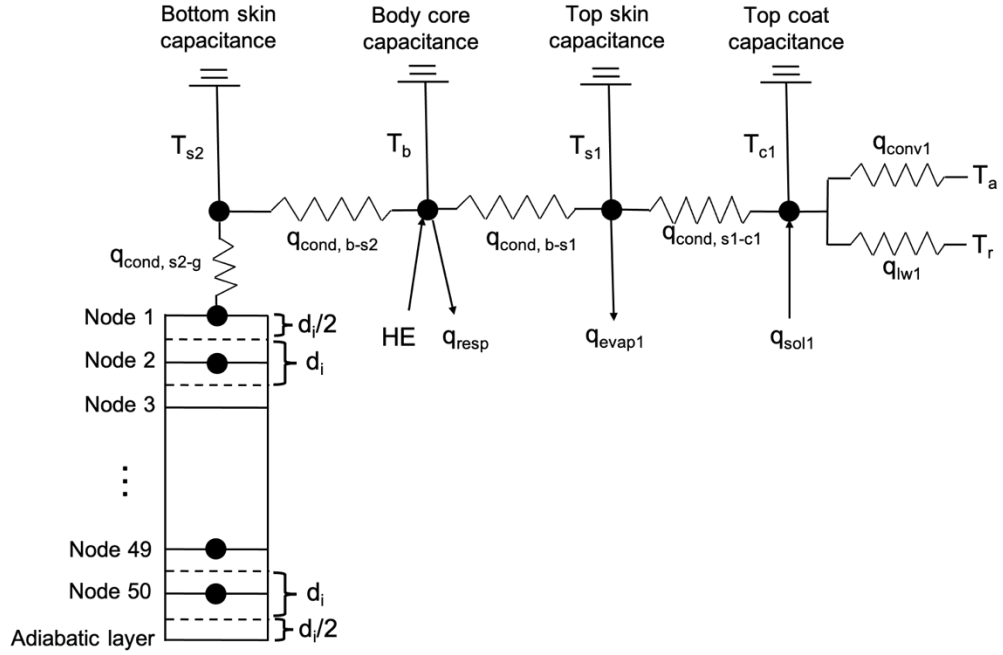

Figure 1. The thermal network diagram of the heat balance model for a dairy cow standing (A) up and lying down (B). T_b = Body temperature, T_{s1} = Top skin temperature (K), T_{s2} = Bottom skin temperature (K), T_{c1} = Top coat temperature (K), T_{c2} = Bottom coat temperature (K), T_a = Air temperature (K), T_r = Surrounding radiant temperature (K), HE = Heat production (W), q_{resp} = Heat dissipation through respiration (W), $q_{cond, b-s1}$ = Heat conduction between body core and top skin (W), $q_{cond, b-s2}$ = Heat conduction between body core and bottom skin (W), q_{evap1} = Heat dissipation through evaporation through sweating at the top skin (W), q_{evap2} = Heat dissipation through evaporation through sweating at the bottom skin (W), $q_{cond, s1-c1}$ = Heat conduction between top skin and top coat (W), $q_{cond, s2-c2}$ = Heat conduction between bottom skin and top coat (W), q_{sol1} = Solar radiation at the top coat (W), q_{sol2} = Solar radiation at the bottom coat (W), q_{conv1} = Heat convection at the top coat surface (W), q_{conv2} = Heat convection at the bottom

coat surface (W), q_{lw1} = Long wave radiation between the top coat and surrounding (W), q_{lw2} = Long wave radiation between the bottom coat and surrounding (W), $q_{cond,\ s2\text{-}g}$ = Heat conduction between bottom skin and ground surface (W). For each node, the capacitance is able to store and dissipate heat with time, which brings about transient temperature changes. The arrow indicates the one-way direction of heat flows (HE, q_{resp}, q_{evap1}, q_{evap2}, q_{sol1} and q_{sol2}), while the other heat flows can happen in either direction to or from the node. When the animal lies down (B), the vertical distance from the bottom skin to adiabatic layer is divided into 50 nodes, with the distance between each of two nodes d_i equal to 0.01 m, and the dashed lines represent the center of each control volume. The bottom coat capacitance was not accounted and T_{s2} is the same as T_{c2} when the animal lies down.

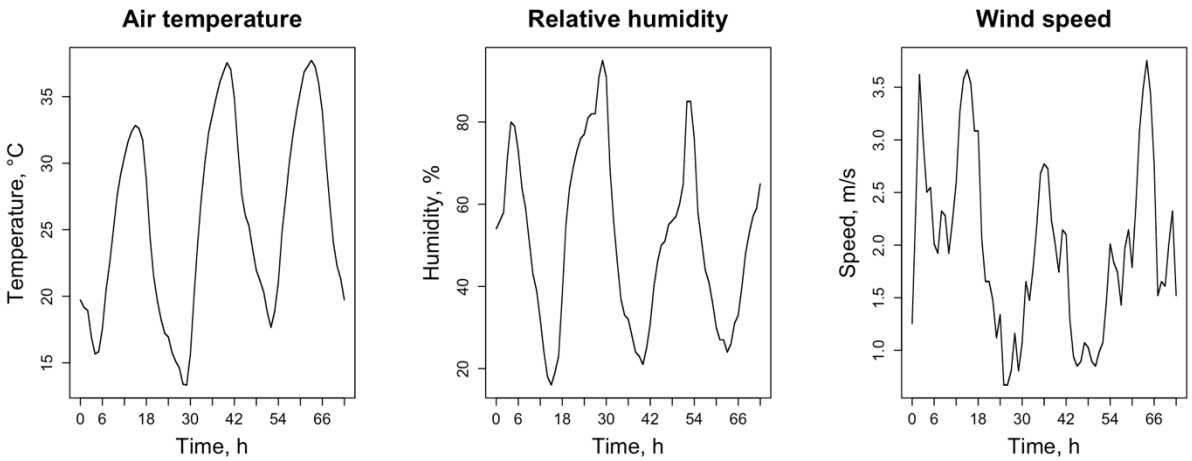

Figure 2. Air temperature, relative humidity and wind speed in Davis (CA) from July 26 to 28, 2019.

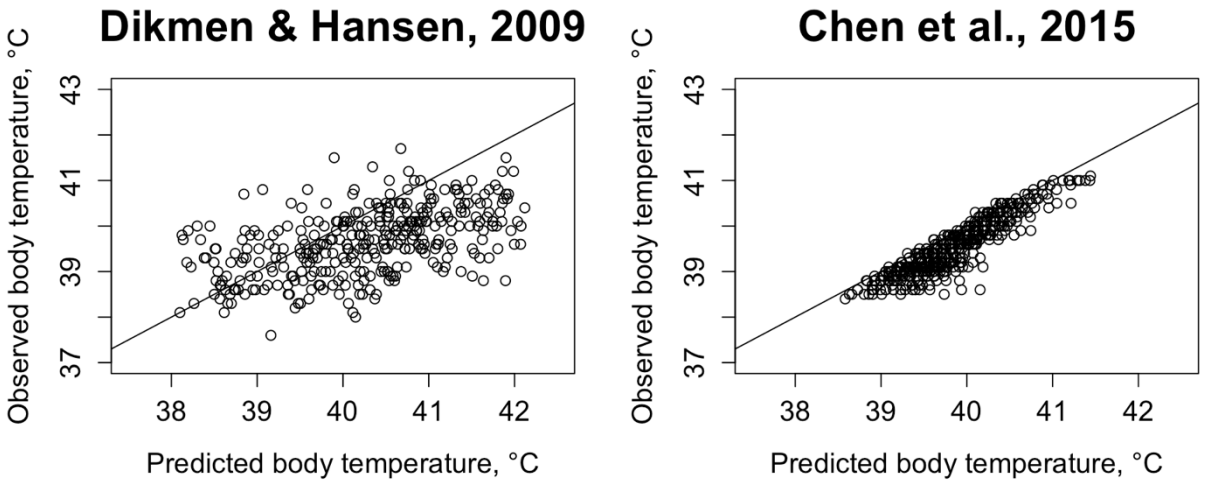

Figure 3. Observed body temperatures from Dikmen and Hansen (2009) and Chen et al. (2015) against predicted body temperatures based on the thermal balance model. The solid line (y = x) represents a perfect prediction.

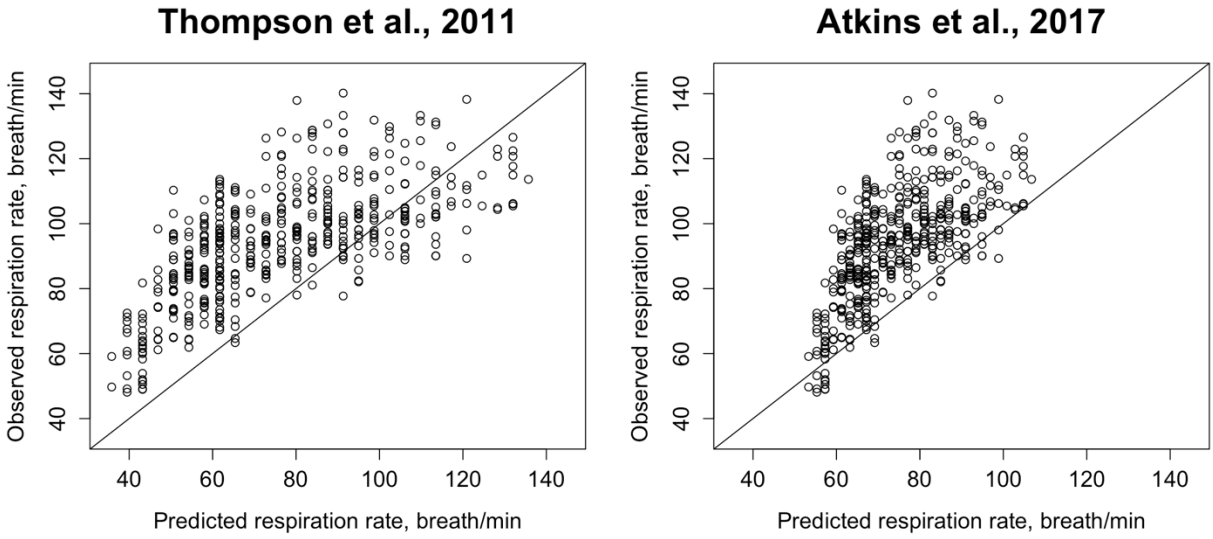

Figure 4. Observed respiration rate from Chen et al. (2015) against predicted respiration rate based on y = 37x – 1385 (Thompson et al., 2011) and y = 19.8x – 707 (Atkins et al., 2017), where x is body temperature (°C) and y is respiration rate (breath/min). The solid line represents a perfect prediction.

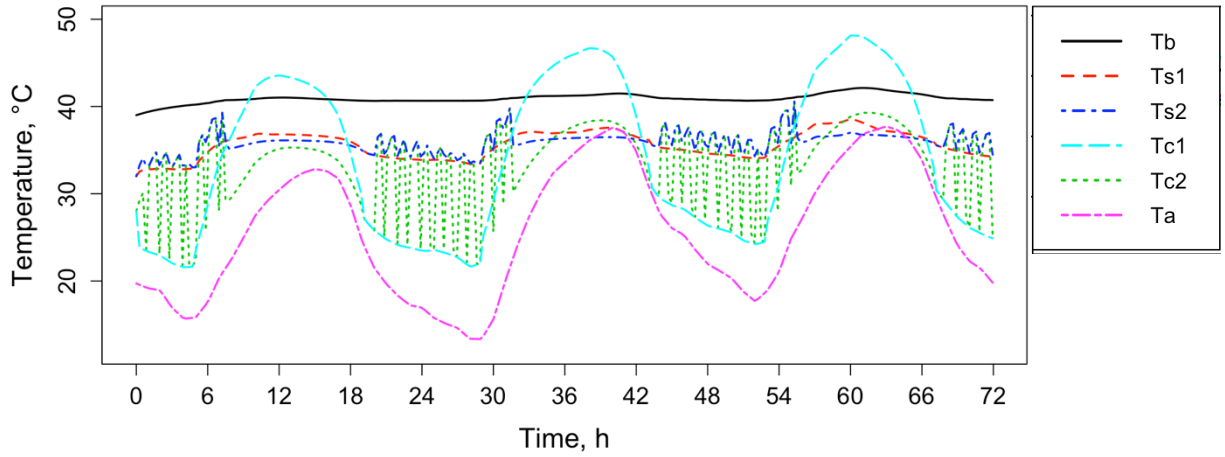

Figure 5. Simulation of body temperature (T_b), top (T_{s1}) and bottom (T_{s2}) skin temperature, and top (T_{c1}) and bottom (T_{c2}) coat temperature based on the air temperature (T_a), relative humidity and wind speed in Davis (CA) from July 26 to 28, 2019.

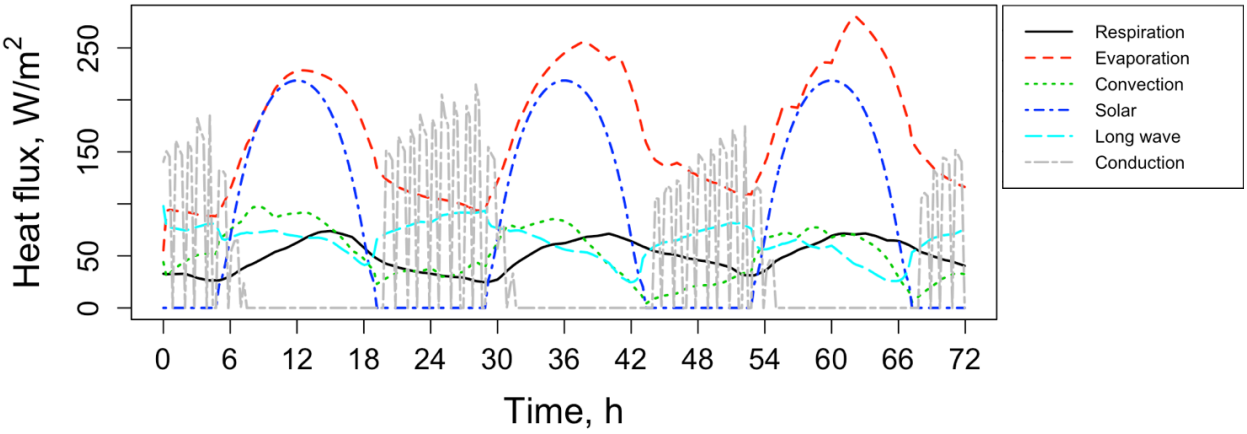

Figure 6. Simulated heat flux of respiration, evaporation, convection, solar radiation, long wave radiation and conduction between animal and ground based on the weather condition in Davis (CA) from July 26 to 28, 2019. Evaporation, convection, solar radiation, and long wave radiation are shown as the weighted average heat flux (e.g., evaporation = 0.8 evaporation at the top skin + 0.2 evaporation at the bottom skin) at the bottom and top nodes.

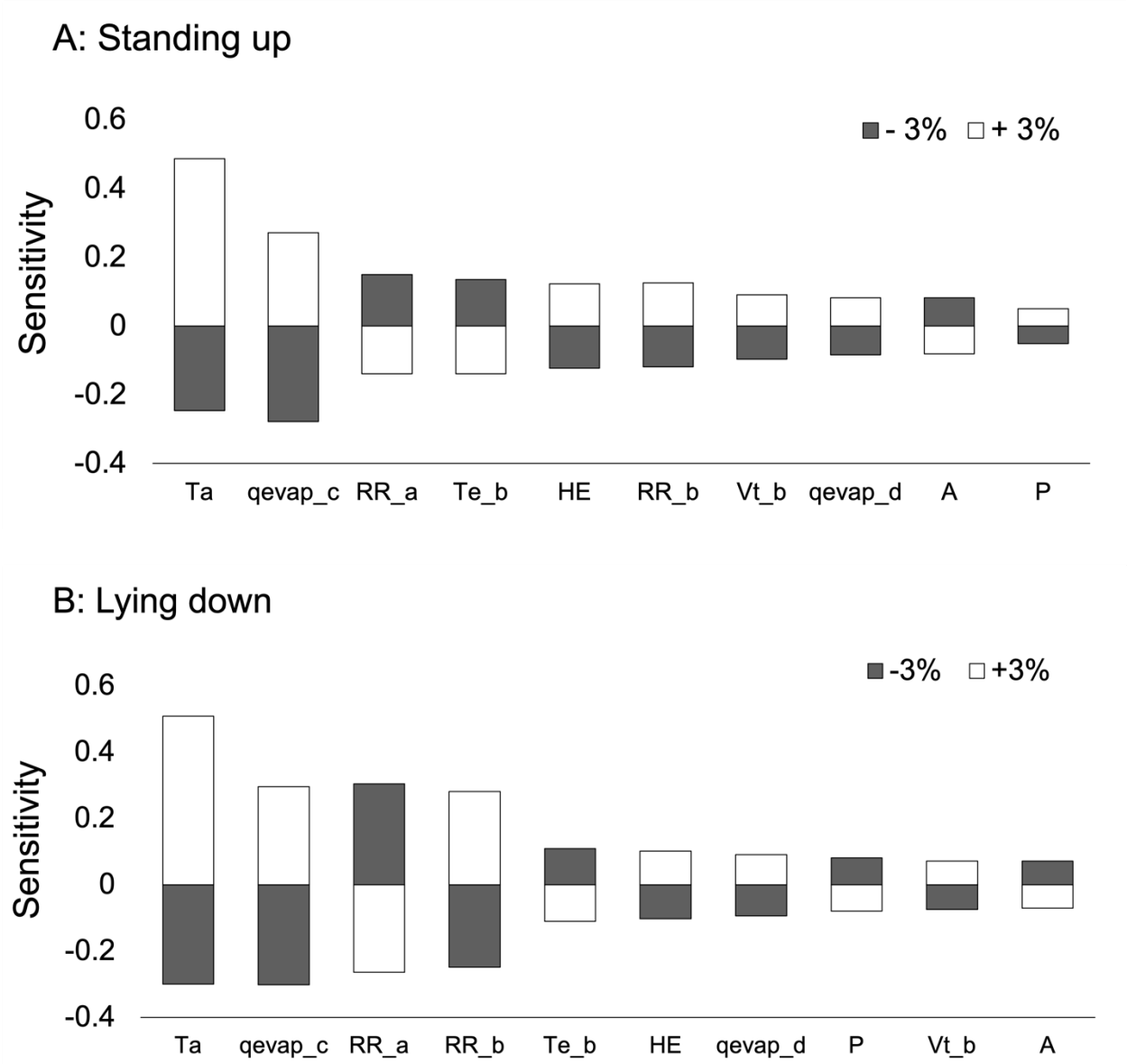

Figure 7. Top 10 sensitive parameters in the local sensitivity analyses for a dairy cow standing up (A) and lying down (B) when changing the parameters ± 3%. Ta = Air temperature (K), qevap_c = Parameter c for evaporation rate (dimensionless), RR_a = Parameter a for respiration rate (dimensionless), Te_b = Parameter b for exhaled air temperature, HE = Heat production (W), RR_b = Parameter b for respiration rate (dimensionless), Vt_b = Parameter b for tidal volume (dimensionless), qevap_d = Parameter d for evaporation rate (dimensionless), A = Animal surface area (m^2), P = Air pressure (Pa).

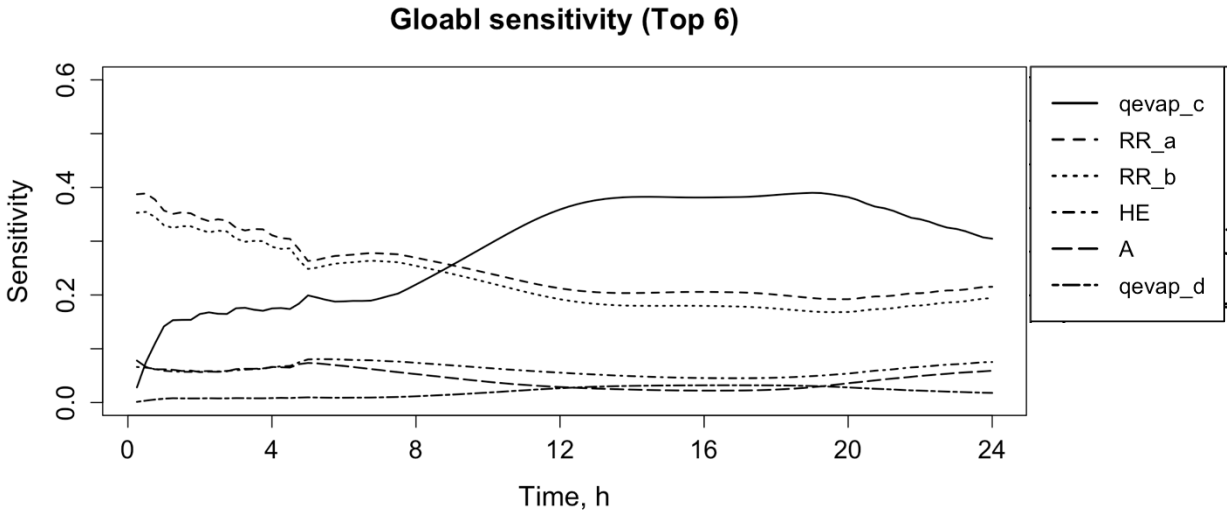

Figure 8. Global sensitivity (top 6) of the parameters throughout 24 h. qevap_c = Parameter c for evaporation rate, RR_a = Parameter a for respiration rate, RR_b = Parameter b for respiration rate, HE = Heat production (W), A = Animal surface area (m^2), qevap_d = Parameter d for evaporation rate (dimensionless).

Appendix A

Detailed description of variables and equations used in the thermal balance model are as follows.

Variables and parameters

Table A1. Description of all variables and parameters used in the model

Symbol	Description	Unit	Reference
A	Animal surface area	m^2	Brody, 1945
a_0	Atmospheric transmittance coefficient, intercept	dimensionless	Hottel, 1976
a_1	Atmospheric transmittance coefficient, slope	dimensionless	Hottel, 1976
Ah/A	The ratio of shadow area to body area	dimensionless	Monteith and Unsworth, 2013
Al	Altitude	km	-
a_s	Skin parameter, 1.11 for lactating animals and 1.17 for nonlactating ones	dimensionless	Smith and Baldwin, 1974
BW	Animal body weight	kg	-
C_f	Drag coefficient	dimensionless	Gebremedhin and Wu, 2001
c_h	Heat production coefficient, 44.1 for high production cows (milk yield $\geqslant$ 30 kg/d), 38.7 for intermediate production cows (milk yield < 30 kg/d) and 29.7 for dry cows.	dimensionless	Purwanto et al., 1990
c_p	Specific heat of air, 1006	J kg^{-1} K^{-1}	-
c_{psoil}	Specific heat of soil, 1784	J kg^{-1} K^{-1}	Najib et al., 2020
c_{pb}	Specific heat capacity of body core, 3472	J kg^{-1} K^{-1}	Gebremedhin et al., 2016
c_{pc}	Specific heat capacity of coat, 1006.43	J kg^{-1} K^{-1}	Gebremedhin et al., 2016
c_{ps}	Specific heat capacity of skin, 3472	J kg^{-1} K^{-1}	Gebremedhin et al., 2016
D	Diffusive coefficient of water vapor	m^2 s^{-1}	Gebremedhin and Wu, 2001
d	Characteristic diameter	m	Ehrlemark ,1988
d_a	Laminar thickness	m	Gebremedhin and Wu, 2001
d_c	Coat thickness, 0.0025	m	Bertipaglia et al., 2005

d_h	Hair diameter, 0.0625	mm	Bertipaglia et al., 2005
d_i	Distance between two nodes underground, 0.01	m	-
D_o	Diffusive coefficient of water vapor under T_o and P_o, 2.2 $\times 10^{-5}$	$m^2\ s^{-1}$	Gebremedhin and Wu, 2001
Gsc	Solar constant, 1367	$W\ m^{-2}$	Duffie and Beckman, 2013
HE	Heat production rate	W	Purwanto et al., 1990; NRC (2001)
h_c	Convection coefficient	$W\ m^{-2}\ K^{-1}$	Monteith and Unsworth, 2013
h_m	Mass transfer coefficient	$m\ s^{-1}$	Gebremedhin and Wu, 2001
k	Atmospheric transmittance coefficient, rate	dimensionless	Hottel, 1976
k_a	Air conductivity, 0.024	$W\ m^{-1}\ k^{-1}$	Gebremedhin et al., 2016
k_{eff}	Effective thermal conductivity	$W\ m^{-1}\ K^{-1}$	Gebremedhin et al., 2001
k_f	Fur conductivity, 0.26	$W\ m^{-1}\ k^{-1}$	Gebremedhin et al., 2016
k_{soil}	Soil conductivity, 1,64	$W\ m^{-1}\ k^{-1}$	Najib et al., 2020
k_x	Horizontal thermal conductivity	$W\ m^{-1}\ K^{-1}$	Gebremedhin and Wu, 2001
k_y	Vertical thermal conductivity	$W\ m^{-1}\ K^{-1}$	Gebremedhin and Wu, 2001
l	Body length, 2.15	m	Gebremedhin and Wu, 2001
M_b	Body core mass	kg	-
M_c	Coat mass	kg	Berman, 2008
ME	Metabolizable energy intake	J	-
M_s	Skin mass	kg	Smith and Baldwin, 1974
Mw	Molar mass of water, 18	$g\ mol^{-1}$	-
n	Julian day number, 1 to 365	d	-
Nu	Nusselt number	dimensionless	Gebremedhin and Wu, 2001
P	Air pressure	Pa	-
p_c	Proportion of contact surface to the whole animal surface area, 0.2	Dimensionless	Ortiz et al., 2015
P_o	Atmospheric pressure, 101325	Pa	-

Pr	Prandtl number, 0.7	dimensionless	Gebremedhin and Wu, 2001
$Pw, sat(T_a)$	Saturation vapor pressure at T_a	Pa	Murray, 1967
$Pw, sat(T_e)$	Saturation vapor pressure at T_e	Pa	Murray, 1967
$Pw, sat(T_{s1})$	Saturation vapor pressure at T_{s1}	Pa	Murray, 1967
$Pw, sat(T_{s2})$	Saturation vapor pressure at T_{s2}	Pa	Murray, 1967
$Pw(T_a)$	Vapor pressure at T_a	Pa	-
$q''_{cond, b-s1}$	Heat conduction between body core and top skin	W m^{-2}	-
$q''_{cond, b-s2}$	Heat conduction between body core and bottom skin	W m^{-2}	-
$q''_{cond, i}$	Heat conduction flux at node i underground	W m^{-2}	-
$q''_{cond, s1-c1}$	Heat conduction between top skin and top coat	W m^{-2}	-
$q''_{cond, s2-c2}$	Heat conduction between bottom skin and bottomcoat	W m^{-2}	-
$q''_{cond, s2-g}$	Heat conduction between bottom skin and ground	W m^{-2}	-
q''_{conv1}	Heat convection at top coat surface	W m^{-2}	-
q''_{conv2}	Heat convection at bottom coat surface	W m^{-2}	-
q''_{evap1}	Heat evaporation through sweating at top skin	W m^{-2}	Silva and Maia, 2011; Gebremedhin and Wu, 2001
q''_{evap2}	Heat evaporation through sweating at bottom skin	W m^{-2}	Silva and Maia, 2011; Gebremedhin and Wu, 2001
q''_{lat}	Latent heat transfer	W m^{-2}	Monteith and Unsworth, 2013
q''_{lw1}	Long wave radiation at top coat	W m^{-2}	-
q''_{lw2}	Long wave radiation at bottom coat	W m^{-2}	-
q''_{resp}	Heat loss through respiration	W m^{-2}	McGovern, 2000; da Silva et al., 2002; Monteith and Unsworth, 2013
q''_{sen}	Sensible heat transfer	W m^{-2}	Monteith and Unsworth, 2013
q''_{sol1}	Solar radiation at top coat	W m^{-2}	Turnpenny et al., 2000a
q''_{sol2}	Solar radiation at bottom coat	W m^{-2}	Turnpenny et al., 2000a
R	Molar gas constant, 8.314	J mol^{-1} K^{-1}	-

R_d	Gas constant, 287	J kg^{-1} K^{-1}	-
RE	Retained energy	J	-
Re	Reynolds number	dimensionless	Gebremedhin and Wu, 2001
RH	Relative humidity	%	-
RR	Respiration rate	breath s^{-1}	Thompson et al., 2011
r_{sg}	Heat conduction resistance between the skin and the ground surface, 0.1	m^2 K W^{-1}	Radoń et al., 2014
S_b	Direct radiation	W·m^{-2}	Duffie and Beckman, 2013
Sc	Schmidt number	Dimensionless	Gebremedhin and Wu, 2001
S_d	Diffuse radiation	W m^{-2}	Duffie and Beckman, 2013
S_e	Extraterrestrial radiation	W m^{-2}	Duffie and Beckman, 2013
St	Standard time	h	-
T_a	Air temperature	K	-
T_b	Body temperature	K	-
T_{black}	Black globe temperature	K	-
T_{c1}	Top coat temperature	K	-
T_{c1}	Bottom coat temperature	K	-
T_{dp}	Dew point temperature	°C	Sonntag, 1990
T_e	Exhaled air temperature	K	Maia et al., 2005
T_g	Ground surface temperature	K	Thompson, 2011
$T_{g,\,i}$	Ground temperature at node i, for i = 1, …, 50	K	-
T_o	0 Celsius degree in Kelvins, 273.15	K	-
T_r	Radiant temperature of environment	K	Kuehn et al., 1970; Thorsson et al., 2007; Thompson et al., 2014a
T_{s1}	Top skin temperature	K	-
T_{s2}	Bottom skin temperature	K	-

T_{sky}	Sky temperature	K	Duffie and Beckman, 2013
Tv_a	Virtual temperature of inhaled air	K	Monteith and Unsworth, 2013
Tv_e	Virtual temperature of exhaled air	K	Monteith and Unsworth, 2013
u	Wind speed	$m\ s^{-1}$	-
v	Kinematic viscosity of air	$m^2\ s^{-1}$	Gebremedhin and Wu, 2001
V_t	Tidal volume	$m^3\ breath^{-1}$	Stevens, 1981
α_s	Solar altitude angle, $\pi/2 - \theta_z$	rad	-
δ	Declination	rad	Monteith and Unsworth, 2013
γ	Azimuth angle	rad	-
γ_a	Animal angle (the angle between the animal long axis and south direction), $-\pi/2$ to $\pi/2$	rad	-
γ_s	Solar azimuth angle	rad	Monteith and Unsworth, 2013
ε_c	Emissivity of coat, 0.98	Dimensionless	Maia, 2005
θ_z	Zenith angle	rad	Monteith and Unsworth, 2013
λ	Latent heat of vaporization of water, 2430	$J\ g^{-1}$	Monteith and Unsworth, 2013
μ	Dynamic viscosity of air	$kg\ m^{-1}\ s^{-1}$	-
π	Constant, 3.14	-	-
ρ	Air density	$kg\ m^{-3}$	-
ρ_c	Reflection coefficient of coat, 0.3	dimensionless	Turnpenny et al., 2000b
ρc_p	Volumetric heat capacity of air	$J\ m^{-3}\ K^{-1}$	-
ρ_g	Reflection coefficient of ground, 0.25 for grass, 0.08 for wet dark soil, 0.13 for dry dark soil, 0.10 for wet light soil and 0.18 for dry light soil	dimensionless	Campbell and Norman, 1998
ρ_h	Fur density, 9.87	$hairs\ mm^{-2}$	Bertipaglia et al., 2005
ρ_{soil}	Soil density, 1559	$kg\ m^{-3}$	Najib et al., 2020
σ	Stefan-Boltzmann constant, 5.67×10^{-8}	$W\ m^{-2}\ K^{-4}$	-

τ_b	Atmospheric transmittance for beam radiation	dimensionless	Hottel, 1976
τ_d	Atmospheric transmittance for diffuse radiation	dimensionless	Liu and Jordan, 1960
φ	Latitude, $-\pi/2$ to $\pi/2$	rad	-
χ_a	Absolute humidity of inhaled air	g m^{-3}	Monteith and Unsworth, 2013
χ_e	Absolute humidity of exhaled air	g m^{-3}	Monteith and Unsworth, 2013
χ_{s1}	Absolute humidity of top skin surface	g m^{-3}	Monteith and Unsworth, 2013
χ_{s2}	Absolute humidity of bottom skin surface	g m^{-3}	Monteith and Unsworth, 2013
ω	Hour angle	rad	Monteith and Unsworth, 2013

Symbol	Description	Unit	Reference
A	Animal surface area	m^2	Brody, 1945
a_0	Atmospheric transmittance coefficient, intercept	dimensionless	Hottel, 1976
a_1	Atmospheric transmittance coefficient, slope	dimensionless	Hottel, 1976
Ah/A	The ratio of shadow area to body area	dimensionless	Monteith and Unsworth, 2013
Al	Altitude	km	-
a_s	Skin parameter, 1.11 for lactating animals and 1.17 for nonlactating ones	dimensionless	Smith and Baldwin, 1974
BW	Animal body weight	kg	-
C_f	Drag coefficient	dimensionless	Gebremedhin and Wu, 2001
c_h	Heat production coefficient, 44.1 for high production cows (milk yield $\geqslant$ 30 kg/d), 38.7 for intermediate production cows (milk yield < 30 kg/d) and 29.7 for dry cows.	dimensionless	Purwanto et al., 1990
c_p	Specific heat of air, 1006	J kg^{-1} K^{-1}	-
c_{psoil}	Specific heat of soil, 1784	J kg^{-1} K^{-1}	Najib et al., 2020
c_{pb}	Specific heat capacity of body core, 3472	J kg^{-1} K^{-1}	Gebremedhin et al., 2016
c_{pc}	Specific heat capacity of coat, 1006.43	J kg^{-1} K^{-1}	Gebremedhin et al., 2016
c_{ps}	Specific heat capacity of skin, 3472	J kg^{-1} K^{-1}	Gebremedhin et al., 2016

D	Diffusive coefficient of water vapor	$m^2\ s^{-1}$	Gebremedhin and Wu, 2001
d	Characteristic diameter	m	Ehrlemark ,1988
d_a	Laminar thickness	m	Gebremedhin and Wu, 2001
d_c	Coat thickness, 0.0025	m	Bertipaglia et al., 2005
d_h	Hair diameter, 0.0625	mm	Bertipaglia et al., 2005
d_i	Distance between two nodes underground, 0.01	m	-
D_o	Diffusive coefficient of water vapor under T_o and P_o, 2.2×10^{-5}	$m^2\ s^{-1}$	Gebremedhin and Wu, 2001
Gsc	Solar constant, 1367	$W\ m^{-2}$	Duffie and Beckman, 2013
HE	Heat production rate	W	Purwanto et al., 1990; NRC (2001)
h_c	Convection coefficient	$W\ m^{-2}\ K^{-1}$	Monteith and Unsworth, 2013
h_m	Mass transfer coefficient	$m\ s^{-1}$	Gebremedhin and Wu, 2001
k	Atmospheric transmittance coefficient, rate	dimensionless	Hottel, 1976
k_a	Air conductivity, 0.024	$W\ m^{-1}\ k^{-1}$	Gebremedhin et al., 2016
k_{eff}	Effective thermal conductivity	$W\ m^{-1}\ K^{-1}$	Gebremedhin et al., 2001
k_f	Fur conductivity, 0.26	$W\ m^{-1}\ k^{-1}$	Gebremedhin et al., 2016
k_{soil}	Soil conductivity, 1,64	$W\ m^{-1}\ k^{-1}$	Najib et al., 2020
k_x	Horizontal thermal conductivity	$W\ m^{-1}\ K^{-1}$	Gebremedhin and Wu, 2001
k_y	Vertical thermal conductivity	$W\ m^{-1}\ K^{-1}$	Gebremedhin and Wu, 2001
l	Body length, 2.15	m	Gebremedhin and Wu, 2001
M_b	Body core mass	kg	-
M_c	Coat mass	kg	Berman, 2008
ME	Metabolizable energy intake	J	-
M_s	Skin mass	kg	Smith and Baldwin, 1974
Mw	Molar mass of water, 18	$g\ mol^{-1}$	-
n	Julian day number, 1 to 365	d	-

Nu	Nusselt number	dimensionless	Gebremedhin and Wu, 2001
P	Air pressure	Pa	-
P_o	Atmospheric pressure, 101325	Pa	-
Pr	Prandtl number, 0.7	dimensionless	Gebremedhin and Wu, 2001
Pw, sat(T_a)	Saturation vapor pressure at T_a	Pa	Murray, 1967
Pw, sat(T_e)	Saturation vapor pressure at T_e	Pa	Murray, 1967
Pw, sat(T_s)	Saturation vapor pressure at T_s	Pa	Murray, 1967
Pw(T_a)	Vapor pressure at T_a	Pa	-
$q''_{cond, b-s}$	Heat conduction between body core and upper skin	W m^{-2}	-
$q''_{cond, b-s'}$	Heat conduction between body core and lower skin	W m^{-2}	-
$q''_{cond, i}$	Heat conduction flux at node i underground	W m^{-2}	-
$q''_{cond, s-c}$	Heat conduction between upper skin and coat	W m^{-2}	-
$q''_{cond, s'-c}$	Heat conduction between lower skin and coat	W m^{-2}	-
$q''_{cond, s'-g}$	Heat conduction between skin and ground	W m^{-2}	-
q''_{conv}	Heat convection at coat surface	W m^{-2}	-
q''_{evap}	Heat evaporation through sweating	W m^{-2}	Silva and Maia, 2011; Gebremedhin and Wu, 2001
q''_{lat}	Latent heat transfer	W m^{-2}	Monteith and Unsworth, 2013
q''_{lw}	Long wave radiation	W m^{-2}	-
q''_{resp}	Heat loss through respiration	W m^{-2}	McGovern, 2000; da Silva et al., 2002; Monteith and Unsworth, 2013
q''_{sen}	Sensible heat transfer	W m^{-2}	Monteith and Unsworth, 2013
q''_{sol}	Solar radiation	W m^{-2}	Turnpenny et al., 2000a
R	Molar gas constant, 8.314	J mol^{-1} K^{-1}	-
R_d	Gas constant, 287	J kg^{-1} K^{-1}	-
RE	Retained energy	J	-

Re	Reynolds number	dimensionless	Gebremedhin and Wu, 2001
RH	Relative humidity	%	-
RR	Respiration rate	breath s^{-1}	Thompson et al., 2011
r_{sg}	Heat conduction resistance between the skin and the ground surface, 0.1	m^2 K W^{-1}	Radoń et al., 2014
S_b	Direct radiation	$W \cdot m^{-2}$	Duffie and Beckman, 2013
Sc	Schmidt number	Dimensionless	Gebremedhin and Wu, 2001
S_d	Diffuse radiation	W m^{-2}	Duffie and Beckman, 2013
S_e	Extraterrestrial radiation	W m^{-2}	Duffie and Beckman, 2013
St	Standard time	h	-
T_a	Air temperature	K	-
T_b	Body temperature	K	-
T_{black}	Black globe temperature	K	-
T_c	Coat temperature	K	-
T_{dp}	Dew point temperature	°C	Sonntag, 1990
T_e	Exhaled air temperature	K	Maia et al., 2005
T_g	Ground surface temperature	K	Thompson, 2011
$T_{g,\,i}$	Ground temperature at node i, for i = 1, …, 50	K	-
T_o	0 Celsius degree in Kelvins, 273.15	K	-
T_r	Radiant temperature of environment	K	Kuehn et al., 1970; Thorsson et al., 2007; Thompson et al., 2014a
T_s	Upper skin temperature	K	-
$T_{s'}$	Lower skin temperature	K	-
T_{sky}	Sky temperature	K	Duffie and Beckman, 2013
Tv_a	Virtual temperature of inhaled air	K	Monteith and Unsworth, 2013
Tv_e	Virtual temperature of exhaled air	K	Monteith and Unsworth, 2013

u	Wind speed	$m\ s^{-1}$	-
v	Kinematic viscosity of air	$m^2\ s^{-1}$	Gebremedhin and Wu, 2001
V_t	Tidal volume	$m^3\ breath^{-1}$	Stevens, 1981
α_s	Solar altitude angle, $\pi/2 - \theta_z$	rad	-
δ	Declination	rad	Monteith and Unsworth, 2013
γ	Azimuth angle	rad	-
γ_a	Animal angle (the angle between the animal long axis and south direction), $-\pi/2$ to $\pi/2$	rad	-
γ_s	Solar azimuth angle	rad	Monteith and Unsworth, 2013
ε_c	Emissivity of coat, 0.98	Dimensionless	Maia, 2005
θ_z	Zenith angle	rad	Monteith and Unsworth, 2013
λ	Latent heat of vaporization of water, 2430	$J\ g^{-1}$	Monteith and Unsworth, 2013
μ	Dynamic viscosity of air	$kg\ m^{-1}\ s^{-1}$	-
π	Constant, 3.14	-	-
ρ	Air density	$kg\ m^{-3}$	-
ρ_c	Reflection coefficient of coat, 0.3	dimensionless	Turnpenny et al., 2000b
ρc_p	Volumetric heat capacity of air	$J\ m^{-3}\ K^{-1}$	-
ρ_g	Reflection coefficient of ground, 0.25 for grass, 0.08 for wet dark soil, 0.13 for dry dark soil, 0.10 for wet light soil and 0.18 for dry light soil	dimensionless	Campbell and Norman, 1998
ρ_h	Fur density, 9.87	$hairs\ mm^{-2}$	Bertipaglia et al., 2005
ρ_{soil}	Soil density, 1559	$kg\ m^{-3}$	Najib et al., 2020
σ	Stefan-Boltzmann constant, 5.67×10^{-8}	$W\ m^{-2}\ K^{-4}$	-
τ_b	Atmospheric transmittance for beam radiation	dimensionless	Hottel, 1976
τ_d	Atmospheric transmittance for diffuse radiation	dimensionless	Liu and Jordan, 1960
φ	Latitude, $-\pi/2$ to $\pi/2$	rad	-

χ_a	Absolute humidity of inhaled air	g m^{-3}	Monteith and Unsworth, 2013
χ_e	Absolute humidity of exhaled air	g m^{-3}	Monteith and Unsworth, 2013
χ_s	Absolute humidity of skin surface	g m^{-3}	Monteith and Unsworth, 2013
ω	Hour angle	rad	Monteith and Unsworth, 2013

Differential equations

$$d(M_b\, c_{pb}\, T_b)/dt = HE - A\,[p_c\, q''_{cond,\, b\text{-}s1} + (1 - p_c)\, q''_{cond,\, b\text{-}s2} + q''_{resp}] \quad (A.1.1)$$

$$d[(1 - p_c)M_s\, c_{ps}\, T_{s1}]/dt = (1 - p_c)\, A\, (q''_{cond,\, b\text{-}s1} - q''_{cond,\, s1\text{-}c} - q''_{evap1}) \quad (A.1.2)$$

$$d(p_c\, M_s\, c_{ps}\, T_{s2})/dt = \begin{cases} p_c\, A\, (q''_{cond,\, b\text{-}s2} - q''_{cond,\, s2\text{-}c} - q''_{evap2}), \text{ when standing up} \\ p_c\, A\, (q''_{cond,\, b\text{-}s2} - q''_{cond,\, s2\text{-}g}), \text{ when lying down} \end{cases} \quad (A.1.3)$$

$$d[(1 - p_c)M_c\, c_{pc}\, T_{c1}]/dt = (1 - p_c)\, A\, (q''_{cond,\, s1\text{-}c1} + q''_{sol1} - q''_{conv1} - q''_{lw1}) \quad (A.1.4)$$

$$d(p_c\, M_c\, c_{pc}\, T_{c2})/dt = \begin{cases} p_c\, A\, (q''_{cond,\, s2\text{-}c2} + q''_{sol2} - q''_{conv2} - q''_{lw2}), \text{ when standing up} \\ 0, \text{ when lying down} \end{cases} \quad (A.1.5)$$

$$A = 0.15\, BW^{0.56} \quad (A.1.6)$$

Given that the coat and skin thickness are very small compared to the body diameter, the surface areas of body core, skin and coat were considered as the same.

$$M_s = a_s\, BW^{0.51} \quad (A.1.7)$$

$$M_c = 0.0022\, A \quad (A.1.8)$$

$$M_b = BW - M_s \quad (A.1.9)$$

Coat mass is very small and can be ignored when calculating body core mass.

Heat production

$$HE = (ME - RE)/86400 \quad (A.2.1)$$

Or

$$HE = c_h\, BW^{0.75}/3.6 \quad (A.2.2)$$

The heat production can be calculated based NRC (2001) as 2.1, or be roughly estimated using 2.2 (Purwanto et al., 1990).

Heat conduction between body core and skin

$$q''_{cond,\ b\text{-}s1} = \rho c_p\ (T_b - T_{s1})/r_{s1} \quad \text{(A.3.1)}$$

$$r_{s1} = \max\ (-5.44\ (T_{s1} - 273.15) + 225),\ 29) \quad \text{(A.3.2)}$$

$$\rho c_p = c_p\ P/(R_d\ T_a) \quad \text{(A.3.3)}$$

$$q''_{cond,\ b\text{-}s2} = \rho c_p\ (T_b - T_{s2})/r_{s2} \quad \text{(A.3.4)}$$

$$r_{s2} = \max\ (-5.44\ (T_{s2} - 273.15) + 225),\ 29) \quad \text{(A.3.5)}$$

Heat loss through respiration

$$q''_{resp} = q''_{sen} + q''_{lat} \quad \text{(A.4.1)}$$

$$q''_{sen} = V_t\ RR\ \rho c_p\ (Tv_e - Tv_a)/A \quad \text{(A.4.2)}$$

$$q''_{lat} = \lambda\ V_t\ RR\ (\chi_e - \chi_a)/A \quad \text{(A.4.3)}$$

$$V_t = 0.0198\ (60\ RR)^{-0.463} \quad \text{(A.4.4)}$$

$$RR = [37\ (Tb - 273.15) - 1385]/60 \quad \text{(A.4.5)}$$

$$T_e = 9.47 + 1.18\ (T_a - 273.15) - 0.01278\ (T_a - 273.15)^2 + 273.15 \quad \text{(A.4.6)}$$

$$Tv_e = T_e\ [1 + 0.38\ Pw,\ sat(T_e)/P] \quad \text{(A.4.7)}$$

$$Tv_a = Ta\ [1 + 0.38\ Pw(T_a)/P] \quad \text{(A.4.8)}$$

$$Pw,\ sat(T_e) = 611\ \exp\ [17.27\ (T_e - 273.15)/(T_e - 35.86)] \quad \text{(A.4.9)}$$

$$Pw,\ sat(T_a) = 611\ \exp\ [17.27\ (T_a - 273.15)/(T_a - 35.86)] \quad \text{(A.4.10)}$$

$$Pw\ (T_a) = Pw,\ sat(T_a)\ RH \quad \text{(A.4.11)}$$

$$\chi_e = Mw\ Pw,\ sat(T_e)/(R\ T_e) \quad \text{(A.4.12)}$$

$$\chi_a = Mw\ Pw(Ta)/(R\ Ta) \quad \text{(A.4.13)}$$

Heat conduction between skin and coat

$$q''_{cond,\ s1\text{-}c1} = k_{eff}\ (T_{s1} - T_{c1})/d_c \quad \text{(A.5.1)}$$

$$k_{eff} = 0.5\ (k_x + k_y) \quad \text{(A.5.2)}$$

$$k_x = (\rho_h\ \pi\ d_h^2/4)\ k_f + (1 - \rho_h\ \pi\ d_h^2/4)\ k_a \quad \text{(A.5.3)}$$

$$k_y = k_a \left(1/\rho_h^{0.5} - d_h\right) \rho_h^{0.5} + d_h k_a k_f/(d_h k_a + (1/\rho_h^{0.5} - d_h) k_f) \quad \text{(A.5.4)}$$

$$q''_{cond,\ s2\text{-}c2} = k_{eff} (T_{s2} - T_{c2})/d_c \quad \text{(A.5.5)}$$

Heat evaporation through sweating

$$q''_{evap1} = \min (31.5 + 3.67 \exp[(T_{s1} - 301.05)/2.19],\ \lambda (\chi_{s1} - \chi_a)/[1/h_m + (d_c + d_a)/D]) \quad \text{(A.6.1)}$$

$$\chi_{s1} = Mw\ Pw,\ sat(T_{s1})/(R\ T_{s1}) \quad \text{(A.6.2)}$$

$$Pw,\ sat(T_{s1}) = 611 \exp [17.27 (T_{s1} - 273.15)/(T_{s1} - 35.86)] \quad \text{(A.6.3)}$$

$$h_m = (D/d)\ 0.28\ Re^{0.6}\ Sc^{0.44} \quad \text{(A.6.4)}$$

$$d = 0.06\ BW^{0.39} \quad \text{(A.6.5)}$$

$$D = D_o (P_o / P) (T_a / T_o)^{3/2} \quad \text{(A.6.6)}$$

$$Re = u\ d/v \quad \text{(A.6.7)}$$

$$v = \mu/\rho \quad \text{(A.6.8)}$$

$$\rho = P/(R_d\ T_a) \quad \text{(A.6.9)}$$

$$\mu = (0.00452 (T_a - 273.15) + 1.734) \times 10^{-5} \quad \text{(A.6.10)}$$

A.6.10 is empirically fitted for T_a ranging from 15 °C to 45 °C.

$$Sc = v/D \quad \text{(A.6.11)}$$

$$d_a = 2\ v/(u\ C_f) \quad \text{(A.6.12)}$$

$$C_f = 2\ Sc^{2/3}\ h_m/u \quad \text{(A.6.13)}$$

$$q''_{evap2} = \min (31.5 + 3.67 \exp[(T_{s2} - 301.05)/2.19],\ \lambda (\chi_{s2} - \chi_a)/[1/h_m + (d_c + d_a)/D]) \quad \text{(A.6.14)}$$

$$\chi_{s2} = Mw\ Pw,\ sat(T_{s2})/(R\ T_{s2}) \quad \text{(A.6.15)}$$

$$Pw,\ sat(T_{s2}) = 611 \exp [17.27 (T_{s2} - 273.15)/(T_{s2} - 35.86)] \quad \text{(A.6.16)}$$

Heat convection at coat surface

$$q''_{conv1} = h_c (T_{c1} - T_a) \quad \text{(A.7.1)}$$

$$h_c = Nu\ k_a/d \quad \text{(A.7.2)}$$

$$Nu = \begin{cases} (0.43 + 0.5\ Re^{0.5})\ Pr^{0.38}, & 1 < Re \leq 10^3 \\ 0.25\ Re^{0.6}\ Pr^{0.38}, & Re > 10^3 \end{cases} \quad (A.7.3)$$

$$q''_{conv2} = h_c\ (T_{c2} - T_a) \quad (A.7.4)$$

Heat flux through long wave radiation

$$q''_{lw1} = \sigma\ \varepsilon_c\ (T_{c1}^4 - T_r^4) \quad (A.8.1)$$

$$T_r = (T_{sky} + T_g)/2 \quad (A.8.2)$$

Or

$$T_r = (T_{black}^4 + 1.1 \times 10^{-8}\ u^{0.6}\ (T_{black} - T_a)/2.029)^{0.25} \quad (A.8.3)$$

When outdoors, T_r is calculated as 8.2 (Thompson et al., 2014); When indoors, T_r is estimated using T_{black} as 8.3 (Kuehn et al., 1970; Thorsson et al., 2007).

$$T_{sky} = T_a\ [0.711 + 0.0056\ T_{dp} + 0.000073\ T_{dp}^2 + 0.013\ \cos(15\ St\ \pi/180)]^{0.25} \quad (A.8.4)$$

$$T_{dp} = 243.12\ [\log(RH/100) + 17.62\ (T_a - 273.15)/(T_a - 30.03)]\ /\ (17.62 - [\log(RH/100) + 17.62\ (T_a - 273.15)/(T_a - 30.03)]) \quad (A.8.5)$$

$$T_g = 1.33\ (T_a - 273.15) - 2.65\ (T_a - 273.15)^{0.5} + 3.21\ \log(S_b + S_d + 1) + 3.5 + 273.15 \quad (A.8.6)$$

$$q''_{lw2} = \sigma\ \varepsilon_c\ (T_{c2}^4 - T_r^4) \quad (A.8.7)$$

Heat flux through solar radiation

$$q''_{sol1} = (A\ (1 - \rho_c)\ ((Ah/A)\ S_b + 0.5\ S_d + (0.5 - p_c)\ \rho_g\ (S_b + S_d)))/((1 - p_c)\ A) \quad (A.9.1)$$

$$q''_{sol2} = \rho_g\ (S_b + S_d) \quad (A.9.2)$$

$$Ah/A = \text{cosec}\ \alpha_s\ [(2/\pi)\ (l/d)\ (1 - \cos^2\alpha_s \cos^2\gamma)^{0.5} + \cos\alpha_s \cos\gamma]/[2\ (l/d + 1)] \quad (A.9.3)$$

$$\gamma = |\gamma_s - \gamma_a| \quad (A.9.4)$$

$$\gamma_s = \text{sign}(\omega)\ |\cos^{-1}[(\cos\theta_z \sin\varphi - \sin\delta)\ /\ \sin\theta_z \cos\varphi]| \quad (A.9.5)$$

$$\cos\theta_z = \cos\varphi \cos\delta \cos\omega + \sin\varphi \sin\delta \quad (A.9.6)$$

$$\delta = 23.45\ \sin(2\pi\ (284 + n)/365)\ \pi/180 \quad (A.9.7)$$

$$\omega = 15\ (St - 12)\ \pi/180 \quad (A.9.8)$$

$$S_b = S_e \tau_b \quad \text{(A.9.9)}$$

$$S_d = S_e \tau_d \quad \text{(A.9.10)}$$

$$S_e = Gsc\ [1 + 0.033 \cos(2\pi\ n /365)] \cos \theta_z \quad \text{(A.9.11)}$$

$$\tau_b = a_0 + a_1 \exp(-k/\cos \theta_z) \quad \text{(A.9.12)}$$

$$a_0 = 0.4237 - 0.00821\ (6 - Al)^2 \quad \text{(A.9.13)}$$

$$a_1 = 0.5055 + 0.00595\ (6.5 - Al)^2 \quad \text{(A.9.14)}$$

$$k = 0.2711 + 0.01858\ (2.5 - Al)^2 \quad \text{(A.9.15)}$$

A.9.12 to A.9.15 were obtained under the condition of one standard atmosphere with 23 km visibility and altitudes less than 2.5 km. The equations must be used cautiously outside the scope.

$$\tau_d = 0.271 - 0.294\ \tau_b \quad \text{(A.9.16)}$$

Heat flux through conduction between skin and ground surface when the animal lies down

$$q''_{cond,\ s2\text{-}g} = (T_{s2} - T_{g,\ 1})/r_{sg} \quad \text{(A.10.1)}$$

The vertical distance from contacting surface to adiabatic layer was divided into 50 nodes. Heat conduction at node 1 was calculated as:

$$q''_{cond,\ 1} = q''_{cond,\ s2\text{-}g} - k_{soil}\ (T_{g,\ 1} - T_{g,\ 2})/(d_i/2) \quad \text{(A.10.2)}$$

The heat flux at node i ($q''_{cond,\ i}$, W m^{-2}) for i = 2 to 49 was calculated as:

$$q''_{cond,\ i} = k_{soil}\ [(T_{g,\ i-1} - T_{g,\ i}) - (T_{g,\ i} - T_{g,\ i+1})]/d_i \quad \text{(A.10.3)}$$

The heat flux at the last node 50 was calculated as:

$$q''_{cond,\ 50} = k_{soil}\ [(T_{g,\ 49} - T_{g,\ 50}) - (T_{g,\ 50} - T_{adl})]/(d_i/2) \quad \text{(A.10.4)}$$

Differential equation for node i underground

$$d(d_i\ \rho_{soil}\ c_{psoil}\ T_{g,\ i})/dt = q''_{cond,\ i} \quad \text{(A.10.5)}$$

Appendix B

Table B1. The amount of time lying down throughout 24 h in the simulation

Time	Time lying down (%/h)
0000 to 0100	62
0100 to 0200	70
0200 to 0300	60
0300 to 0400	65
0400 to 0500	37
0500 to 0600	80
0600 to 0700	80
0700 to 0800	40
0800 to 0900	0
0900 to 1000	0
1000 to 1100	0
1100 to 1200	0
1200 to 1300	0
1300 to 1400	0
1400 to 1500	0
1500 to 1600	0
1600 to 1700	0
1700 to 1800	0
1800 to 1900	0
1900 to 2000	0
2000 to 2100	62
2100 to 2200	68
2200 to 2300	60
2300 to 2400	67

Appendix C

Table C1. Parameters analyzed in the sensitivity analysis

Parameter*	Description	Unit	Baseline value	Equation
A	Animal surface area	m^2	5.39	1.1 to 1.5
a_0	Atmospheric transmittance coefficient, intercept	dimensionless	0.13	9.12
a_1	Atmospheric transmittance coefficient, slope	dimensionless	0.76	9.12
c_p	Specific heat of air	J kg^{-1} K^{-1}	1006	3.3
c_{pb}	Specific heat capacity of body core	J kg^{-1} K^{-1}	3472	1.1
c_{pc}	Specific heat capacity of coat	J kg^{-1} K^{-1}	1006.43	1.4, 1.5
c_{ps}	Specific heat capacity of skin	J kg^{-1} K^{-1}	3472	1.2, 1.3
c_{psoil}	Specific heat capacity of soil	J kg^{-1} K^{-1}	1784	10.5
d	Characteristic diameter	m	0.8	6.7
d_c	Coat thickness	m	0.0025	5.1, 5.5
HE	Heat production rate	W	1240	1.1
k	Atmospheric transmittance coefficient, rate	dimensionless	0.39	9.12
k_{eff}	Effective thermal conductivity	W m^{-1} K^{-1}	0.028	5.1, 5.5
k_{soil}	Soil conductivity	W m^{-1} K^{-1}	1.64	10.2, 10.3, 10.4
l	Body length, 2.15	m	2.15	9.3
M_b	Body core mass	kg	570.95	1.1
M_c	Coat mass	kg	0.012	1.4, 1.5
M_s	Skin mass	kg	29.05	1.2, 1.3
P	Air pressure	Pa	101325	3.3, 4.7, 4.8, 6.6, 6.9
qevap_a	Parameter a for evaporation rate	-	31.5	6.1, 6.14
qevap_b	Parameter b for evaporation rate	-	3.67	6.1, 6.14
qevap_c	Parameter c for evaporation rate	-	27.9	6.1, 6.14

qevap_d	Parameter d for evaporation rate	-	2.19	6.1, 6.14
RH	Relative humidity	%	18	4.11, 8.5
RR_a	Parameter a for respiration rate	-	37	4.5
RR_b	Parameter b for respiration rate	-	1385	4.5
rs_a	Parameter a for skin resistance	-	–0.0544	3.2, 3.5
rs_b	Parameter b for skin resistance	-	2.25	3.2, 3.5
T_a	Air temperature	K	307.15	3.3, 4.6, 4.8, 4.10, 4.11, 4.13, 6.6, 6.9, 7.1, 7.4, 8.3 to 8.6
T_{adl}	Temperature at the adiabatic layer	K	289.31	10.4
Te_a	Parameter a for exhaled air temperature	-	9.47	4.6
Te_b	Parameter b for exhaled air temperature	-	1.18	4.6
Te_c	Parameter c for exhaled air temperature	-	0.01278	4.6
Tg_a	Parameter a for ground temperature	-	1.33	8.6
Tg_b	Parameter b for ground temperature	-	2.65	8.6
Tg_c	Parameter c for ground temperature	-	3.21	8.6
Tg_d	Parameter d for ground temperature	-	3.5	8.6
Tsky_a	Parameter a for sky temperature	-	0.711	8.4
Tsky_b	Parameter b for sky temperature	-	0.0056	8.4
Tsky_c	Parameter c for sky temperature	-	0.000073	8.4
Tsky_d	Parameter d for sky temperature	-	0.013	8.4
u	Wind speed	$m\ s^{-1}$	2.86	6.7, 6.12, 8.3
Vt_a	Parameter a for tidal volume	-	0.0198	4.4
Vt_b	Parameter b for tidal volume	-	-0.463	4.4
γ_a	Animal angle	rad	$\pi/4$	9.4

ρ_c	Reflection coefficient of coat	dimensionless	0.03	9.1
ρ_g	Reflection coefficient of ground	dimensionless	0.08	9.1, 9.2
ρ_{soil}	Soil density	kg m^{-3}	1559	10.5
τd_a	Parameter a for atmospheric transmittance of diffuse radiation	-	0.271	9.15
τd_b	Parameter b for atmospheric transmittance of diffuse radiation	-	0.294	9.16

Parameter*	Description	Unit	Baseline value	Equation
A	Animal surface area	m^2	5.39	1.1 to 1.4
a_0	Atmospheric transmittance coefficient, intercept	dimensionless	0.13	9.11
a_1	Atmospheric transmittance coefficient, slope	dimensionless	0.76	9.11
c_p	Specific heat of air	J kg^{-1} K^{-1}	1006	3.3
c_{pb}	Specific heat capacity of body core	J kg^{-1} K^{-1}	3472	1.1
c_{pc}	Specific heat capacity of coat	J kg^{-1} K^{-1}	1006.43	1.4
c_{ps}	Specific heat capacity of skin	J kg^{-1} K^{-1}	3472	1.2, 1.3
c_{psoil}	Specific heat capacity of soil	J kg^{-1} K^{-1}	1784	10.4
d	Characteristic diameter	m	0.8	6.7
d_c	Coat thickness	m	0.0025	5.1
HE	Heat production rate	W	1240	1.1
k	Atmospheric transmittance coefficient, rate	dimensionless	0.39	9.11
k_{eff}	Effective thermal conductivity	W m^{-1} K^{-1}	0.028	5.1
k_{soil}	Soil conductivity	W m^{-1} K^{-1}	1.64	10.2, 10.3
l	Body length, 2.15	m	2.15	9.2
M_b	Body core mass	kg	570.95	1.1
M_c	Coat mass	kg	0.012	1.4
M_s	Skin mass	kg	29.05	1.2, 1.3

P	Air pressure	Pa	101325	3.3, 4.7, 4.8, 6.6, 6.9
qevap_a	Parameter a for evaporation rate	-	31.5	6.1
qevap_b	Parameter b for evaporation rate	-	3.67	6.1
qevap_c	Parameter c for evaporation rate	-	27.9	6.1
qevap_d	Parameter d for evaporation rate	-	2.19	6.1
RH	Relative humidity	%	18	4.11, 8.5
RR_a	Parameter a for respiration rate	-	37	4.5
RR_b	Parameter b for respiration rate	-	1385	4.5
rs_a	Parameter a for skin resistance	-	–0.0544	3.2
rs_b	Parameter b for skin resistance	-	2.25	3.2
T_a	Air temperature	K	307.15	3.3, 4.6, 4.8, 4.10, 4.11, 4.13, 6.6, 6.9, 7.1, 8.3 to 8.6
T_{adl}	Temperature at the adiabatic layer	K	289.31	10.3
Te_a	Parameter a for exhaled air temperature	-	9.47	4.6
Te_b	Parameter b for exhaled air temperature	-	1.18	4.6
Te_c	Parameter c for exhaled air temperature	-	0.01278	4.6
Tg_a	Parameter a for ground temperature	-	1.33	8.6
Tg_b	Parameter b for ground temperature	-	2.65	8.6
Tg_c	Parameter c for ground temperature	-	3.21	8.6
Tg_d	Parameter d for ground temperature	-	3.5	8.6
Tsky_a	Parameter a for sky temperature	-	0.711	8.4
Tsky_b	Parameter b for sky temperature	-	0.0056	8.4
Tsky_c	Parameter c for sky temperature	-	0.000073	8.4
Tsky_d	Parameter d for sky temperature	-	0.013	8.4

u	Wind speed	m s^{-1}	2.86	6.7, 6.12, 8.3
Vt_a	Parameter a for tidal volume	-	0.0198	4.4
Vt_b	Parameter b for tidal volume	-	-0.463	4.4
γ_a	Animal angle	rad	$\pi/4$	9.3
ρ_c	Reflection coefficient of coat	dimensionless	0.03	9.1
ρ_g	Reflection coefficient of ground	dimensionless	0.08	9.1
ρ_{soil}	Soil density	kg m^{-3}	1559	10.4
τd_a	Parameter a for atmospheric transmittance of diffuse radiation	-	0.271	9.15
τd_b	Parameter b for atmospheric transmittance of diffuse radiation	-	0.294	9.15

*All the parameters were analyzed through both local and global sensitivity analyses, except RH, T_a and u, which were only analyzed through a local sensitivity analysis.

Chapter 3: A multivariate model to predict greenhouse gas emission, manure excretion and water intake in dairy cattle

J. Li[1], D. P. Casper[2] and E. Kebreab[1]

[1]Department of Animal Science, University of California, Davis, CA 95616; [2]Casper's Calf Ranch, Freeport, IL 61032

Abstract

Although several models exist that predict greenhouse gas emissions, water intake and excretion variables, most if not all, are univariate models considering one output at a time. Multivariate techniques consider the relationships between variables in an overarching way and quantify the relationship between them. The study aimed to evaluate the environmental impact of dairy cattle by considering relevant outputs simultaneously. Three multivariate Bayesian regression models were developed to predict enteric methane (CH_4, g/d), carbon dioxide (CO_2, kg/d), water intake ($Water_{in}$, kg/d), volatile solids (VS, kg/d), biodegradable VS (dVS, kg/d), fecal DM (F_{DM}, kg/d), fecal water (F_W, kg/d), fecal carbon (F_C, g/d), fecal nitrogen (F_N, g/d), total urine (U_t, kg/d), urine carbon (U_C, g/d) and urine nitrogen (U_N, g/d) for lactating cows, nonlactating cows and heifers. In addition, milk yield (kg/d) was predicted for lactating cows. The model selection was conducted through a bidirectional selection method, selecting covariates from variables of diet compositions and animal status. The final selected models were evaluated through K-fold cross validation and assessed using root mean square prediction error (RMSPE). The results showed that DMI was the most important covariate present in all the equations with the exception of predicting U_t for nonlactating cows. Most model predictions had reasonable accuracy (RMSPE < 25%), except Fw (RMSPE = 38.6%) and U_C (34.9%) for lactating cows, $Water_{in}$ (RMSPE = 53.7%) and U_t (RMSPE = 56.1%) for nonlactating cows, and

CO_2 (RMSPE = 34.1%), $Water_{in}$ (RMSPE = 79.7%), U_C (RMSPE = 38.4%) and U_t (RMSPE = 43.9%) for heifers. The models provided an assessment of greenhouse gas emissions and manure excretions of dairy farms, which can be integrated with other models to evaluate the environmental impact of dairy production systems.

Key words: dairy cattle, greenhouse gas emissions, manure excretion, multivariate model, water intake

Introduction

The environmental impact of livestock, including greenhouse gas (GHG) emissions, manure excretion and water usage has been investigated in several studies. For example, the GHG emissions from agriculture are estimated to account for 14.5% of global anthropogenic GHG emissions (Gerber et al., 2013), while methane (CH_4) from enteric fermentation of livestock is responsible for 40% of agricultural GHG emissions in the United States (Tubiello et al., 2013). Several studies have investigated the mitigation strategies (e.g., Waghorn et al., 2008; Klop et al., 2016; Honan et al., 2021), measurements (e.g., Pinares-Patiño et al., 2008; Hammond et al., 2016), and prediction (e.g., Moraes et al., 2014; Appuhamy et al., 2016a; Niu et al., 2018) of enteric CH_4 emissions for dairy cattle.

Manure produced by animals generates CH_4, nitrous oxide (N_2O) and ammonia (NH_3) through decomposition, hydrolysis, nitrification and denitrification processes, which makes it another important source of pollutants (Li et al., 2012). The organic matter (or volatile solids, VS) in manure is closely related to the potential CH_4 production from manure and is used as a factor for CH_4 production estimation in the Intergovernmental Panel on Climate Change (IPCC) Tier 2 methodology (IPCC, 2019). However, lignin in manure is resistant to anaerobic digestion and does not contribute to CH_4 production, therefore VS without lignin, also known as

biodegradable VS (dVS) is a better variable for manure CH_4 production estimation (Appuhamy et al., 2018). Various prediction models dealing with whole farm emissions, including emissions at animal, manure or soil level have been developed in recent years (e.g., Li et al., 2012; Rotz et al., 2014). The quantification of detailed manure compositions, including carbon, nitrogen and water content, can provide inputs for the whole-farm models. Water intake is essential to milk production, and in predicting manure water excretion and overall water footprint at animal level.

Most extant models for the prediction of GHG emissions, excretion and water intake are univariate (e.g., Appuhamy et al., 2014; Niu et al., 2018). However, univariate models do not take correlations between response variables into consideration and may lead to model bias (Moraes et al., 2015). Most emissions and manure excretion variables are highly correlated with each other, so a multivariate model is more suitable during development of a prediction model for multiple response variables simultaneously. Van Lingen et al. (2018) developed a multivariate model to predict emissions and excretion for dairy cows, but the model only includes CH_4, dVS and manure nitrogen as the response variables. In this study, we aimed to develop a multivariate model to predict CH_4, CO_2, VS, dVS, manure carbon and nitrogen, water intake and milk production in dairy cows. Because most studies focus on the environmental effects of lactating cows alone, we expanded the model to include nonlactating cows and heifers to enable the assessment of emissions, excretion and water intake at the whole farm level.

Materials and Methods

Data Sources

A dataset containing individual records of CH_4 production, excretion and water intake from Holstein and Jersey lactating (n = 1111, Holstein = 1038, Jersey = 73) and nonlactating (n = 591, Holstein = 575, Jersey = 16) cows, and Holstein, Jersey and Angus-Hereford cross heifers (n =

414, Holstein = 220, Jersey = 109, Angus-Hereford cross = 85) was assembled. Records were collected in 53 trials at the former USDA Energy Metabolism Unit at Beltsville, Maryland from 1963 to 1995. Descriptive statistics for diet composition, type of animal, methane production and manure excretion are shown in Table 1.

Multivariate Model

In order to predict environmental and production outcomes in dairy cattle, 13 variables including CH_4 (g/d), CO_2 (kg/d), water intake ($Water_{in}$, kg/d), VS (kg/d), dVS (kg/d), fecal DM (F_{DM}, kg/d), fecal water (F_W, kg/d), fecal carbon (F_C, g/d), fecal nitrogen (F_N, g/d), total urine (U_t, kg/d), urine carbon (U_C, g/d), urine nitrogen (U_N, g/d) and milk yield (MY, kg/d), were considered for prediction by a multivariate model for dairy cows. However, VS and dVS were not available directly in the dataset. Urine OM is approximately 4 times of urine carbon (Dijkstra et al. 2013), therefore, VS was calculated as the sum of measured fecal OM and 4 times the measured U_C, i.e., VS = fecal OM + 4 U_C (Appuhamy et al., 2018). Then dVS was obtained by subtracting fecal lignin from VS.

The following notations are used to present the details of model development. We used n, j, k, t and to m represent the number of observations, studies, animals, response variables and covariates, respectively. A Bayesian multivariate model was constructed as follows:

$$\mathbf{Y} = \mathbf{X}\,\mathbf{B} + \mathbf{Z_1}\,\mathbf{\Delta} + \mathbf{Z_2}\,\mathbf{A} + \mathbf{E} \qquad [i]$$

where $\mathbf{Y}$ is an n × t matrix, with each row representing the response variables of each observation; $\mathbf{X}$ (n × m), $\mathbf{Z_1}$ (n × j) and $\mathbf{Z_2}$ (n × k) are the design matrices relating $\mathbf{B}$, $\mathbf{\Delta}$ and $\mathbf{A}$ to $\mathbf{Y}$; $\mathbf{B}$ is an m × t matrix with each row representing the regression coefficients predicting each response variable; $\mathbf{\Delta}$ is a j × t matrix with each row representing the study random effects on each response variable; $\mathbf{A}$ is k × t matrix with each row representing the animal random effects

on each response variable; **E** is an n × t error matrix. Animal was included as a random effect because one animal was used in multiple studies and had multiple observations in the dataset. To understand the distributions of study, animal and error effect, consider **Δ**, **A** and **E** matrices as stacked column-wise **δ**, **α** and **ϵ** vectors:

$$\boldsymbol{\Delta} = [\boldsymbol{\delta_1} \quad \boldsymbol{\delta_2} \quad \dots \quad \boldsymbol{\delta_t}], \mathbf{A} = [\boldsymbol{\alpha_1} \quad \boldsymbol{\alpha_2} \quad \dots \quad \boldsymbol{\alpha_t}], \mathbf{E} = [\boldsymbol{\epsilon_1} \quad \boldsymbol{\epsilon_2} \quad \dots \quad \boldsymbol{\epsilon_t}],$$

$$\boldsymbol{\delta} = \begin{bmatrix} \boldsymbol{\delta_1} \\ \boldsymbol{\delta_2} \\ \vdots \\ \boldsymbol{\delta_t} \end{bmatrix}, \boldsymbol{\alpha} = \begin{bmatrix} \boldsymbol{\alpha_1} \\ \boldsymbol{\alpha_2} \\ \vdots \\ \boldsymbol{\alpha_t} \end{bmatrix}, \boldsymbol{\epsilon} = \begin{bmatrix} \boldsymbol{\epsilon_1} \\ \boldsymbol{\epsilon_2} \\ \vdots \\ \boldsymbol{\epsilon_t} \end{bmatrix} \quad \text{[ii]}$$

where $\boldsymbol{\delta_p}$ (j × 1), $\boldsymbol{\alpha_p}$ (k × 1) and $\boldsymbol{\epsilon_p}$ (n × 1) are p^{th} column of the **Δ**, **A** and **E**, respectively for p = 1 to t. Then the distribution of **δ**, **α** and **ϵ** was:

$$\begin{bmatrix} \boldsymbol{\delta} \\ \boldsymbol{\alpha} \\ \boldsymbol{\epsilon} \end{bmatrix} \sim N\left(\begin{bmatrix} \mathbf{0} \\ \mathbf{0} \\ \mathbf{0} \end{bmatrix}, \begin{bmatrix} \mathbf{I_j} \otimes \mathbf{G_\delta} & \mathbf{0} & \mathbf{0} \\ \mathbf{0} & \mathbf{I_k} \otimes \mathbf{G_\alpha} & \mathbf{0} \\ \mathbf{0} & \mathbf{0} & \mathbf{I_n} \otimes \mathbf{R_\epsilon} \end{bmatrix} \right) \quad \text{[iii]}$$

where $\mathbf{I_j}$, $\mathbf{I_k}$ and $\mathbf{I_n}$ are identity matrices of order j, k and n, respectively; $\mathbf{G_\delta}$, $\mathbf{G_\alpha}$ and $\mathbf{R_\epsilon}$ are unstructured covariance matrices of order t for **δ**, **α** and **ϵ**, respectively. Minimally informative distributions were specified for the priors so that the inference is mostly influenced by the observed data (Gelman et al., 2004). All the regression coefficients were set to follow a normal prior with 0 mean and variance equal to 10^{10}. Inverse Wishart priors were specified with degrees of freedom equal to 0.1 and scale matrix equal to $10^4\,\mathbf{I_t}$, where $\mathbf{I_t}$ is an identity matrix of order t.

Covariates for model selection included breed, DMI (kg/d), OM intake (OMI, kg/d), days in milk (DIM, d), BW (kg), milk yield (MY, kg/d), milk protein (mPro, %), milk fat (mFat, %), and dietary contents of DM (% of diet), NDF (% of DM), ADF (% of DM), CP (% of DM), EE (% of DM), lignin (% of DM) and ash (% of DM). Although MY was a response variable, it was used as a covariate for predicting other response variables in the model for lactating cows but not used when MY was a response variable. The pairwise Pearson's correlations among the covariates are

shown in Figure 1. In order to avoid the collinearity, covariates with correlation greater than 0.5 were not used to predict one response variable at the same time. Model selection was based on deviance information criterion (DIC). A decrease of DIC value by more than 10 units indicates a substantial improvement by an additional covariate (Spiegelhalter et al., 2002). Otherwise, the covariate was considered unnecessary. Given the multivariate model contained 13 response variables and 15 covariates, the computation load of a greedy search for the best model was extremely heavy. Instead, a bidirectional selection was conducted in this study (Draper and Smith, 1998). At each step, all possible additions and deletions of a single covariate were made, and the action that improves DIC the most was taken. The procedure was repeated until no improvement can be made, or the improvement of DIC was less than 10 units, for each of the response variable one by one.

The Markov Chain Monte Carlo (MCMC) was generated using Gibbs sampling. After checking the MCMC convergence based on graphical methods, including trace, autocorrelation and running mean plots (Roy, 2020), the chain length was set to be 1.1×10^5 with the first 10^4 iterations removed as burn-in and chain thinning of 25. All the models were developed using the MCMCglmm package (Hadfield, 2010) in R (R Core Team, 2020).

Model Evaluation

The three multivariate models for three animal groups were evaluated using the K-fold cross-validation method (Efron and Tibshirani, 1993), in which folds were individual studies (K = number of studies). Each fold was used as a validation set, and its predicted response variables were calculated based on the model fitted from the remaining folds. The goodness of model prediction was assessed by the root mean square prediction error (RMSPE; Bibby and

Toutenburg, 1977), RMSPE to standard deviation of observed values ratio (RSR; Moriasi et al., 2007), mean bias (MB) and slope bias (SB). The calculation of the assessment is:

$$MSPE = \sum_{i=1}^{n}\left(Y_i - \widehat{Y}_i\right)^2/n \quad [iv]$$

$$RMSPE = \sqrt{MSPE} \quad [v]$$

$$RSR = RMSPE/S_o \quad [vi]$$

$$MB = (\overline{P} - \overline{O})^2 \quad [vii]$$

$$SB = (S_p - r\,S_o)^2 \quad [viii]$$

Where Y_i and $\widehat{Y}_i$ are observed and predicted value of *i*th observation, respectively; S_o and Sp are the standard deviation of observations and predictions, respectively; $\overline{O}$ and $\overline{P}$ are the mean of observation and prediction, respectively; r is the Pearson's correlation between observations and predictions. Briefly, RMSPE implies the model performance, while RSR quantifies the relative magnitude of RMSPE compared to observed data variance. A value of RSR between 0 and 1 indicates acceptable model performance. MSPE is decomposed to MB and SB to identify the source of model biases. In the results, RMSPE is presented as a percentage to the observation mean, while MB and SB are presented as percentages to MSPE.

Results and Discussion

The final selected multivariate models for lactating cows, nonlactating cows and heifers are shown in Tables 2, 3 and 4, respectively. Given some information may not be available on farm, previous studies built multiple models for GHG emission and nutrient excretion using information from different levels. For example, Appuhamy et al. (2014) and Niu et al. (2018) built models at the animal level (DMI, milk production, milk composition, etc.), diet level (nutrient composition) or both so that users can select an appropriate model based on the available information to them. The major concern was DMI because individual feed intake

records are rarely kept on farm. However, the models containing DMI had much lower RMSPE than those without it (Appuhamy et al., 2014; Niu et al., 2018), indicating DMI is an important covariate explaining the variation of GHG production and nutrient excretion. Although DMI may not be available at the individual level, DMI at the group level can easily be obtained from farms to estimate the average herd GHG emission and nutrient excretion, which is of interest in this study. Therefore, multiple models with different levels of covariates were not considered and only the best multivariate model was presented.

The average pairwise Pearson's correlation among the response variables were 0.59, 0.50 and 0.53 for lactating cows, nonlactating cows and heifers, respectively (Figure 2), which indicated the necessity of using multivariate models. CH_4, CO_2, F_{DM}, F_N, F_C, F_w, VS and dVS are highly correlated with other for all three animal groups, probably because GHG emission and fecal excretion are all directly affected by DMI, which provides substrate from them. Urine variables are not as correlated with other variables, especially for nonlactating cows. $Water_{in}$ is highly correlated with U_t for nonlactating cows and heifers, but not as correlated for lactating cows, probably because water intake is used for both milk and urine production in lactating cows.

All the equations contained an intercept for lactating and nonlactating cows, but all the equations for heifers did not except F_W, F_C, and F_N. The intercepts were excluded from those equations because they were highly varied (SD > 10 × mean), which could cause model bias, mean bias specifically, and undermine the cross validation. The most important factor of predicting GHG emissions and nutrient excretions was feed intake, which was contained in all the equations except the U_t equation for nonlactating cows. Appuhamy et al. (2018) predicted VS and dVS using OMI instead of DMI, because OMI excludes ash and is more relevant to manure OM excretions. Although OMI improved the model compared to DMI in some equations, we

found minor differences between models replacing DMI with OMI or vice versa. Breed was not present in any equations in the final selected models. Similarly, Moraes et al. (2014) did not find any significant effects of breed on emissions when dietary compositions and animal status were considered, indicating a similar biological process of producing GHG production and manure excretions shared by bovine breeds (Klevenhusen et al., 2011).

GHG Production

The prediction of enteric CH_4 production (Equation 1, 14 and 26 in Tables 2, 3, and 4) involved DMI for all three animal groups, because DMI provides substrate for microbial fermentation to produce CH_4 (Niu et al., 2018). Dietary structural and non-structural carbohydrate concentrations have an impact on the profile of volatile fatty acids in the rumen (Bannink et al., 2008). Structural carbohydrates are positively correlated with CH_4 production (Moe and Tyrrell, 1979; Bannink et al., 2008), which was represented through the positive coefficients of ADF and NDF in the CH_4 production equations for lactating cows and heifers. However, Equation 14 did not contain NDF or ADF, indicating other factors might have a more important effect for nonlactating cows. Dietary EE presented in the CH_4 production equation for nonlactating cows had a negative coefficient, which agrees with previous studies showing that inclusion of lipids in the diet has a CH_4 mitigation effect (e.g., Beauchemin et al., 2008; Moate et al., 2011). However, the CH_4 production equation for lactating cows contained MY and mFat instead of EE. The positive coefficient of mFat may be due to the relationship between acetate production and milk fat. Acetate is required for *de novo* milk fat synthesis, and it is also associated with the generation of hydrogen for methanogenesis in the rumen (Moraes et al., 2014). The negative coefficient of MY may be explained by the energy balance between CH_4

emission and milk production, because the carbon in gas energy could be used for milk production if not eructated out as CH_4.

Kirchgessner et al. (1991) reported the estimation of CO_2 production through DMI and BW, or through MY and BW. However, BW was not present in any CO_2 production equations in this study, probably because the variance of BW was largely captured by DMI. The CO_2 production equation for lactating cows (Equation 2) also contained CP as a covariate, but the coefficient was smaller than 0.1, indicating a small effect of dietary CP content on CO_2 production. Pedersen et al. (2008) reported a linear increase of CO_2 emission with the increase of respiration quotient, which can be estimated based on dietary compositions including CP. Note that the mean bias was large (94.2%) for CO_2 prediction equation of heifers, which indicates that a proper intercept is required. However, the intercept was not fit because the variance was very large as discussed above. A larger dataset for heifer is required to accurately estimate an intercept.

Milk Production and Water Intake

In the final selected model for lactating cows (Equation 4), MY was predicted using DMI, DIM and CP. This is expected because milk production is closely related to DMI (NRC, 2001) and DIM (Wood, 1967). Dietary CP provides nitrogen source for rumen microbes and affects the rumen-available protein, which in turn profoundly affects milk yield (Nocek and Russell, 1988).

Besides DMI, dietary DM and ash were present in the $Water_{in}$ equations (Equation 3, 16 and 28), which agrees with a previous study by Appuhamy et al. (2016b). Although the RMSPE of $Water_{in}$ was large for nonlactating cows (53.7%), the MB and SB were both small, indicating a part of $Water_{in}$ variance was not captured by the equation. For heifers, both the RMSPE and MB was large, indicating a better intercept is required. Water consumption of animals is highly dependent on the ambient temperature (Khelil-Arfa et al., 2014), which was not available in our

dataset and needs to be considered in future studies. On the other hand, the RMSPE of $Water_{in}$ for lactating cows (21.7%) was much lower. Milk production highly relies on the water consumption, because milk consists around 87% water. The presence of MY in the equation might compensate the lack of data on ambient temperature.

Manure Excretion

The F_{DM} of lactating cows (Equation 5) was positively associated with ADF and negatively associated with CP, which is reasonable because increasing dietary lignocellulose causes decreased DM digestibility (Van Soest, 1965) and increased dietary CP tends to decrease F_{DM} (Tomlinson et al., 1996). In the F_{DM} equation for nonlactating cows (Equation 17), NDF was present instead, probably in a similar role to ADF. However, CP was absent in Equation 17, which agrees with Wilkerson et al. (1997) that fecal excretion for nonlactating cows is mainly dependent on DMI and dietary NDF level. Nennich et al. (2005) reported an equation to estimate fecal excretion for heifers using DMI and BW, however, we only found a significant effect of DMI on F_{DM} for heifers (Equation 29).

Increasing dietary CP level can increase nitrogen excretion (Broderick, 2003), which was represented by the positive association of CP with nitrogen excretion (F_N and U_N) for all animal categories. Lignin was positively associated with F_N for lactating cows and heifers (Equation 6 and 30), and NDF was positive associated with U_N for nonlactating cows (Equation 22), which might be due to the inhibition of fiber on digestibility (Lloyd et al., 1961). Previous studies reported a significant effect of BW on nitrogen excretion (Wilkerson et al., 1997; Appuhamy et al., 2014), however, we only found such effect on U_N for lactating cows (Equation 10). In addition, MY was negatively associated with U_N, suggesting an increase of nitrogen efficiency with increasing of MY (Wilkerson et al., 1997). Dietary EE was positively associated with F_N for

heifers (Equation 30), which could be explained by the decrease of CP digestibility due to increase of EE level (NRC 2001).

Dietary CP and ADF were significantly associated with F_C for lactating cows (Equation 7), which agrees with Nousiainen et al. (2009) reporting the positive and negative effects of CP and ADF on feed digestibility. Besides, mFat and mPro were also positively and negatively associated with F_C for lactating cows, respectively, which might be due to the association between indigestible non-fiber carbohydrates and milk compositions (Firkins et al., 2001; Cabrita et al., 2007). Only ADF was present in the F_C equations for nonlactating cows and heifers though (Equation 19 and 31). Dietary CP and BW were positively associate with U_C for lactating cows (Equation 11), which agrees with the result obtained by (Appuhamy et al., 2014). Increasing CP level is associated with increasing urinary purine, thus increases U_C (Colmenero and Broderick, 2006). There was a large MB (44.1%) for the prediction of U_C for heifers, indicating a proper intercept was required through a larger dataset.

Dietary ADF was positively related to F_W across all the animal categories (Equation 8, 20 and 32). This could be due to the positive association of ADF with saliva input to the rumen, which in turn increases F_W (Appuhamy et al., 2014). Dietary CP content was negatively related to F_W in the Equation 8 and 32, which could be explained by the elevated blood urea concentrations due to increasing CP intake, causing water transfer from gut to blood and ending up with less water in feces (Silanikove and Tadmore, 1989). Dietary DM and DIM were also negatively related to F_W for lactating cows, indicating that less dietary water content tends to decrease F_W and cows in early lactation excrete less water in feces (Appuhamy et al., 2014). Dietary CP was positively associated with U_t for lactating cows (Equation 9), probably due to higher protein level leading to more urine (Gonda and Lindberg, 1994). Dietary sodium and

potassium have shown significant effects on the urine output (Bannik et al., 1999; Spek et al., 2012), which could be the reason that dietary ash was present in the U_t equations for nonlactating cows and heifers (Equation 21 and 33). The RMSPE of the two equations was quite large (56.1 and 43.9%, respectively), but SB were small for both nonlactating cows and heifers, and MB (12%) was only medium for heifers, which indicates that other covariates not present in our dataset may be required for better prediction.

Manure VS and dVS were predicted through feed intake (DMI or OMI) and structural carbohydrates (NDF or ADF), which is consistent with the negative relationship of dietary structural carbohydrates with feed digestibility (Lloyd et al., 1961). However, Equation 25, 36 and 37 included feed intake as the only covariate, which might be due to higher NDF level in the diet and smaller DMI of nonlactating cows and heifers so that two covariates confounded with each other.

Conclusions

Three multivariate models of GHG emissions, manure excretion and water intake, along with milk production, were developed for lactating cows, nonlactating cows and heifer. All the models required DMI as the most important covariate. Most equations predicted the response variables with reasonable accuracy (RMSPE < 25%), except Fw and U_C for lactating cows, $Water_{in}$ and U_t for nonlactating cows, and CO_2, $Water_{in}$, U_C and U_t for heifers. The prediction of these variables may require additional variables outside the dataset in this study or a nonlinear equation to obtain a better prediction.

Acknowledgements

Research was partially supported by the California Air Resources Board (Sacramento, CA), the Sesnon Endowed Chair program (University of California, Davis), and the USDA National Institute of Food and Agriculture Multistate Research Project NC-2040 (Washington, DC).

References

Appuhamy, J. A. D. R. N., J. France, and E. Kebreab. 2016a. Models for predicting enteric methane emissions from dairy cows in North America, Europe, and Australia and New Zealand. Glob. Chang. Biol. 22:3039–3056.

Appuhamy, J. A. D. R. N., J. V. Judy, E. Kebreab, and P. J. Kononoff. 2016b. Prediction of drinking water intake by dairy cows. J. Dairy Sci. 99:7191–7205.

Appuhamy, J. A. D. R. N., L. E. Moraes, C. Wagner-Riddle, D. P. Casper, and E. Kebreab. 2018. Predicting manure volatile solid output of lactating dairy cows. J. Dairy Sci. 101:820–829.

Appuhamy, J. A. D. R. N., L. E. Moraes, C. Wagner-Riddle, D.P. Casper, J. France, and E. Kebreab. 2014. Development of mathematical models to predict volume and nutrient composition of fresh manure from lactating Holstein cows. Anim. Prod. Sci. 54:1927–1938.

Bannink, A., H. Valk, and A. M. Van Vuuren. 1999. Intake and excretion of sodium, potassium, and nitrogen and the effects on urine production by lactating dairy cows. J. Dairy Sci. 82:1008–1018.

Bannink, A., J. France, S. Lopez, W. J. J. Gerrits, E. Kebreab, S. Tamminga, and J. Dijkstra. 2008. Modelling the implications of feeding strategy on rumen fermentation and functioning of the rumen wall. Anim. Feed Sci. Technol. 143:3–26.

Beauchemin, K.A., M. Kreuzer, F. O'Mara, and T. A. McAllister. 2008. Nutritional management for enteric methane abatement: a review. Aust. J. Exp. Agric. 48:21–27.

Bibby, J. and T. Toutenburg. 1977. Prediction and Improved Estimation in Linear Models. John Wiley & Sons, Chichester.

Broderick, G. A. 2003. Effects of varying dietary protein and energy levels on the production of lactating dairy cows. J. Dairy Sci. 86:1370–1381.

Cabrita, A. R. J., R. J. B. Bessa, S. P. Alves, R. J. Dewhurst, and A. J. M. Fonseca. 2007. Effects of dietary protein and starch on intake, milk production, and milk fatty acid profiles of dairy cows fed corn silage-based diets. J. Dairy Sci. 90:1429–1439.

Colmenero, J. O., and G. A. Broderick. 2006. Effect of dietary crude protein concentration on milk production and nitrogen utilization in lactating dairy cows. J. Dairy Sci. 89:1704–1712.

Draper, N. R., and H. Smith. 1998. Applied regression analysis (Vol. 326). John Wiley & Sons.

Efron, B., and R. J. Tibshirani. 1993. An Introduction to the Bootstrap. Chapman and Hall, New York.

Firkins, J. L., M. L. Eastridge, N. R. St-Pierre, and S. M. Noftsger. 2001. Effects of grain variability and processing on starch utilization by lactating dairy cattle. J. Anim. Sci. 79(suppl_E): E218–E238.

Gerber, P. J., H. Steinfeld, B. Henderson, A. Mottet, C. Opio, J. Dijkman, A. Falcucci, and G. Tempio. 2013. Tackling climate change through livestock - A global assessment of emissions and mitigation opportunities. Food and Agriculture Organization of the United Nations (FAO), Rome.

Gelman, A., J. Carlin, H. Stern, and D. Rubin. 2004. Bayesian data analysis. Pages 62–67 in Texts in Statistical Science. Chapman and Hall, London, UK.

Gonda, H. L., and J. E. Lindberg. 1994. Evaluation of dietary nitrogen utilization in dairy cows based on urea concentrations in blood, urine and milk, and on urinary concentration of purine derivatives. Acta Agric. Scand. A Anim. Sci. 44:236–245.

Hadfield, J. D. 2010. MCMC methods for multi-response generalized linear mixed models: the MCMCglmm R package. J. Stat. Softw. 33:1–22.

Hammond, K. J., G. C. Waghorn, and R. S. Hegarty. 2016. The GreenFeed system for measurement of enteric methane emission from cattle. Anim. Prod. Sci. 56:181–189.

Honan, M., X. Feng, J. M. Tricarico, and E. Kebreab. 2021. Feed additives as a strategic approach to reduce enteric methane production in cattle: modes of action, effectiveness and safety. Anim. Prod. Sci.

IPCC. 2019. 2019 refinement to the 2006 IPCC guidelines for national greenhouse gas inventories. IGES, Kanagawa, Japan: Intergovernmental Panel on Climate Change.

Khelil-Arfa, H., P. Faverdin, and A. Boudon. 2014. Effect of ambient temperature and sodium bicarbonate supplementation on water and electrolyte balances in dry and lactating Holstein cows. J. Dairy Sci. 97:2305–2318.

Kirchgessner, M., W. Windisch, H. L. Müller, and M. Kreuzer. 1991. Release of methane and of carbon dioxide by dairy cattle. Agribiol. Res. 44:91–102.

Klevenhusen, F., S. M. Bernasconi, M. Kreuzer, and C. R. Soliva. 2011. Experimental validation of the intergovernmental panel on climate change default values for ruminant- derived methane and its carbon-isotope signature. Anim. Prod. Sci. 50:159–167.

Klop, G., B. Hatew, A. Bannink, and J. Dijkstra. 2016. Feeding nitrate and docosahexaenoic acid affects enteric methane production and milk fatty acid composition in lactating dairy cows. J. Dairy Sci. 99:1161–1172.

Li, C., W. Salas, R. Zhang, C. Krauter, A. Rotz, and F. Mitloehner. 2012. Manure-DNDC: a biogeochemical process model for quantifying greenhouse gas and ammonia emissions from livestock manure systems. Nutr. Cycl. Agroecosyst. 93:163–200.

Lloyd, L. E., H. F. M. Jeffers, E. Donefer, and E. W. Crampton. 1961. Effect of four maturity stages of timothy hay on its chemical composition, nutrient digestibility and nutritive value index. J. Anim. Sci. 20:468–473.

Moate, P. J., S. R. O. Williams, C. Grainger, M. C. Hannah, R. J. Eckard. 2011. Comparison of cold pressed canola, brewers grains and hominy meal as dietary supplements suitable for reducing enteric methane emission from lactating cows. Anim. Feed Sci. Technol. 166:254–264.

Moe, P. W., and H. F. Tyrrell. 1979. Methane production in dairy cows. J. Dairy Sci. 62:1583–1586.

Moraes, L. E., A. B. Strathe, J. G. Fadel, D. P. Casper, and E. Kebreab. 2014. Prediction of enteric methane emissions from cattle. Glob. Chang. Biol. 20:2140–2148.

Moraes, L. E., E. Kebreab, A. B. Strathe, J. Dijkstra, J. France, D. P. Casper, and J. G. Fadel. 2015. Multivariate and univariate analysis of energy balance data from lactating dairy cows. J. Dairy Sci. 98:4012–4029.

Moriasi, D.N., J. G. Arnold, M. W. Van Liew, R. L. Bingner, R. D. Harmel, and T. L. Veith. 2007. Model evaluation guidelines for systematic quantification of accuracy in watershed simulations. Trans. ASABE. 50:885–900.

National Research Council. 2001. Nutrient Requirements of Dairy Cattle. 7th rev. ed. Natl. Acad. Sci., Washington, DC.

Nennich, T. D., J. H. Harrison, L. M. Vanwieringen, D. Meyer, A. J. Heinrichs, W. P. Weiss, N. R. St-Pierre, R. L. Kincaid, D. L. Davidson, and E. Block. 2005. Prediction of manure and nutrient excretion from dairy cattle. J. Dairy Sci. 88:3721–3733.

Niu, M., E. Kebreab, A. N. Hristov, J. Oh, C. Arndt, A. Bannink, A. R. Bayat, A. F. Brito, T. Boland, D. Casper, and L. A. Crompton. 2018. Prediction of enteric methane production, yield, and intensity in dairy cattle using an intercontinental database. Glob. Chang. Biol. 24:3368–3389.

Nocek, J. E., and J. Russell. 1988. Protein and energy as an integrated system. Relationship of ruminal protein and carbohydrate availability to microbial synthesis and milk production. J. Dairy Sci. 71:2070–2107.

Nousiainen, J., M. Rinne, and P. Huhtanen. 2009. A meta-analysis of feed digestion in dairy cows. 1. The effects of forage and concentrate factors on total diet digestibility. J. Dairy Sci. 92:5019–5030.

Owen, J. J., and W. L. Silver. 2015. Greenhouse gas emissions from dairy manure management: A review of field-based studies. Glob. Chang. Biol. 21:550–565.

Pedersen, S., V. Blanes-Vidal, H. Joergensen, A. Chwalibog, A. Haeussermann, M. J. W. Heetkamp, and A. J. A. Aarnink. 2008. Carbon dioxide production in animal houses: A literature review. Agricultural Engineering International: CIGR Journal.

Pinares-Patiño, C. S., A. Machmüller, G. Molano, A. Smith, J. B. Vlaming, and H. Clark. 2008. The SF6 tracer technique for measurements of methane emission from cattle–effect of tracer permeation rate. Can. J. Anim. Sci. 88:309–320.

Roque, B. M., J. K. Salwen, R. Kinley, and E. Kebreab. 2019. Inclusion of Asparagopsis armata in lactating dairy cows' diet reduces enteric methane emission by over 50 percent. J. Clean. Prod. 234:132–138.

R Core Team (2020). R: A language and environment for statistical computing. R Foundation for Statistical Computing, Vienna, Austria. https://www.R-project.org/.

Rotz, C. A., F. Montes, S. D. Hafner, A. J. Heber, and R. H. Grant. 2014. Ammonia emission model for whole farm evaluation of dairy production systems. J. Environ. 43:1143–1158.

Roy, V. 2020. Convergence diagnostics for Markov chain Monte Carlo. Annual Review of Statistics and Its Application. 7:387–412.

Silanikove, N. I. S. S. I. M., and A. M. N. O. N. Tadmor. 1989. Rumen volume, saliva flow rate, and systemic fluid homeostasis in dehydrated cattle. Am. J. Physiol. Regul. Integr. Comp. Physiol. 256:R809–R815.

Smith, P., H. Clark, H. Dong, E. A. Elsiddig, H. Haberl, R. Harper, J. House, M. Jafari, O. Masera, C. Mbow, and N. H. Ravindranath. 2014. Agriculture, forestry and other land use (AFOLU). Cambridge University Press, Cambridge, UK and New York, NY, USA.

Spek, J. W., A. Bannink, G. Gort, W. H. Hendriks, and J. Dijkstra. 2012. Effect of sodium chloride intake on urine volume, urinary urea excretion, and milk urea concentration in lactating dairy cattle. J. Dairy Sci. 95:7288–7298.

Spiegelhalter, D. J., N. Best, B. P. Carlin, and A. Van der Linde. 2002. Bayesian measures of model complexity and fit. J. R. Stat. Soc. Series B Stat. Methodol. 64: 583–639.

Tomlinson, A. P., W. J. Powers, H. H. Van Horn, R. A. Nordstedt, and C. J. Wilcox. 1996. Dietary protein effects on nitrogen excretion and manure characteristics of lactating cows. Trans. ASABE. 39:1441–1448.

Tubiello, F. N., M. Salvatore, S. Rossi, A. Ferreira, N. Fitton, and P. Smith. 2013. The FAOSTAT database of greenhouse gas emissions from agriculture. Environ. Res. Lett. 8:015009.

Van Lingen, H. J., J. G. Fadel, A. Bannink, J. Dijkstra, J. M. Tricarico, D. Pacheco, D. P. Casper, and E. Kebreab. 2018. Multi-criteria evaluation of dairy cattle feed resources and animal characteristics for nutritive and environmental impacts. Animal. 12:s310–s320.

Van Soest, P. J. 1965. Symposium on factors influencing the voluntary intake of herbage by ruminants: voluntary intake in relation to chemical composition and digestibility. J. Anim. Sci. 24:834–843.

Waghorn, G. C., H. Clark, V. Taufa, and A. Cavanagh. 2008. Monensin controlled-release capsules for methane mitigation in pasture-fed dairy cows. Aust. J. Exp. Agric. 48:65–68.

Wilkerson, V.A., D. R. Mertens, and D. P. Casper. 1997. Prediction of excretion of manure and nitrogen by Holstein dairy cattle. J. Dairy Sci. 80:3193–3204.

Wood, P. D. P. 1967. Algebraic model of the lactation curve in cattle. Nature 216:164–165.

Tables and Figures

Table 1. Descriptive statistics of diet compositions, animal status emission and excretion for the dataset used in this study

Item[1]	Lactating cows (n = 1111)			Nonlactating cows (n = 591)			Heifers (n = 414)		
	Mean (SD)	Min	Max	Mean (SD)	Min	Max	Mean (SD)	Min	Max
CP, % of DM	16.2 (2.5)	5.2	23.5	16.0 (2.4)	4.9	21.8	15.6 (2.9)	10.4	23.6
NDF, % of DM	34.3 (7.5)	14.9	76.1	36.3 (10.0)	14.0	74.0	41.2 (14.9)	13.2	78.3
ADF, % of DM	20.0 (4.2)	7.7	47.1	21.6 (6.9)	5.0	47.4	24.6 (11.4)	4.3	48.3
Lignin, % of DM	4.4 (1.4)	0.5	9.4	4.8 (2.0)	0.8	14.3	5.2 (2.7)	0.4	13.5
EE, % of DM	2.8 (1.0)	1.0	7.0	2.7 (0.9)	0.8	7.6	2.9 (1.1)	0.9	6.3
Ash, % of DM	6.4 (1.1)	3.7	12.1	7.3 (2.3)	3.5	22.1	6.4 (1.9)	3.1	13.7
DM, % of diet	65.3 (19.8)	30.2	97.4	67.9 (20.9)	19.4	98.7	56.2 (27.0)	19.7	97.0
DMI, kg	16.5 (4.3)	3.9	29.4	6.7 (2.0)	2.3	13.4	5.4 (1.6)	1.8	12.8
OMI, kg	15.4 (4.0)	3.6	27.3	6.2 (1.9)	2.1	12.8	5.0 (1.5)	1.7	11.9
DIM, d	162 (82.1)	11.0	488	-	-	-	-	-	-
BW, kg	594 (88.6)	302	854	668 (88.4)	328	893	345 (72.9)	195	542.0
MY, kg/d	23.3 (10.3)	0.1	56.6	-	-	-	-	-	-
mPro, %	3.3 (0.4)	2.3	5.8	-	-	-	-	-	-
mFat, %	3.67 (0.75)	1.42	7.6	-	-	-	-	-	-
CH_4, g/d	298 (91.8)	68.3	551	162 (43.1)	42.4	322.9	119 (37.6)	47.9	248
CO_2, kg/d	10.6 (2.1)	3.7	17.1	6.4 (1.3)	2.2	10.3	4.6 (1.1)	2.4	8.5
$Water_{in}$, kg/d	60.5 (28.3)	2.0	121.3	24.6 (14.9)	1.0	124.4	14.3 (10.8)	0.2	109.2
VS, kg/d	5.9 (1.8)	1.5	12.1	2.2 (0.9)	0.7	6.1	1.9 (0.7)	0.4	7.8
dVS, kg/d	5.3 (1.6)	1.4	11.4	2.0 (0.8)	0.7	5.8	1.7 (0.6)	0.4	7.6
F_{DM}, kg/d	5.5 (1.8)	1.1	11.2	1.9 (0.8)	0.5	5.5	1.7 (0.6)	0.3	4.1
F_W, kg/d	27.1 (10.2)	4.8	65.9	8.1 (4.1)	1.5	29.7	6.6 (3.0)	1.0	21.6
F_C, g/d	2541 (798.2)	539	5208	882 (383.9)	215	2626	789 (302.2)	143	2017
F_N, g/d	150 (54.8)	35.1	377.6	51.2 (19.1)	13.2	125.2	46.9 (18.3)	11.8	119.4
U_t, kg/d	17.5 (8.9)	4.4	138.3	15.9 (11.4)	2.5	103.8	9.6 (5.0)	1.8	31.8
U_C, g/d	232 (99.9)	12.1	1925	137 (71.0)	29.2	1115	99.5 (78.7)	29.4	237.4
U_N, g/d	152 (65.8)	22.3	363	108 (37.1)	17.0	248	71.7 (34.2)	18.1	212.5

[1]MY = milk yield, mPro = milk protein, mFat = milk fat, VS = volatile solids, dVS = biodegradable volatile solids, F_{DM} = fecal DM, F_W = fecal water, F_C = fecal carbon, F_N = fecal nitrogen, U_t = total urine, U_C = urine carbon, U_N = urine nitrogen

Table 2. Selected multivariate model and root mean square prediction error (RMSPE, % of observed mean) for enteric CH_4 (g/d), CO_2 (kg/d), water intake ($Water_{in}$, kg/d), milk yield (MY, kg/d), fecal DM (F_{DM}, kg/d), fecal nitrogen (F_N, g/d), fecal carbon (F_C, g/d), fecal water (F_w, kg/d), total urine (U_t, kg/d), urine nitrogen (U_N, g/d), urine carbon (U_C, g/d), VS (kg/d) and dVS (kg/d) of lactating cows (n = 1111).

Eq.	Selected model[1]	Model performance[2]			
		RMSPE, %	RSR	MB, %	SB, %
(1)	$CH_4 = -108.00\ (13.96) + 17.65\ (0.56) \times DMI + 3.04\ (0.40) \times ADF + 25.86\ (1.95) \times mFat - 1.89\ (0.22) \times MY$	16.7	0.54	0.66	4.4
(2)	$CO_2 = 2.77\ (1.18) + 0.39\ (0.019) \times DMI + 0.077\ (0.033) \times CP$	7.5	0.38	0.58	4.5
(3)	$Water_{in} = -19.98\ (9.08) + 2.71\ (0.28) \times DMI + 0.35\ (0.11) \times DM + 0.48\ (0.11) \times MY$	21.7	0.49	0.29	8.3
(4)	$MY = 10.59\ (2.11) + 0.93\ (0.050) \times DMI - 0.058\ (0.0017) \times DIM + 0.4\ (0.084) \times CP$	10.6	0.33	0.13	0.15
(5)	$F_{DM} = -0.34\ (1.23) + 0.38\ (0.019) \times DMI - 0.084\ (0.032) \times CP + 0.047\ (0.015) \times ADF$	14.9	0.41	0.14	3.1
(6)	$F_N = -62.71\ (7.14) + 10.22\ (0.19) \times DMI + 2.00\ (0.33) \times CP + 2.59\ (0.56) \times Lignin$	10.8	0.34	0.18	0.50
(7)	$F_C = 149.3\ (116.55) + 177.51\ (2.56) \times DMI + 19.93\ (2.29) \times ADF - 42.22\ (4.18) \times CP + 35.27\ (11.36) \times mFat - 111.47\ (19.32) \times mPro$	14.7	0.39	0.0011	2.4
(8)	$F_w = -4.07\ (2.69) + 2.08\ (0.046) \times DMI + 0.42\ (0.036) \times ADF - 0.35\ (0.076) \times CP - 0.068 \times (0.022)\ DM - 0.0076\ (0.0016) \times DIM$	38.6	0.92	0.23	3.3
(9)	$U_t = 1.11\ (2.84) + 0.65\ (0.094) \times DMI + 0.71\ (0.14) \times CP - 0.24\ (0.037) \times MY$	20.6	0.83	0.64	0.32
(10)	$U_N = -242.33\ (11.69) + 9.59\ (0.38) \times DMI + 16.24\ (0.49) \times CP + 0.053\ (0.014) \times BW - 2.47\ (0.15) \times MY$	20.3	0.47	0.020	7.4

(11)	U_C = –215.88 (31.58) + 8.54 (0.84) × DMI + 11.20 (1.35) × CP + 0.14 (0.035) × BW + 10.85 (2.40) × Lignin	34.9	0.91	0.47	1.1
(12)	VS = –1.56 (1.10) + 0.41 (0.020) × OMI + 0.061 (0.015) × ADF	10.5	0.35	0.84	0.016
(13)	dVS = –1.25 (1.10) + 0.37 (0.020) × OMI + 0.025 (0.010) × NDF	11.3	0.37	0.73	0.011

[1]Model parameters are reported as posterior means and standard deviation in parenthesis. DMI is in kg/d; CP, NDF, ADF and Lignin are in % of dietary DM; mFat = milk fat, %; mPro = milk protein, %; DM is % of as-fed diet; DIM = day in milk; BW is in kg; OMI = organic matter intake, kg/d.
[2]RMSPE = Root mean square prediction error, expressed as a percentage of observed mean; RSR = Ratio of RMSPE to observed standard deviation; MB = Mean bias, expressed as a percentage of MSPE; SB = Slope bias, expressed as a percentage of MSPE.

Table 3. Selected multivariate model and root mean square prediction error (RMSPE, % of observed mean) for enteric CH_4 (g/d), CO_2 (kg/d), water intake ($Water_{in}$, kg/d), fecal DM (F_{DM}, kg/d), fecal nitrogen (F_N, g/d), fecal carbon (F_C, g/d), fecal water (F_w, kg/d), total urine (U_t, kg/d), urine nitrogen (U_N, g/d), urine carbon (U_C, g/d), VS (kg/d) and dVS (kg/d) of nonlactating cows (n = 591).

Eq.	Selected model[1]	Model performance[2]			
		RMSPE, %	RSR	MB, %	SB, %
(14)	CH_4 = 45.43 (5.99) + 17.84 (0.48) × DMI – 2.40 (1.11) × EE	15.9	0.59	1.6	0.58
(15)	CO_2 = 2.87 (1.17) + 0.57 (0.057) × OMI	9.4	0.45	0.21	1.8
(16)	$Water_{in}$ = 8.58 (4.21) + 1.15 (0.31) × DMI + 0.91 (0.35) × Ash	53.7	0.35	0.46	0.37
(17)	F_{DM} = –1.16 (1.24) + 0.35 (0.054) × DMI + 0.023 (0.012) × NDF	14.9	0.39	1.9	1.6
(18)	F_N = –27.14 (3.35) + 9.11 (0.18) × DMI + 1.16 (0.16) × CP	14.7	0.32	2.5	1.3
(19)	F_C = –526.36 (33.35) + 151.36 (2.56) × DMI + 19.24 (0.82) × ADF	13.9	0.42	4.1	0.48
(20)	F_w = –6.38 (1.33) + 1.58 (0.069) × DMI + 0.20 (0.021) × ADF	21.0	0.98	1.0	0.0062
(21)	U_t = 8.84 (2.78) – 0.14 (0.067) × ADF + 1.22 (0.25) × Ash	56.1	0.93	0.53	0.15
(22)	U_N = –124.87 (9.79) + 12.16 (0.44) × DMI + 8.15 (0.44) × CP + 0.44 (0.10) × NDF	19.1	0.56	8.64	0.36
(23)	U_C = 5.68 (18.13) + 14.54 (1.54) × DMI + 3.90 (1.62) × Ash	22.6	0.97	1.06	0.68
(24)	VS = –0.84 (1.24) + 0.36 (0.058) × OMI + 0.039 (0.016) × ADF	15.5	0.39	0.97	1.33
(25)	dVS = –0.16 (1.18) + 0.32 (0.055) × DMI	19.2	0.49	3.7	0.077

[1]Model parameters are reported as posterior means and standard deviation in parenthesis. DMI is in kg/d; CP, NDF, ADF, EE and Ash are in % of dietary DM; OMI = organic matter intake, kg/d.
[2]RMSPE = Root mean square prediction error, expressed as a percentage of observed mean; RSR = Ratio of RMSPE to observed standard deviation; MB = Mean bias, expressed as a percentage of MSPE; SB = Slope bias, expressed as a percentage of MSPE.

Table 4. Selected multivariate model and root mean square prediction error (RMSPE, % of observed mean) for enteric CH_4 (g/d), CO_2 (kg/d), water intake ($Water_{in}$, kg/d), fecal DM (F_{DM}, kg/d), fecal nitrogen (F_N, g/d), fecal carbon (F_C, g/d), fecal water (F_w, kg/d), total urine (U_t, kg/d), urine nitrogen (U_N, g/d), urine carbon (U_C, g/d), VS (kg/d) and dVS (kg/d) of heifers (n = 414).

Eq.	Selected model[1]	Model performance[2]			
		RMSPE, %	RSR	MB, %	SB, %
(26)	CH_4 = 16.64 (0.56) × DMI + 0.86 (0.12) × NDF	20.0	0.63	5.6	0.014
(27)	CO_2 = 0.62 (0.070) × OMI	34.1	1.4	94.2	0.12
(28)	$Water_{in}$ = 1.69 (0.23) × DMI + 0.093 (0.054) × DM + 1.18 (0.27) × Ash	79.7	0.58	30.2	0.028
(29)	F_{DM} = 0.34 (0.066) × DMI	22.0	0.43	1.4	1.3
(30)	F_N = –35.040 (20.10) + 9.40 (0.20) × DMI + 1.17 (0.17) × CP + 1.57 (0.25) × Lignin + 2.22 (0.48) × EE	16.8	0.33	0.27	1.5
(31)	F_C = –369.69 (42.91) + 160.22 (2.56) × DMI + 12.25 (0.79) × ADF	12.7	0.60	26.6	0.17
(32)	F_w = –2.75 (19.80) + 1.38 (0.075) × DMI + 0.16 (0.028) × ADF – 0.098 (0.060) × CP	24.8	0.84	10.6	1.5
(33)	U_t = 0.53 (0.11) × DMI + 1.27 (0.13) × Ash	43.9	0.98	12.0	0.21
(34)	U_N = –71.25 (21.92) + 10.72 (0.43) × DMI + 5.31 (0.35) × CP	23.6	0.49	3.2	6.9
(35)	U_C = 13.38 (2.12) × DMI	38.4	1.0	44.1	2.9
(36)	VS = 0.37 (0.066) × DMI	22.7	0.59	4.5	0.0048
(37)	dVS = 0.36 (0.069) × OMI	23.0	0.60	6.6	0.057

[1]Model parameters are reported as posterior means and standard deviation in parenthesis. DMI is in kg/d; CP, NDF, ADF, EE and Ash are in % of dietary DM; OMI = organic matter intake, kg/d.

[2]RMSPE = Root mean square prediction error, expressed as a percentage of observed mean; RSR = Ratio of RMSPE to observed standard deviation; MB = Mean bias, expressed as a percentage of MSPE; SB = Slope bias, expressed as a percentage of MSPE.

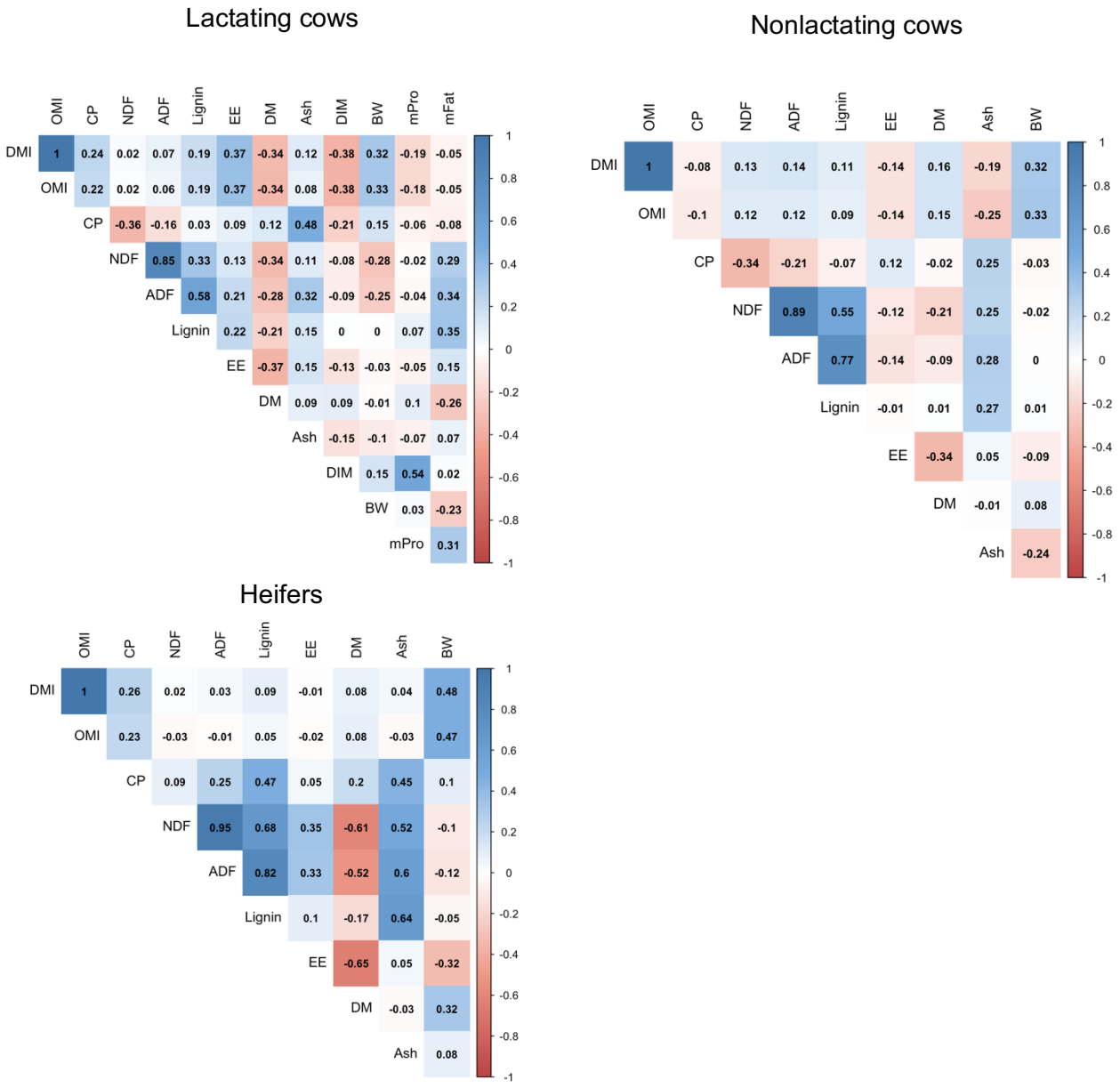

Figure 1. Heatmaps of pairwise Pearson's correlations among covariates for lactating cows, nonlactating cows and heifers. Covariates included CP (% of DM), NDF (% of DM), ADF (% of DM), Lignin (% of DM), EE (% of DM), Ash (% of DM), DM (% of diet), DMI (kg), OMI (kg), DIM = Days in milk (d), BW (kg), mPro = Milk protein (%) and mFat = Milk fat (%). Covariates for nonlactating cows and heifers did not include DIM, mPro and mFat.

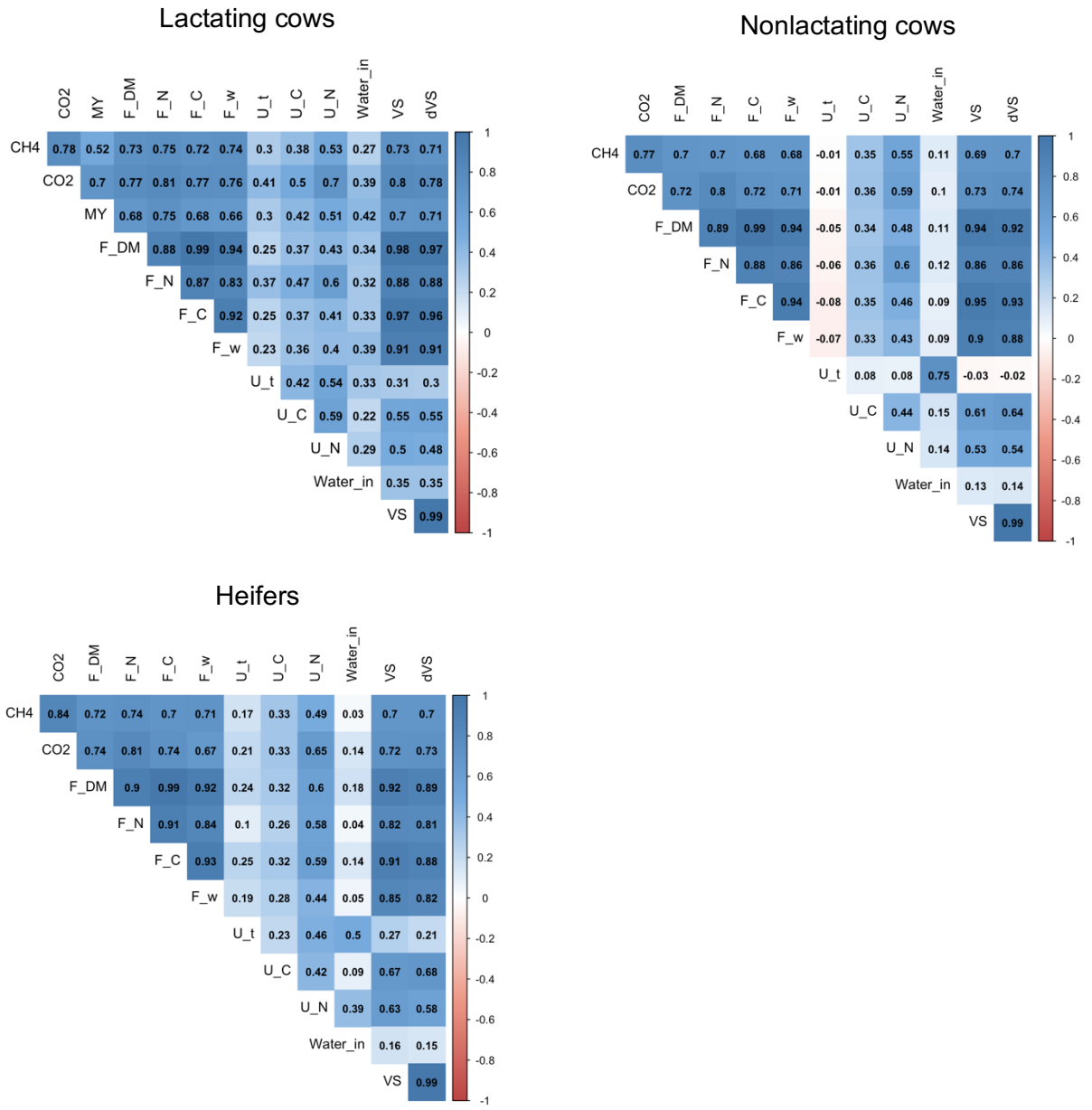

Figure 2. Heatmaps of pairwise Pearson's correlations among CH_4 (g/d), CO_2 (kg/d), milk yield (MY, kg/d), water intake ($Water_{in}$, kg/d), fecal DM (F_{DM}, kg/d), fecal nitrogen (F_N, g/d), fecal carbon (F_C, g/d), fecal water (F_W, kg/d), total urine (U_t, kg/d), urine nitrogen (U_N, g/d), urine carbon (U_C, g/d), VS (kg/d) and dVS (kg/d) for lactating cows, nonlactating cows and heifers.

Chapter 4: A simulation study at farm level using nonlinear ration formulation, thermal balance, emission and excretion models

Abstract

The objective of this chapter is to integrate information from a nonlinear ration formulation model, a thermal balance model, and emission and excretion models to evaluate the environment impact of dairy cattle and the effect of climate on dairy cattle at the farm level. A simulation study was conducted for a dairy herd with 550 heifers and 1000 cows, which included 16% of early-lactation, 23% of mid-lactation, 46% of late-lactation and 15% of nonlactating cows. A ration was designed for each animal group using mixed integer nonlinear programming, then the ration was used to estimate the greenhouse gas (GHG) emissions and manure excretion for all animals. Thermal balance for lactating and nonlactating cows was predicted under a typical California summer weather condition using the thermal balance model, which used the ration designed to estimate the heat production. Based on the ration designed using the herd average characteristics, the daily as-fed feeds consumed included 4.1 tons of corn silage, 12.2 tons of cracked corn grain, 2.9 tons of grass silage, 3.9 tons of soybean meal, 5.1 tons of bermudagrass hay and 0.22 ton of dibasic calcium phosphate. The total daily feed cost was $4,773. Using the ration designed for each animal group, the total GHG emission was 23.6 tons of CO_2 equivalents, including 372.6 kg of methane. The total daily manure excretion was 63.6 tons, including 0.4 ton of nitrogen and 3.5 tons of carbon. The thermal balance results showed that the average body temperature for early-, mid-, late-lactation and dry cows were 41.0 °C, 42.2 °C, 40.3 °C and 39.3 °C, respectively. Evaporation was the major heat dissipation method, which accounts for about 50% of the total heat dissipation on average for both lactating and nonlactating cows.

Key words: dairy cattle, simulation, ration, thermal balance, emission, excretion

Introduction

Mathematical modeling has been used to address issues of dairy industry related to improving efficiency and reducing negative impacts on the environment (Bannink et al., 2011; Ryan et al., 2011; Moraes et al., 2015). Many of these issues need to be addressed at the farm level using a systematic whole farm approach. Whole-farm models are able to investigate major farm components, the interactions among these components, and their interaction with the environment (Rotz, et al., 1999). Whole-farm models are valuable because complex dairy systems are difficult to fully investigate by field research (Kebreab et al., 2019). Several whole-farm models were developed for different purposes (e.g., Cabrera et al., 2006; Johnson et al., 2008; Rotz et al., 2012). Cabrera et al. (2006) developed an integrated dairy farm model to reduce environmental impacts, mainly focusing on the nitrogen excretion. Johnson et al. (2008) developed pasture-based model for grazing system. Rotz et al. (2012) developed an integrated farm system model, which is able to simulate crop, dairy, or beef production over years to determine the long-term animal performance, environmental impact, and economics. These models have certain flaws, such as inflexibility and narrow applicability (Kebreab et al., 2019). A new whole-farm model, ruminant farm system model including four integrated biophysical modules of animal, manure, soil, crop and storage, and three system balance modules of water, energy, and economics, is under development (Kebreab et al., 2019). In addition, it incorporates big data artificial intelligence and allows users to adjust the model parameters to achieve the flexibility (Kebreab et al., 2019). The nonlinear ration formulation, thermal balance, greenhouse gas (GHG) emission and manure excretion models developed in previous chapters can be integrated to the ruminant farm system model easily. This study aims at integrating the models described in this dissertation through a simulation study at farm level.

Materials and Methods

Dairy herd simulation

The simulation was conducted on a daily time step. A dairy herd consisting of six groups was simulated: younger and older heifers, early-, mid-, and late lactation cows, and nonlactating cows. The animal characteristics are summarized in Table 1. Calves were not investigated in this dissertation. We assumed a cow group of 1,000 animals containing 16% of early-lactation, 23% of mid-lactation, 46% of late-lactation and 15% of nonlactating cows (Rotz, et al., 1999). Based on the average culling rate and replacement needs in the United States, total number of heifers required to maintain 1,000 cows is at least 528 (Overton and Dhuyvetter, 2020), therefore, we set the heifer group size to be 550, with younger and older heifers each accounting for 50%, respectively.

Ration formulation

Rations for each animal group were designed based on mixed integer nonlinear programming based deterministic global optimization (MINLP_DGO) as described in Chapter 1. Three different sets of feed resources were used for heifers, lactating and nonlactating cows as shown in Table 2. Least cost diet was formulated based on the nutrient requirements and feed ingredients in NRC (2001). Nutrient constraints including net energy requirements for maintenance (NE_M), lactation (NE_L) and growth (NE_G), metabolizable protein (MP) requirement, calcium and phosphorus requirements, along with several ingredient constraints including fat (less than 7% of diet DM), NDF (greater than 25 % and less than 40 % of diet DM) and forage NDF (greater than 19% of diet DM), were considered. In addition, DMI was limited to be less than the predicted DMI in NRC (2001), so that low quality feeds with low price would not be

overfed. Lastly, the forage content was required to be greater than 40% for lactating cows to avoid rumen malfunction.

Emission and excretion

Based on the formulated rations, animal GHG emission and manure excretion, including enteric methane (CH_4), carbon dioxide (CO_2), volatile solids (VS), biodegradable VS (dVS), fecal DM (F_{DM}), fecal water (F_W), fecal carbon (F_C), fecal nitrogen (F_N), total urine (U_t), urine carbon (U_C) and nitrogen (U_N), were predicted for each animal group using the multivariate models described in Chapter 3.

Thermal balance

The thermal balance model described in Chapter 2 was used to predict the thermal condition of lactating and nonlactating cows under hot weather based on the herd average characteristics. Heifers were not included in the thermal balance simulation, because heifers generate less metabolic heat and have greater body surface area relative to body mass, which make them able to dissipate body heat efficiently and more tolerant of heat stress (West, 2003). The heat production rate was estimated using metabolizable energy intake based on the ration minus the retained energy (milk, pregnancy and body weight change). Three days of simulation were run based on the weather condition in Davis, California from July 26 to 28, 2019. Hourly air temperature, relative humidity and wind speed were obtained from Weather Underground (https://www.wunderground.com/weather/us/ca/davis). Weather data were interpolated linearly to provide information of inputs varying on a per second basis, with the average air temperature, relative humidity and wind speed being 25.8 °C (min = 13.3 °C, max = 37.7 °C), 51.0% (min = 16.0 %, max = 95 %) and 2.0 m/s (min = 0.67 m s^{-1}, max = 3.8 m s^{-1}), respectively. Unlike the simulation in Chapter 2, animal thermal balance was simulated for indoor under a roof, which is

a more realistic situation. The proportion of lying down during other time was set based on Drwencke et al. (2020), resulting 11.9 h of lying down per day.

Results and Discussion

Ration formulation

Nutrient requirements and rations formulated for the six animal groups are shown in Table 3. The milk production process requires a large amount of energy and protein, therefore lactating cows had the largest nutrient requirements. Based on the ration designed using the herd average characteristics, the daily total amount of feeds consumed (as-fed basis) was: 15.2 tons of corn silage, 9.5 tons of cracked corn grain, 2.9 tons of grass silage, 4.0 tons of soybean meal, 3.3 tons of bermudagrass hay and 0.22 ton of dibasic calcium phosphate. The total daily feed cost was $4773, which consisted of $675.8 (14.2%) for heifers, $3806.4 (79.7%) for lactating cows and $291 (6.1%) for dry cows. Daily total milk production was 27.4 tons, and the average feed cost was $0.14/kg of milk, which falls in the range 0.1 to 0.2 $/kg of milk reported by Alqaisi and Schlecht (2021).

GHG emission and manure excretion

The GHG emission and manure excretion per animal based on the herd average characteristics are shown in Table 4. Based on the results, the daily total emission of enteric CH_4 and CO_2 were 372.6 kg and 13.1 tons, respectively. The global warming potential of CH_4 is about 28 times of that of CO_2 (IPCC, 2019), therefore the total emission was 23.6 tons of CO_2 equivalents. Many studies have investigated the CH_4 mitigation strategies (Waghorn et al., 2008; Klop et al., 2016; Roque et al., 2019), among which 3- nitrooxypropanol (3NOP) and nitrate have been most widely investigated. Two meta-analyses concluded that, at the average 3NOP dose of 123 mg/kg of DM and nitrate dose of 18g/kg DM of nitrate, the CH_4 mitigation effects

were 32.5% (Dijkstra et al., 2018) and 14.4% (Feng et al., 2020) for lactating cows, respectively. Based on their conclusions, the total CO_2 equivalents could be decreased to 21.1 or 22.5 tons if adding 3NOP at dose of 123 mg/kg of DM or nitrate of 18 g/kg of DM to diets of lactating cows. The CH_4 mitigation effects of 3NOP and nitrate on nonlactating cows and heifers were not fully studied, but lactating cows contributed the most to GHG emission, accounting for 75.5% in our simulation.

Total daily manure ($F_{DM} + F_W + U_t$) excretion was 63.6 tons, including 0.4 ton of nitrogen and 3.5 tons of carbon. Total VS and dVS excretion were 7.8 and 7.0 tons, respectively. Manure OM can generate CH_4, nitrous oxide (N_2O) and ammonia (NH_3) through decomposition, hydrolysis, nitrification and denitrification processes, which makes it an important source of pollutants and has to be controlled (Li et al., 2012). High-production animals have greater nutrient requirements and feed intake but feed efficiency decreases with feed intake (Broderick, 2003; Gourley et al., 2012), so it is important to avoid overfeeding and underfeeding. Overfeeding not only increases unnecessary feed cost, but also increases the environmental impact (Connor, 2015). Feed efficiency can be increased through dietary strategies. Decreasing dietary protein could decrease urine nitrogen excretion without affecting production if energy and protein are well balanced (Dijkstra et al., 2011). Both energy and nitrogen efficiencies are negatively associated with dietary ADF (Phuong et al., 2013), which was also used to estimate F_C and VS in our study. Feed additives such as yeast supplementation (Schingoethe et al., 2004; Moallem et al., 2009) and fibrolytic enzyme (Yang et al., 1999; Holtshausen et al., 2011) could also improve feed efficiency.

Thermal balance

The temperature of changes of body core, skin and coat over three days for lactating and dry cows are shown in Figure 1. The average body temperature for early-, mid-, late-lactation and dry cows were 41.0 °C, 42.2 °C, 40.3 °C and 39.3 °C, respectively. The body temperature was positively associated with heat energy generation, which is dependent on the milk production. Lactating animals are more susceptible to heat stress, especially high-lactating cows (Kadzere et al., 2002), therefore, it is essential to cool lactating cows in order to maintain the milk production. The proportions of heat dissipation through convection, evaporation, long wave radiation, respiration and conduction are shown in Table 5. Different animal groups exhibited a similar pattern that evaporation was the major way to dissipate heat during all the time periods. Sprinkler with fan cooling can increase heat dissipation through evaporation and convection, and has been suggested as an effective cooling strategy (Strickland et al., 1989; Turner et al., 1992). One should note that evaporation rate is affected by the environmental humidity, and low humidity promotes evaporation. When applying cooling sprinklers, small droplets may evaporate before reaching the animal, which increases the environmental humidity and limit the evaporation potential, thus should be avoided (Chen et al., 2015). Another physical cooling strategy is cooling mat, which cool the animal through conductive cooling. However, conduction between the animal and ground surface only accounts for 5 to 6 percent of total heat dissipation on average in the simulation result, since only 20% of the animal surface is accessible to conductive cooling (Ortiz et al., 2015). Drwencke et al. (2020) reported that burying a cooling mat with temperature of 18.8 °C under the bed at depth of 10.2 cm did not effectively mitigate the heat stress, which agrees with our simulation result.

In conclusion, the nonlinear ration formulation model, thermal balance model, and emission and excretion models developed in previous chapters were integrated to gain a better knowledge of nutritional and environmental factors of a dairy system. However, our study did not involve the interaction between calves and the environment, which may be addressed by the future studies.

References

Alqaisi, O., and E. Schlecht. 2021. Feeding Models to Optimize Dairy Feed Rations in View of Feed Availability, Feed Prices and Milk Production Scenarios. Sustainability 13:215.

Bannink, A., M. W. Van Schijndel, and J. Dijkstra. 2011. A model of enteric fermentation in dairy cows to estimate methane emission for the Dutch National Inventory Report using the IPCC Tier 3 approach. Anim. Feed Sci. Technol. 166:603–618.

Broderick, G.A. 2003. Effects of varying dietary protein and energy levels on the production of lactating dairy cows. J. Dairy Sci. 86:1370–1381.

Cabrera, V. E., P. E. Hildebrand, J. W. Jones, D. Letson, and A. De Vries. 2006. An integrated North Florida dairy farm model to reduce environmental impacts under seasonal climate variability. Agric. Ecosyst. Environ. 113:82–97.

Chen, J. M., K. E. Schütz, and C. B. Tucker. 2015. Cooling cows efficiently with sprinklers: Physiological responses to water spray. J. Dairy Sci. 98:6925–6938.

Connor, E.E. 2015. Invited review: Improving feed efficiency in dairy production: challenges and possibilities. Animal 9:395–408.

Dijkstra, J., A. Bannink, J. France, E. Kebreab, and S. Van Gastelen. 2018. Antimethanogenic effects of 3-nitrooxypropanol depend on supplementation dose, dietary fiber content, and cattle type. J. Dairy Sci. 101:9041–9047.

Dijkstra, J., O. Oenema, and A. Bannink. 2011. Dietary strategies to reducing N excretion from cattle: implications for methane emissions. Curr. Opin. Env. Sust. 3:414–422.

Drwencke, A. M., G. Tresoldi, M. M. Stevens, V. Narayanan, A. V. Carrazco, F. M. Mitloehner, T. E. Pistochini, and C. B. Tucker. (2020). Innovative cooling strategies: Dairy cow responses and water and energy use. J. Dairy Sci. 103:5440–5454.

Feng, X.Y., J. Dijkstra, A. Bannink, S. van Gastelen, J. France, and E. Kebreab. 2020. Antimethanogenic effects of nitrate supplementation in cattle: A meta-analysis. J. Dairy Sci. 103:11375–11385.

Gourley, C. J., S. R. Aarons, and J. M. Powell. 2012. Nitrogen use efficiency and manure management practices in contrasting dairy production systems. Agric. Ecosyst. Environ. 147:73–81.

Holtshausen, L., Y. H. Chung, H. Gerardo-Cuervo, M. Oba, and K. A. Beauchemin. 2011. Improved milk production efficiency in early lactation dairy cattle with dietary addition of a developmental fibrolytic enzyme additive. J. Dairy Sci. 94:899–907.

Johnson, I. R., D. F. Chapman, V. O. Snow, R. J. Eckard, A. J. Parsons, M. G. Lambert, and B. R. Cullen. 2008. DairyMod and EcoMod: biophysical pasture-simulation models for Australia and New Zealand. Aust. J. Exp. Agric. 48:621–631.

Kadzere, C. T., M. R. Murphy, N. Silanikove, and E. Maltz, E. 2002. Heat stress in lactating dairy cows: a review. Livest. Prod. Sci.77:59–91.

Kebreab, E., K. F. Reed, V. E. Cabrera, P. A. Vadas, G. Thoma, and J. M. Tricarico. 2019. A new modeling environment for integrated dairy system management. Anim. Front. 9:25–32.

Klop G., B. Hatew, A. Bannink, J. Dijkstra. Feeding nitrate and docosahexaenoic acid affects enteric methane production and milk fatty acid composition in lactating dairy cows. J. Dairy Sci. 99, 2016, 1161-1172.

Li, C., Salas, W., Zhang, R., Krauter, C., Rotz, A. and Mitloehner, F., 2012. Manure-DNDC: a biogeochemical process model for quantifying greenhouse gas and ammonia emissions from livestock manure systems. Nutrient Cycling in Agroecosystems, 93(2), pp.163-200.

Moallem, U., H. Lehrer, L. Livshitz, M. Zachut, and S. Yakoby. 2009. The effects of live yeast supplementation to dairy cows during the hot season on production, feed efficiency, and digestibility. J. Dairy Sci. 92:343–351.

Moraes, L.E., E. Kebreab, A. B. Strathe, J. Dijkstra, J. France, D. P. Casper, and J. G. Fadel. 2015. Multivariate and univariate analysis of energy balance data from lactating dairy cows. J. Dairy Sci. 98:4012–4029.

NRC. 2001. Nutrient Requirements of Dairy Cattle. 7th ed. National Academy Press, Washington, DC.

Ortiz, X.A., J. F. Smith, F. Rojano, C. Y. Choi, J. Bruer, T. Steele, N. Schuring, J. Allen, and R. J. Collier. 2015. Evaluation of conductive cooling of lactating dairy cows under controlled environmental conditions. J. Dairy Sci. 98:1759–1771.

Overton, M.W., and K. C. Dhuyvetter. 2020. Symposium review: An abundance of replacement heifers: What is the economic impact of raising more than are needed?. J. Dairy Sci. 103:3828–3837.

Phuong, H. N., N. C. Friggens, I. J. M. De Boer, and P. Schmidely. 2013. Factors affecting energy and nitrogen efficiency of dairy cows: A meta-analysis. J. Dairy Sci. 96:7245–7259.

Roque, B. M., J. K. Salwen, R. Kinley, and E. Kebreab. 2019. Inclusion of Asparagopsis armata in lactating dairy cows' diet reduces enteric methane emission by over 50 percent. J. Clean. Prod. 234:132–138.

Rotz, C.A., M. S. Corson, D. S. Chianese, F. Montes, S.D. Hafner, and C.U. Coiner. 2012. The integrated farm system model. References manual, version, 3.

Rotz, C.A., D. R. Mertens, D.R. Buckmaster, M.S. Allen, and J. H. Harrison. 1999. A dairy herd model for use in whole farm simulations. J. Dairy Sci. 82:2826–2840.

Ryan, W., D. Hennessy, J. J. Murphy, T. M. Boland, and L. Shalloo. 2011. A model of nitrogen efficiency in contrasting grass-based dairy systems. J. Dairy Sci. 94:1032–1044.

Schingoethe, D.J., K. N. Linke, K. F. Kalscheur, A. R. Hippen, D. R. Rennich, and I. Yoon. 2004. Feed efficiency of mid-lactation dairy cows fed yeast culture during summer. J. Dairy Sci. 87:4178–4181.

Strickland, J. T., R. A. Bucklin, R. A. Nordstedt, D. K. Beede, and D. R. Bray. 1989. Sprinkler and fan cooling system for dairy cows in hot, humid climates. Appl. Eng. Agric. 5:231–236.

Turner, L.W., J. P. Chastain, R. W. Hemken, R. S. Gates, and W. L. Crist. 1992. Reducing heat stress in dairy cows through sprinkler and fan cooling. Appl. Eng. Agric. 8:251–256.

Waghorn, G.C., H. Clark, V. Taufa, and A. Cavanagh. 2008. Monensin controlled-release capsules for methane mitigation in pasture-fed dairy cows. Aust. J. Exp. Agric. 48:65–68.

Weather Underground. (2019). Davis, CA weather condition. Accessed July 29, 2019. https://www.wunderground.com/weather/us/ca/davis.

West, J.W. 2003. Effects of heat-stress on production in dairy cattle. J. Dairy Sci. 86:2131–2144.

Yang, W.Z., K. A. Beauchemin, and L. M. Rode. 1999. Effects of an enzyme feed additive on extent of digestion and milk production of lactating dairy cows. J. Dairy Sci. 82:391–403.

Tables and Figures

Table 1. Average animal characteristics of the six animal groups in the simulation

	Younger heifers	Older heifers	Early-lactation cows	mid-lactation cows	Late-lactation cows	Nonlactating cows
Number of animals	275	275	160	230	460	150
Body weight, kg	200	450	650	620	680	720
Parity	-	-	2	2	2	2
Milk production, kg	-	-	35	45	25	-
Milk protein, %	-	-	3	3	3	-
Milk fat, %	-	-	3.5	3.5	3.5	-
Days in milk, d	-	-	50	150	250	-
Days of pregnancy, d	0	90	0	60	160	260
Age, month	6	18	-	-	-	-

Table 2. Chemical compositions (% of DM) and price ($/kg of DM) of feeds for heifers, lactating and nonlactating cows

Feed[1]	CP	EE	NDF	ADF	Ca	P	TDN[2]	Price
Corn silage	8.8	3.2	45.0	28.1	0.28	0.26	68.8	0.18
Cracked corn grain	9.4	4.2	9.5	3.4	0.04	0.30	85.0	0.18
Grass silage	17.6	2.9	54.5	35.7	0.89	0.36	56.7	0.24
Soybean meal	49.9	1.6	14.9	10.0	0.40	0.71	80.0	0.38
Legume silage	21.9	2.2	43.2	35.2	1.36	0.35	56.8	0.31
Cotton seed	23.5	19.3	50.3	40.1	0.17	0.60	77.2	0.26
Grass hay	13.3	2.5	57.7	36.9	0.66	0.29	59.7	0.24
Bermudagrass hay	10.4	2.7	73.3	36.8	0.49	0.27	52.9	0.16
Beet pulp	10.0	1.1	45.8	23.1	0.91	0.09	69.1	0.27
Calcium phosphate dibasic	0	0	0	0	22.0	19.3	0	0.96

[1]Feeds used for heifers: corn silage, cracked corn grain, grass silage and calcium phosphate dibasic; feeds used for lactating cows: corn silage, cracked corn grain, soybean meal, legume silage, cotton seed, grass hay, bermudagrass hay and calcium phosphate dibasic; feeds used for nonlactating cows: corn silage, grass silage, soybean meal, bermudagrass hay and calcium phosphate dibasic.

[2]TDN are the standard values from the NRC (2001) table.

Table 3. Nutrient requirements and feed ration per animal for the six animal groups

	Younger heifers	Older heifers	Early-lactation cows	Mid-lactation cows	Late-lactation cows	Nonlactating cows
Nutrient requirement[1]						
NE_M, Mcal/d	4.6	8.5	10.6	10.2	11.0	10.4
NE_L, Mcal/d	0	0	24.3	31.2	17.3	3.4
NE_G, Mcal/d	1.7	1.9	0.64	0.62	0.66	0.64
MP, g/d	461.1	460.7	2366.7	3024.4	1788.1	765.3
Calcium, g/d	17.0	19.8	64.8	76.1	53.6	32.7
Phosphorus, g/d	11.6	10.5	54.6	69.0	41.2	16.1
Ingredient (kg of DM)						
Corn silage	0	1.1	7.5	0	5.9	7.5
Cracked corn grain	2.2	3.9	7.6	11.2	6.4	-
Grass silage	3.0	1.4	-	-	-	0
Soybean meal	-	-	4.6	4.9	3.2	1.3
Legume silage	-	-	0	0	0	-
Cotton seed	-	-	0	0	0	-
Grass hay	-	-	0	0	0	-
Bermudagrass hay	-	-	0.73	10.9	0.57	0
Beet pulp	-	-	-	-	-	0
Calcium phosphate dibasic	0.04	0.07	0.21	0.22	0.18	0.1
Chemical composition (% of DM)						
CP	13.9	10.9	18.0	17.1	17.1	14.8
NDF	34.9	25.0	25.8	35.9	25.7	40.0
ADF	21.7	14.4	15.0	17.9	14.9	25.1
Fat	3.4	3.71	3.2	3.1	3.2	2.9
Ca	0.7	0.5	0.5	0.5	0.5	0.6
P	0.5	0.5	0.6	0.5	0.6	0.6
Diet cost ($/animal)	1.2	1.3	4.8	5.9	3.7	2.0

NE_M = Net energy for maintenance; NE_L = Net energy for lactation; NE_G = Net energy for growth; MP = Metabolizable protein

Table 4. Average GHG emission and manure excretion per animal of the six animal groups

	Younger heifers	Older heifers	Early-lactation cows	Mid-lactation cows	Late-lactation cows	Nonlactating cows
CH_4, g/d	119.3	130.0	326.2	432.4	267.0	197.2
CO_2, kg/d	3.0	3.8	12.2	14.7	10.4	7.7
Fecal DM, kg/d	1.8	2.2	6.7	9.4	5.1	2.9
Fecal nitrogen, g/d	43.8	50.2	188.8	257.5	141.9	71.0
Fecal carbon, g/d	734.2	843.9	3134.7	4409.2	2396.4	1304.4
Fecal water, kg/d	6.6	7.4	34.6	47.0	24.2	12.7
Total urine, kg/d	10.9	9.3	19.0	20.1	17.8	12.3
Urine nitrogen, g/d	57.0	55.4	198.3	216.7	165.3	120.8
urine carbon, g/d	70.1	86.6	272.7	327.6	227.5	158.4
VS, kg/d	1.9	2.4	7.4	10.0	5.7	3.2
dVS, kg/d	1.8	2.2	6.7	9.1	5.1	2.7

Table 5. The average percentage (%) of heat dissipation (J) through convection, evaporation, long wave radiation, respiration and conduction during different time periods for the simulation of early-, mid-, late-lactation and dry cows based on the weather condition in Davis (CA) from July 26 to 28, 2019.

	0000 to 0600 h	0600 to 1200 h	1200 to 1800 h	1800 to 2400 h	Entire day
Early-lactation					
Convection	13.2	10.4	2.2	7.2	8.2
Evaporation	34.4	56.9	71.1	46.5	52.4
Long wave radiation	27.8	6.5	0.43	21.2	13.8
Respiration	15.9	21.0	25.4	19.8	20.6
Conduction	8.7	5.3	0.94	5.3	5.0
Mid-lactation					
Convection	12.2	9.5	2.3	6.9	7.7
Evaporation	38.7	58.1	70.2	48.7	54.2
Long wave radiation	24.9	6.1	0.76	18.9	12.5
Respiration	16.3	21.5	25.7	20.4	21.0
Conduction	7.9	4.8	0.94	4.9	4.6
Late-lactation					
Convection	13.9	11.3	2.0	7.5	8.6
Evaporation	31.7	55.6	72.0	44.4	51.0
Long wave radiation	30.2	6.8	0.12	23.1	15.0
Respiration	15.1	20.6	24.8	19.2	20.0
Conduction	9.1	5.7	0.95	5.7	5.3
Dry cow					
Convection	14.9	12.7	1.6	7.9	9.3
Evaporation	28.8	54.6	73.0	42.3	49.7
Long wave radiation	33.5	7.3	0.50	26.1	16.9
Respiration	13.2	18.9	23.9	17.6	18.4
Conduction	9.7	6.3	0.97	6.1	5.8

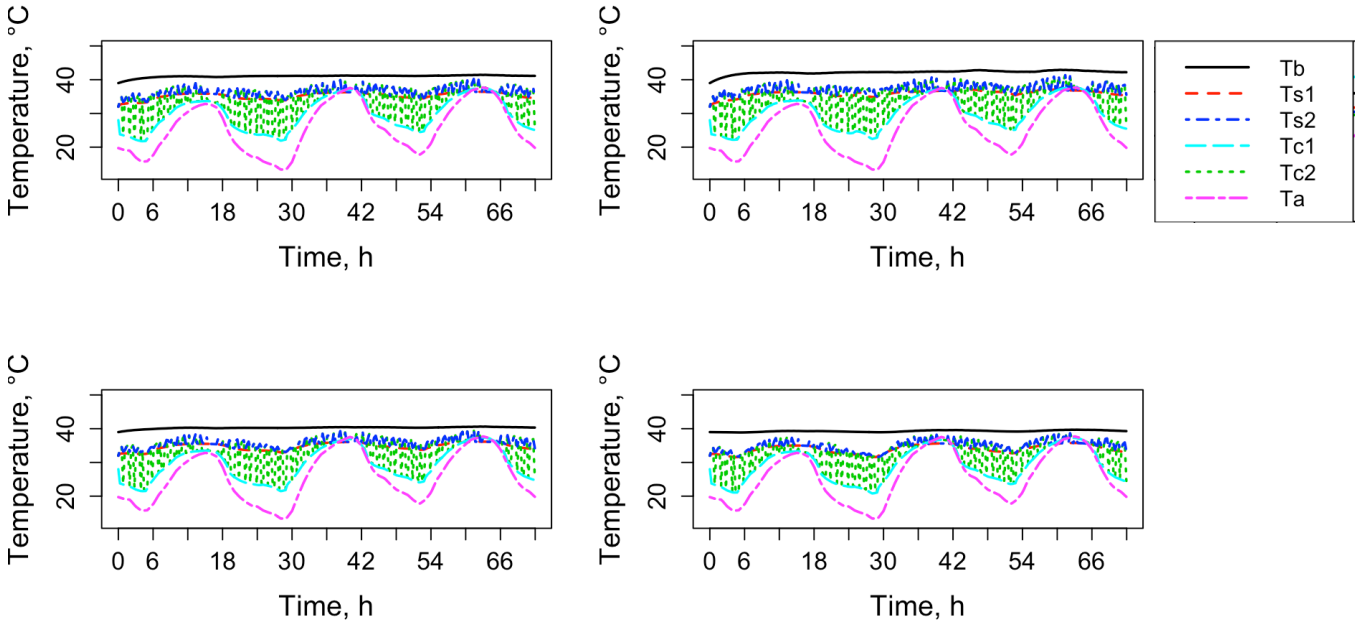

Figure 1. Simulated body (T_b), top skin (T_{s1}), bottom skin (T_{s2}), top coat (T_{c1}) and bottom coat (T_{c2}) temperature of early-, mid-, late-lactation and dry cows based on the weather condition in Davis (CA) from July 26 to 28, 2019.